UAB
Universitat Autònoma de Barcelona

School of Engineering

Department of Chemical Engineering

CHARACTERIZATION OF S-OXIDIZING BIOMASS THROUGH RESPIROMETRIC TECHNIQUES UNDER ANOXIC AND AEROBIC CONDITIONS

PhD Thesis

Supervised by:

Dr. David Gabriel Buguña & Dr. Xavier Gamisans Noguera

MABEL MORA GARRIDO

Bellaterra, October 2014

DAVID GABRIEL BUGUÑA, professor agregat del Departament d'Enginyeria Química de la Universitat Autònoma de Barcelona, i **XAVIER GAMISANS NOGUERA**, Catedràtic d'Escola Universitària,

CERTIFIQUEM:

Que l'enginyera química **MARIA ISABEL MORA GARRIDO** ha realitzat sota la nostra direcció el treball titulat: **"CHARACTERIZATION OF S-OXIDIZING BIOMASS THROUGH RESPIROMETRIC TECHNIQUES UNDER ANOXIC AND AEROBIC CONDITIONS"**, el qual es presenta en aquesta memòria i que constitueix la seva Tesi per a optar al Grau de Doctor per la Universitat Autònoma de Barcelona.

I perquè en prengueu coneixement i consti als efectes oportuns, presentem a l'Escola d'Enginyeria de la Universitat Autònoma de Barcelona l'esmentada Tesi, signant el present certificat a

Bellaterra, 30 d'octubre de 2014

David Gabriel Buguña   Xavier Gamisans Noguera

A mis ángeles de la guarda

CONTENTS

<u>**Chapter 1**</u>

MOTIVATIONS AND THESIS OVERVIEW

<u>**Chapter 2**</u>

INTRODUCTION

<u>**Chapter 3**</u>

OBJECTIVES

<u>**Chapter 4**</u>

GENERAL MATERIALS AND METHODS

<u>**Chapter 5**</u>

DEVELOPMENT OF AN ANOXIC RESPIROMETRIC TECHNIQUE TO CHARACTERIZE SO-NR MIXED CULTURES OBTAINED FROM DESULFURIZING BIOTRICKLING FILTERS

Chapter 6

COUPLING RESPIROMETRY AND TITRIMETRY TO INVESTIGATE THE KINETICS OF THIOSULFATE-DRIVEN AUTOTROPHIC DENITRIFICATION AND THE EFFECT OF NITRITE ACCLIMATION

Chapter 7

KINETIC AND STOICHIOMETRIC CHARACTERIZATION OF ANOXIC SULFIDE OXIDATION BY SO-NR MIXED CULTURES OBTAINED FROM ANOXIC BIOTRICKLING FILTERS

Chapter 8

PRELIMINARY STUDY ON LFS RESPIROMETRY APPLICATION TO CHARACTERIZE SULFIDE, ELEMENTAL SULFUR AND THIOSULFATE OXIDATION KINETICS AND STOICHIOMETRY UNDER AEROBIC CONDITIONS BY SOB

Chapter 9

STUDY ON THE APPLICATION OF HETEROGENEOUS RESPIROMETRY TO CHARACTERIZE H_2S OXIDIZING BIOFILM FROM DESULFURIZING BIOTRICKLING FILTERS

SUMMARY

Monitoring the biological activity in biotrickling filters (BTF) is difficult since it implies estimating biomass concentration and its growth yield, which can hardly be measured in immobilized biomass systems. In this study, the characterization of sulfur oxidizing biomass (SOB) obtained from different desulfurizing BTFs was performed through the application of respirometric and titrimetric techniques.

The study performed with SO-NR biomass and thiosulfate as electron donor revealed that no competitive inhibition occurred when nitrate and nitrite were present in the medium. Moreover, final bioreaction products depended on the initial $S_2O_3^{2-}$-S/NO_3^--N ratio although such ratio did not affect thiosulfate oxidation or denitrification rates. Moreover, respirometric profiles showed that the specific nitrite uptake rate depended on the biomass characteristics. Then, the coupling of respirometry and titrimetry was the method used to solve the two-step denitrification ($NO_3^- \rightarrow NO_2^- \rightarrow N_2$) stoichiometry. Afterwards, a kinetic model describing denitrification associated to thiosulfate oxidation was calibrated and validated through the estimation of several kinetic parameters from the fitting of experimental respirometric profiles using the stoichiometry previously solved. The profiles were obtained using either nitrate or nitrite as electron acceptors for acclimated and non-acclimated biomass to nitrite. Finally, sulfide was used as electron donor and again a kinetic model was proposed, calibrated and validated using the procedure developed in previous chapters.

After the characterization of SOB under anoxic conditions, the LFS respirometry was used in order to find out which were the mechanisms involved in biological sulfide oxidation under aerobic conditions. Other physical-chemical phenomena, as H_2S stripping or chemical oxidation of $H_2S_{(aq)}$, were characterized since they might cause interference over the biological activity measurement. Besides the stoichiometry of the process, a kinetic model describing each of the reactions occurring during sulfide oxidation was calibrated and validated. No product selectivity was found related with the O_2/S ratio available in the medium. Moreover, it was found that sulfide was preferentially consumed and oxidized to elemental sulfur even though an excess of oxygen was present in the medium. The shrinking particle equation was included in the kinetic model to describe elemental sulfur oxidation since the oxygen profile could not be described with a simple Monod equation.

As an innovative technique, the heterogeneous respirometry was applied to assess the biological activity of immobilized cells (biofilm). Mass transport and the activity of sulfide-oxidizing biofilms attached on two types of packed beds, originated from operative biotrickling filters, were studied under aerobic conditions. A mathematical model for the determination of kinetic-related parameters such as the maximum OUR and morphological properties of biofilm was developed and calibrated. It was found that the oxygen diffusion rate was the limiting step in the case of very active biofilms.

RESUM

La monitorització de l'activitat biològica en biofiltres percoladors és complexa ja que implica l'estimació de la concentració de biomassa i el rendiment de creixement. Aquestes dades no són senzilles de calcular quan la biomassa creix de forma immobilitzada. En aquesta tesi es porta a terme la caracterització de biomassa sulfur-oxidant extreta de diferents biofiltres percoladors, emprats per a la desulfuració de biogas, a través de tècniques respiromètriques i titrimètriques.

Durant l'estudi realitzat amb biomassa SO-NR i tiosulfat com a donador d'electrons, no es va observar competència entre el consum de nitrat i de nitrit. Els productes finals de la reacció depenien de la relació inicial $S_2O_3^{2-}$-S/NO_3^--N però aquesta relació no tenia efectes sobre les velocitats de consum de tiosulfat ni de desnitrificació. Dels perfils respiromètrics també es va observar que els consums específics de nitrit depenien de les característiques de la biomassa. La respirometria anòxica acoblada a la titrimetria va ser la metodologia emprada per a resoldre l'estequiometria de la desnitrificació en dues etapes ($NO_3^- \rightarrow NO_2^- \rightarrow N_2$). El model cinètic proposat per a descriure la desnitrificació es va calibrar i validar estimant els paràmetres cinètics que descrivien els perfils respiromètrics fent servir nitrat i nitrit amb biomassa aclimatada i no aclimatada a nitrit. Finalment, un cop a desnitrificació va ser ben caracteritzada, es va utilitzar sulfur com a donador d'electrons i es va proposar, calibrar i validar un model cinètic que descrivís completament el procés biològic.

Un cop caracteritzada la biomassa SO-NR es va utilitzar la respirometria LFS per a estudiar els mecanismes implicats a la oxidació biològica de sulfur i sofre en condicions aeròbies. Fenòmens com l'stripping o oxidació química del suflur també es va caracteritzar ja que podien interferir a la mesura de l'activitat biològica. L'estequiometria del procés així com els mecanismes de degradació i el model cinètic es van proposar. El model es va calibrar i validar amb els perfils respiromètrics sense incloure cap selectivitat cap a la formació de sofre o sulfat en funció de la relació O_2/S disponible. Es va observar que els bacteris consumien preferentment el sulfur tot i haver un excés d'oxigen al medi. En aquest cas es va utilitzar un model de consum de partícules per a descriure la oxidació del sofre ja que l'equació de Monod no descrivia un perfil tan sensible com el de l'oxigen dissolt.

L'últim estudi inclòs en aquesta tesi és el d'aplicació d'una tècnica novedosa, la respirometria heterogènia, per a avaluar l'activitat biològica de les cèl·lules en estat immobilitzat. Es van estudiar els fenòmens de transferència de matèria, així com l'activitat sulfur-oxidant amb dos tipus de material de rebliment obtinguts de biofiltres percoladors. Es va desenvolupar un model matemàtic per a determinar els coeficients cinètics així com les propietats morfològiques del biofilm. Es va observar que la difusió de l'oxigen és el pas limitant en aquells biofilms amb elevada activitat biològica.

RESUMEN

La monitorización de la actividad biológica en biofiltros percoladores es compleja ya que implica la estimación de la concentración de biomasa y del rendimiento celular. Estos datos no son sencillos de calcular en aquellos sistemas en los que la biomasa crece de manera inmovilizada. En esta tesis se ha llevado a cabo la caracterización de biomasa sulfuro-oxidante extraída de distintos biofiltros percoladores, utilizados para la desulfuración de biogás, mediante la aplicación de técnicas respirométricas.

Durante el estudio realizado con biomasa SO-NR y tiosulfato como donador de electrones no se observó competencia entre el consumo de nitrato y de nitrito. Los productos finales de la reacción dependieron de la relación inicial $S_2O_3^{2-}$-S/NO_3^--N pero esta relación no tuvo efectos sobre las velocidades de oxidación de tiosulfato ni de desnitrificación. Además, los perfiles respirométricos mostraron que los consumos específicos de nitrito dependían de las características de la biomasa. La respirometría acoplada a la titrimetría fue el método empleado para resolver la estequiometría de la desnitrificación en dos etapas ($NO_3^- \rightarrow NO_2^- \rightarrow N_2$). El modelo cinético propuesto para describir los perfiles respirométricos se calibró y validó mediante la estimación de los parámetros cinéticos utilizando la estequiometria previamente calculada. Las respirometrías se realizaron con biomasa tanto aclimatada como no aclimatada a nitrito. Finalmente, se utilizó sulfuro y de nuevo se propuso, calibró y validó un modelo cinético que describiese el proceso completamente.

Una vez caracterizada la biomasa SO-NR se utilizó la respirometría LFS para estudiar los mecanismos implicados en la oxidación biológica de sulfuro y azufre en condiciones aerobias. Fenómenos como el stripping o la oxidación química de sulfuro también se caracterizaron ya que podían interferir en la medida de la actividad biológica. Además de la estequiometría del proceso, se propusieron los mecanismos de degradación y un modelo cinético que también se calibró y validó con los perfiles respirométricos. No se encontró selectividad hacia la formación de azufre o sulfato en función de la relación O_2/S sino que se observó que las bacterias consumían el sulfuro preferentemente incluso aunque hubiese un exceso de oxígeno en el medio. En este caso se utilizó un modelo de consumo de partículas para describir la oxidación del azufre ya que la ecuación de Monod no describía un perfil tan sensible como el de oxígeno disuelto.

El último estudio incluido en esta tesis es el de aplicación de una nueva técnica, la respirometría heterogénea, para evaluar la actividad biológica de las células en estado inmovilizado. Se estudiaron los fenómenos de transferencia de materia así como la actividad sulfuro-oxidante con dos tipos de material de relleno obtenidos de biofiltros percoladores. Se desarrolló un modelo matemático para determinar los coeficientes cinéticos así como las propiedades morfológicas del biofilm. Finalmente se observó que la difusión del oxígeno es el paso limitante en aquellos biofilms con elevada actividad biológica.

LIST OF ABBREVIATIONS

BTF - Biotrickling filter

CSTR – Continuous stirred tank reactor

DGGE – Denaturing gradient gel electrophoresis

DNA - Deoxyribonucleic acid

DO - Dissolved oxygen

EBRT – Empty bed residence time

EC – Elimination capacity

EDTA – Ethylenediaminetetraacetic acid

FIM – Fisher information matrix

FSS – Fixed suspended solids

GFM – Gas flow meter

HR – Heterogeneous respirometer

HRT – Hydraulic retention time

MFC – Mass flow controller

PCR – Polymerase chain reaction

PR – Pall ring

PUF – Polyurethane foam

RE – Removal efficiency

RNA - Ribonucleic acid

RTL – Research and Testing Laboratory

SNitUR – Specific nitrite uptake rate

SNUR – Specific nitrate uptake rate

SOB – Sulfur oxidizing or S-oxidizing bacteria/biomass

SO-NR – Sulfide-oxidizing nitrate-reducing

STUR – Specific thiosulfate uptake rate

TSS – Total suspended solids

VSS – Volatile suspended solids

Chapter 1

MOTIVATIONS AND THESIS OVERVIEW

1. MOTIVATIONS AND THESIS OVERVIEW

1.1. MOTIVATIONS

The development of this thesis has been done in the Department of Chemical Engineering of the UAB, in the Research Group on Biological Treatment and Valorisation of Liquid and Gas Effluents (GENOCOV) within the project "Monitorización, modelización y control para la opmitización de biofiltros percoladores de desulfuración anóxicos y aerobios" (MICROBIOFIN). The project proposes the use of a variety of techniques for monitoring the biofiltration process. These techniques are respirometry and titrimetry for defining the biodegradation mechanisms and obtaining the kinetics of the process, advanced molecular biology techniques based on massive sequencing of the genetic material present in the reactor for the identification and monitoring of the microbial populations, and microsensors for biofilm characterization. The experimental data obtained together with the development of rigorous models will allow the prediction of the bioreactors behavior in different situations, besides being a powerful tool for the design, the optimization and the control of the bioreactors. Among the abovementioned research topics, this thesis is focused particularly in the characterization of the S-oxidizing biomass obtained from desulfurizing biotrickling filters through respirometric and titrimetric techniques. It must be pointed out that this thesis directly drives to a further knowledge and optimization of biofiltration systems, which is the main objective of the research project.

1.2. THESIS OVERVIEW

In this first chapter of the thesis the motivations and the thesis overview are presented. In Chapter 2, the general introduction is presented. In the introduction, information about the desulfurization of biogas through biotrickling filters, the microbial sulfur metabolism and the application of respirometric and titrimetric techniques for biomass characterization is provided. This information facilitates the understanding of the following chapters since many basic topics and concepts are explained. In Chapter 3 the general and the specific objectives of the thesis are stated. Chapter 4 is a compilation of all materials and methods employed during the experimental phase of the thesis. The setups corresponding to suspended and immobilized biomass cultivation as well as the respirometric assays performance are

described in detail. Moreover, in Chapter 4, analytical methods and molecular biology techniques applied to monitor different variables are presented.

Chapters 5, 6, 7, 8 and 9 contain the results obtained during the thesis. In Chapter 5 the development of a respirometric methodology to characterize biomass withdrawn from a desulfurizing biotrickling filter is presented. This methodology is further used in Chapters 6 and 7 to study the mechanisms and kinetics corresponding to two-step denitrification and thiosulfate, elemental sulfur and sulfide oxidation under anoxic conditions. Specifically, in Chapter 6 the coupling of respirometry and titrimetry is used to solve the stoichiometry of two-step denitrification associated to thiosulfate oxidation, which is subsequently used to estimate the corresponding kinetic parameters. Moreover, denitratation and denitritiation are studied in terms of kinetics using biomass acclimated and non-acclimated to nitrite. The knowledge obtained from the previous chapters is applied in chapter 7 to characterize the kinetics corresponding to sulfide oxidation and denitrification. The mechanisms and kinetics corresponding to two-step sulfide oxidation are proposed. Also, in this chapter the confidence intervals of the kinetic parameters are estimated through the Fisher Information Matrix mathematical method. Denaturing Gradient Gel Electrophoresis (DGGE) analysis was also applied in order to study the biomass diversity.

Chapters 8 and 9 are focused on characterizing sulfide oxidizing biomass under aerobic conditions. In Chapter 8 the methodology developed in Chapter 5 to cultivate the biomass and to perform the respirometric tests are adapted to characterize the biomass through the well-known LFS respirometric technique. The mechanisms corresponding to the biological reactions are proposed and the chemical oxidation of sulfide characterized. A kinetic model is calibrated and validated to describe the respirometric profiles. Pyrosequencing analysis is applied in order to study the diversity of the biomass. In Chapter 9 a new methodology to study the kinetics of the biomass immobilized in the packing material is presented: the heterogeneous respirometry. A more complex kinetic model is proposed and calibrated to describe sulfide oxidation under aerobic conditions.

In Chapter 10 the conclusions extracted from the results obtained in previous chapters are exposed and future research topics recommended. Finally, Chapter 11 contains the references used along the thesis.

Chapter 2

INTRODUCTION

2. INTRODUCTION

2.1. DESULFURIZATION OF BIOGAS

2.1.1. Biogas as a sustainable energy source

Biogas is an energy rich gas (from 15 to 30 MJ Nm^{-3}) originated from the anaerobic digestion of organic biodegradable materials such as sewage sludge, municipal wastes, animal manure and others (Cuellar and Webber, 2008; Khalid et al., 2011). The anaerobic digestion is a process in which a wide variety of microorganisms break down biodegradable material in the absence of oxygen to obtain a digested liquid or solid flow, with much lower organic content, and a biogas.

The main constituents of biogas are methane (60-70% v v^{-1}) and carbon dioxide (30-40% v v^{-1}). It also contains significant quantities of undesirable compounds, such as H_2S, mercaptans and siloxanes, depending on the composition of the organic material fermented. Biogas has been evaluated as one of the most energy-efficient and environmentally beneficial technology for bioenergy production, not only because this renewable energy source can be used for replacement of fossil fuels in power and heat production, but also it provides an excellent opportunity for mitigation of greenhouse gases emission. In addition, methane-rich biogas can replace natural gas as a feedstock for producing chemicals and materials (Pathak et al., 2009; Panwar et al., 2011).

2.1.2. Presence of hydrogen sulfide in biogas: detrimental implications on technology, environment and health.

As previously mentioned, the biogas may contain different pollutants that constitute a serious problem not only for the harmful environmental emissions but also for their detrimental effect to any biogas conversion device (Abatzoglou and Boivin, 2009). H_2S, specifically, is a colorless, flammable, extremely hazardous gas, with a "rotten egg" smell, emitted from numerous industrial activities (Syed et al., 2006) and present in biogas at typical concentrations between 50 and 3000 ppm_v (Soreanu et al., 2009). This compound is produced during the anaerobic digestion by sulfate reducing bacteria and is also the principal component in gaseous effluents from wastewater collection and treatment facilities (Cox and Deshusses, 2002). H_2S is highly corrosive and the main responsible of digesters and internal combustion engines deterioration.

Moreover, it might eventually converts to sulfur dioxide in energy recovery processes, which is a precursor to acid rain.

Besides the environmental implications, the toxicological effects of H_2S exposure in human health are numerous. The most direct and dangerous route of exposure is the inhalation which affects the nervous system and can result in unconsciousness, coma and death at concentrations above 500 ppm_v (US-EPA, 2003).

2.1.3. Biological based desulfurization in a biotrickling filter

Physical and chemical processes traditionally used to remove the H_2S from biogas entail high cost associated related with both operation and maintenance of the equipments. For this reason, current technologies are increasingly focused on biological treatment of pollutants since they are attractive from both an economical and technological point of view (Soreanu et al., 2009).

Biogas desulfurization has already been efficiently performed through biofiltration in BTFs (Fortuny et al., 2008; Fernandez et al., 2013). Moreover, desulfurizing BTFs have demonstrated to be economically advantageous when compared to physical-chemical processes such as chemical scrubbers or adsorption towers (Gabriel and Deshusses, 2004). In a BTF, biomass immobilized over the surface of an inert packing material degrades the H_2S previously absorbed in a continuously circulating liquid phase (Cox and Deshusses, 1998; Syed et al., 2006). The dissolved sulfide is biologically oxidized to other sulfur species (basically elemental sulfur, thiosulfate and sulfate) using either oxygen (aerobic conditions) or nitrate (anoxic conditions) as final electron acceptors. In Figure 2.1 the general schema of a BTF is presented. Further details about sulfur compounds biodegradation are specified in section 2.4.

In general, the suitability of the BTFs in environmental applications depends on the characteristics of the pollutant to be removed. In this sense, the pollutant must be biodegradable, soluble in water and non-toxic to the microorganisms. In the case of H_2S these constraints are accomplished but the major problem generated in a desulfurizing BTF is the possible clogging of the bed derived from an excessive production and accumulation of elemental sulfur and, eventually, biomass (Fortuny et al., 2010). The elemental sulfur is solid and is an intermediate oxidation compound which is not further

oxidized to sulfate under an electron acceptor deficiency. For this reason, under aerobic conditions, the main bottle-neck of the process is the maximization of the oxygen transfer from the gas to the liquid phase (Rodriguez et al., 2012). Under anoxic conditions this problem is avoided since nitrate or nitrite are already dissolved in the liquid phase, thus being the availability of a nitrogen source the main limitation.
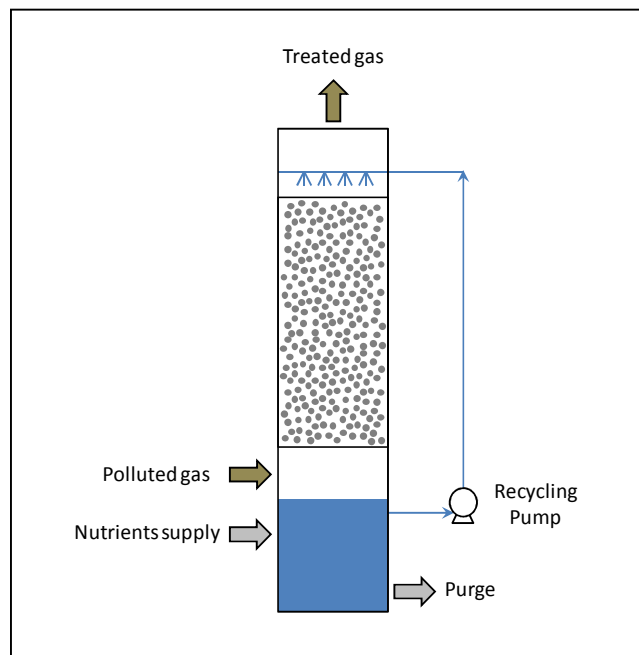
Figure 2.1. General schema of a biotrickling filter for biogas desulfurization

2.2. CHEMISTRY OF HYDROGEN SULFIDE

H_2S is an inorganic volatile gas (boiling point of -60.3 ºC at 1 atm) with a solubility of 3.98 g L^{-1} H_2O (1 atm, 20 ºC). $H_2S_{(aq)}$ is a weak diprotic acid and depending on the pH of the solution three different species may be obtained according to Eqs. 2.1 and 2.2.

$$H_2S + H_2O \leftrightarrow HS^- + H_3O^+ \text{ (pKa}_1 = 7.04) \tag{2.1}$$

$$HS^- + H_2O \leftrightarrow S^{2-} + H_3O^+ \text{ (pKa}_2 = 11.96) \tag{2.2}$$
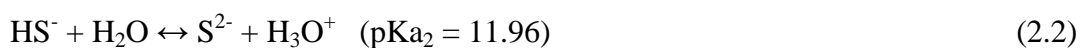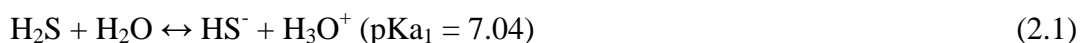
Apart from H_2S, there are several inorganic and organic sulfur compounds that are present in nature, waste gases, biogas, etc. as gas, liquid or solid compounds. H_2S is a highly reactive species and its chemical oxidation has been frequently reported to occur spontaneously in aqueous sulfide solutions with oxygen. The major intermediates and products formed according to Eqs. 2.3 to 2.6 are elemental sulfur (S^0), sulfite (SO_3^{2-}), thiosulfate ($S_2O_3^{2-}$) and sulfate (SO_4^{2-}). Many factors have been reported to affect the chemical oxidation of sulfide but, among them, pH, temperature and presence of catalysts, as transition metals and organic compounds (Obrien and Birkner, 1977), are the most relevant (Cline and Richards, 1969; Chen and Morris, 1972; Buisman et al., 1990; Nielsen et al., 2003; Gonzalez-Sanchez and Revah, 2007).

$$2\ HS^- + O_2 \rightarrow 2\ S^0 + 2\ OH^- \tag{2.3}$$

$$2\ HS^- + 2\ O_2 \rightarrow S_2O_3^{2-} + H_2O \tag{2.4}$$

$$2\ HS^- + 3\ O_2 \rightarrow 2\ SO_3^{2-} + 2\ H^+ \tag{2.5}$$

$$2\ HS^- + 4\ O_2 \rightarrow 2\ SO_4^{2-} + 2\ H^+ \tag{2.6}$$

From the chemical oxidation of aqueous sulfide solutions, other intermediate species are originated due to the reaction between different sulfur species. Eqs. 2.7 to 2.9 are some of the reactions proposed to explain the intermediary formation of polysulfide ions (S_x^{2-}) or thiosulfate at neutral and alkaline pH values (Kleinjan et al., 2005a).

$$HS^- + (x-1)\ S^0 \rightarrow S_x^{2-} + H^+ \tag{2.7}$$

$$S_x^{2-} + 3/2\ O_2 \rightarrow S_2O_3^{2-} + (x-2)/8\ S^0 \tag{2.8}$$

$$S^0 + SO_3^{2-} \rightarrow S_2O_3^{2-} + H^+ \tag{2.9}$$

Polysulfide ions are unbranched chains of sulfur atoms, with different length and one sulfide atom, easily to be recognized for their yellow-to-orange color in solution. At neutral to intermediate alkalinities S_6^{2-}, S_5^{2-} and S_4^{2-} are the dominating species

(Kleinjan et al., 2005a). Hartler et al. (1967) showed that polysulfide formation takes place at the surface of sulfur granules being the reaction rate faster with biologically produced sulfur than with the inorganic sulfur granules. Polysulfides are subject to rapid auto-oxidation when exposed to air being thiosulfate the product of the reaction (Steudel et al., 1986). Moreover, the reaction between sulfide and elemental sulfur can positively influence the biological sulfide oxidation by reducing the concentration of sulfide, which is an inhibiting substrate for S-oxidizing bacteria (Gonzalez-Sanchez and Revah, 2007).

2.3. BIOLOGICAL ELEMENTAL SULFUR

The first detailed description of sulfur bacteria and sulfur globules was given in 1887 by the microbiologist Winogradsky, who described the elemental sulfur inclusions stored in *Beggiatoa sp.* Nowadays it is known that biologically produced elemental sulfur has a white or pale-yellow color, is hydrophilic and has a lower density (1.22 g cm^{-3}) compared to chemically produced sulfur (2 g cm^{-3}) (Guerrero et al., 1984; Janssen et al., 1999; Perry, 2011). Additionally, intracellular sulfur globules refract light and cultures containing them exhibit a milky appearance. Contrary to the biological sulfur, the standard inorganic sulfur flower consists mainly of orthorhombic crystals, traces of polymeric sulfur and cyclo S_7 (bright yellow) which have a completely hydrophobic surface (Kleinjan et al., 2003).

Biological sulfur accumulates, as a transient or a final product, inside or outside the cell depending on the organism, the culture conditions and the reduced sulfur substrate (Dahl and Prange, 2006). An image of a sulfur-excreting *Thiobacillus* is showed in Figure 2.2a (Janssen et al., 1999). Many authors have suggested that the location of the catalyst for HS$^-$ oxidation (cytochromes or quinones) determines whether the sulfur is stored extracellularly or intracellularly (Gray and Knaff, 1982; Then and Truper, 1983; Brune, 1989). Sulfur percentages up to 30% of the cell dry mass have been reported for intracellular sulfur accumulating bacteria as *Beggiatoa sp.* (Nelson et al., 1986b). It must be mentioned that the majority of genera in which cultured bacteria produce intracellular sulfur globules are found in the γ-proteobacteria. As an example, this

includes bacteria in genera *Thiothrix, Beggiatoa, Thiomargarita* and *Thioploca* and the family Chromatiaceae (purple sulfur bacteria) (Maki, 2013).

Studies by X-ray absorption indicated that chemotrophic bacteria produce mainly S_8 rings, long-chain polythionates (^-O_3S-S_n-SO_3^-, n=5-20) and/or long sulfur chains terminated by organic groups (Janssen et al., 1994; Janssen et al., 1999; Prange et al., 2002). A correlation between sulfur speciation and presence of oxygen during growth of bacteria is evident. Therefore, while sulfur chains as organic polysulfanes (R-S_n-R) are present in the anaerobically grown phototrophic sulfur bacteria, sulfur rings and polythionates are present in aerobically grown microorganisms as *Beggiatoa alba* and *Acidithiobacillus ferrooxidans*, respectively. Moreover, sulfur particles are not just formed by sulfur. As an example, intracellular biosulfur particles produced by *Allochromatium vinosoum* (Figure 2.2b) has been studied and consist of a core of sulfur and a surface of polymeric organic compounds, which are probably proteins (Kleinjan et al., 2003; Dahl and Prange, 2006). Extracellularly stored sulfur has also been studied and Steudel et al. (1989) proposed a number of models to define its composition. As an example, sulfur globules excreted by *Acidithiobacillus ferrooxidans* consist of vesicles composed of a sulfur nucleus (mainly S_8 rings and other sulfur rings) with a long-chain polythionate membrane (Steudel et al., 1987).
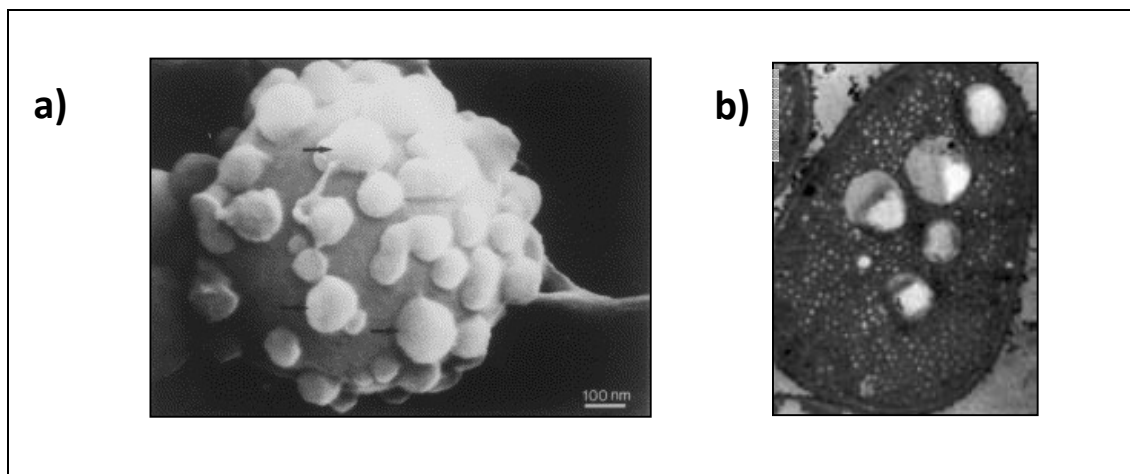
Figure 2.2. Electron micrographs of cells (a) surface of a *Thiobacillus* accumulating extracellular sulfur (Janssen et al., 1999) (b) intracellular sulfur globules from *Allochromatium vinosum* (Dahl and Prange, 2006).

2.4. BIOLOGICAL SULFUR METABOLISM

2.4.1.   The biological sulfur cycle

Microbial processes related with reduction or oxidation of sulfur compounds are based on the biological sulfur cycle (Figure 2.3). Sulfate on the reductive side of the biological sulfur cycle functions as an electron acceptor in metabolic pathways used by a wide range of microorganisms and is converted to sulfide. On the oxidative side, RSC such as sulfide serve as electron donors for phototrophic and chemolithotrophic bacteria, which convert these compounds to S^0 or sulfate (Tang et al., 2009). Moreover, inorganic sulfur can be used either as a sulfur source in assimilatory metabolism or as electron donor/acceptor in the dissimilatory metabolism (Brüser et al., 2000). As can be observed in Figure 2.3 sulfur occurs in a variety of oxidation states (from -2 to +6).
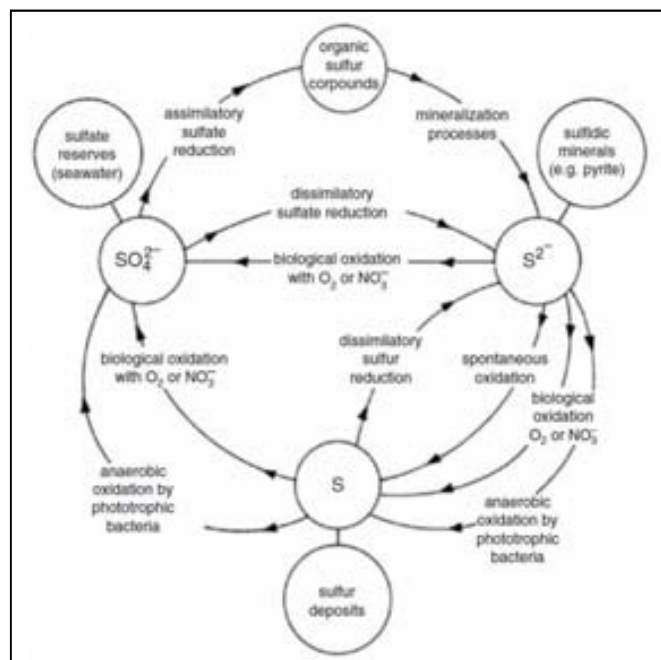
Figure 2.3. The sulfur cycle (Robertson and Kuenen, 2006)

This thesis is specially focused on the oxidative side of the biological sulfur cycle in which the oxidation of RSC as thiosulfate, elemental sulfur and sulfide is involved. In particular, S-oxidation mechanisms related to chemolithotrophic bacteria play an important role in this thesis since species as *Thiobacillus denitrificans* and *Thiothrix sp.* are studied under anoxic and aerobic conditions, respectively.

2.4.2. S-oxidizing bacteria

Sulfur oxidizing bacteria (SOB) comprise a wide number of chemolithotrophic and phototrophic organisms. Traditionally sulfur bacteria included green sulfur bacteria, purple sulfur bacteria and colorless sulfur bacteria, which belong either to the proteobacteria or to the archaebacteria groups. Nowadays, it is well-known that many other phototrophic or chemotrophic species have the ability of lithotrophic and even organoheterotrophic growth on RSC. Specifically, chemolithotrophic SOB use RSC like elemental sulfur, thiosulfate or sulfide as electron donors as well as energy sources for growth. Among chemolithotrophic bacteria, the colorless sulfur bacteria from genus *Acidithiobacillus* and *Thiobacillus* are the most reported in literature for biogas desulfurization. Specifically, *Acidithiobacillus thiooxidans* (Lee et al., 2006), *Thiobacillus novellus* (Chung et al., 1998), *Thiobacillus thioparus* (Ramirez et al., 2009) or *Thiobacillus denitrificans* (Ma et al., 2006). In Table 2.1 a list of representative SOB, that have been described to grow lithotrophically by the oxidation of RSC, is presented.

Regarding to the nature of the carbon source, chemolithotrophic SOB grow autotrophically (inorganic carbon source like CO_2), heterotrophically (organic matter as carbon source) or mixotrophically (inorganic and organic carbon assimilation). Usually, the final product of SOB respiration is sulfate, which is preferred over the formation of other intermediates like elemental sulfur as it yields the most energy. However, sulfate formation will occur if there is enough electron acceptor (e.g. oxygen or nitrate) available. In fact, results from studies performed with *Halothiobacillus* W5, a dominant SOB found in desulfurizing bioreactors, indicated that under severe oxygen limitation the respiratory chain cytochrome c pool was over reduced causing a shift to partial $2e^-$ oxidation of sulfide to sulfur instead of $8e^-$ oxidation to sulfate (Visser et al., 1997; Janssen et al., 2009). On the contrary, Jin et al. (2005) suggested that SOB oxidize elemental sulfur to sulfate under low sulfide concentrations. It has been also suggested by other authors that the O_2/S^{2-} concentration ratio is the key parameter determining whether elemental sulfur of sulfate is produced (Fortuny et al., 2008) although many studies have not found a correlation between the product selectivity and the electron acceptor/S^{2-} ratio (Buisman et al., 1991; Mora et al., 2014a,b).

Table 2.1. Representative lithotrophic S-oxidizing bacteria

BACTERIA	Foto-trophy[1]	Chemo-trophy[1]	Auto-trophy[2]	Optimum pH	Substrate	Product
Chlorobiaceae	+	-	O		HS^-, $S_2O_3^{2-}$, S^0	SO_4^{2-}
α-proteobacteria						
Rhodobacter	-	+	F	5-7	HS^-, $S_2O_3^{2-}$, S^0	SO_4^{2-}
Paracoccus versutus	-	+	F	6-8	HS^-, $S_2O_3^{2-}$, S^0	SO_4^{2-}
Acidiphilium acidophilum	-	+	F	3-4	HS^-, $S_4O_6^{4-}$, S^0	SO_4^{2-}
Thiobacillus novellus	-	+	F	6-8	$S_2O_3^{2-}$, $S_4O_6^{4-}$	SO_4^{2-}
β-proteobacteria						
Thiobacillus thioparus	-	+	O	6-8	HS^-, $S_2O_3^{2-}$, $S_4O_6^{4-}$, S^0	S^0, SO_4^{2-}
Thiobacillus denitrificans	-	+	O	6.8-7.4	HS^-, $S_2O_3^{2-}$, $S_4O_6^{4-}$, S^0	SO_4^{2-}
Thiobacillus aquaesulis	-	+	O	7.5-8	$S_2O_3^{2-}$	SO_4^{2-}
Thiomonas thermosulfatus	-	+	F	5.2-5.6	$S_2O_3^{2-}$, $S_4O_6^{4-}$, S^0	SO_4^{2-}
Thiomonas cuprina	-	+	F	3-4	S^0	SO_4^{2-}
Thiomonas intermedia	-	+	F	5.5-6	HS^-, $S_2O_3^{2-}$, $S_4O_6^{4-}$, S^0	SO_4^{2-}
γ-proteobacteria						
Chromatiaceae	+	+	F		HS^-, $S_2O_3^{2-}$, S^0	SO_4^{2-}
Ectothiorhodospiraceae	+	+	F	7-10	HS^-, $S_2O_3^{2-}$, S^0	S^0, SO_4^{2-}
Beggiatoa	-	+	F	6-8	HS^-, $S_2O_3^{2-}$	SO_4^{2-}
Thioploca	-	+	F	6-8	HS^-	SO_4^{2-}
Acidothiobacillus ferrooxidans	-	+	O	2-4	HS^-, $S_2O_3^{2-}$, $S_4O_6^{4-}$, S^0	SO_4^{2-}
Acidothiobacillus caldus	-	+	O	1-3.5	$S_2O_3^{2-}$	SO_4^{2-}
Acidothiobacillus thiooxidans	-	+	O	2-4	HS^-, $S_2O_3^{2-}$, $S_4O_6^{4-}$, S^0	SO_4^{2-}
Halothiobacillus hydrotermalis	-	+	O	7.5-8	$S_2O_3^{2-}$	SO_4^{2-}
Halothiobacillus halophilus	-	+	O	7	HS^-, $S_2O_3^{2-}$, $S_4O_6^{4-}$, S^0	SO_4^{2-}
Halothiobacillus neapolitanus	-	+	O	6-8	HS^-, $S_2O_3^{2-}$, $S_4O_6^{4-}$, S^0	SO_4^{2-}
Thiomicrospira	-	+	O	6-8	HS^-, $S_2O_3^{2-}$, $S_4O_6^{4-}$	SO_4^{2-}
Thioalkalivibrio versutus	-	+		10-10.2	HS^-, $S_2O_3^{2-}$, S^0	SO_4^{2-}
Thiothrix nivea	-	+	F	6-8.5	HS^-, $S_2O_3^{2-}$, S^0	SO_4^{2-}
Achromatium	-	+			HS^-	SO_4^{2-}
ε-proteobacteria						
Thiovulum	-	+	O	6-8	HS^-	SO_4^{2-}
Sulfurimonas denitrificans	-	+	O	6-8	HS^-, $S_2O_3^{2-}$, $S_4O_6^{4-}$, S^0	SO_4^{2-}
Cyanobacteria						
Oscillatoria	+	-	O	7-10	HS^-	S^0
Gram positive						
Sulfobacillus	-	+			S^0	SO_4^{2-}

[1]: (+) property present (-) property absent; [2]: (O) obligate autotroph (F) facultative autotroph; *Adapted from Brüser et al. (2000), Friedrich et al. (2001), Robertson and Kuenen (2006) and Syed et al. (2006).*

The existence of different oxidation pathways of RSC is a consequence of the wide metabolic and phylogenetic diversity of SOB as well as the ability to use various sulfur compounds. In Figure 2.4 a general schema representing the enzymatic oxidation reactions of the main inorganic sulfur compounds is presented (Suzuki, 1999).
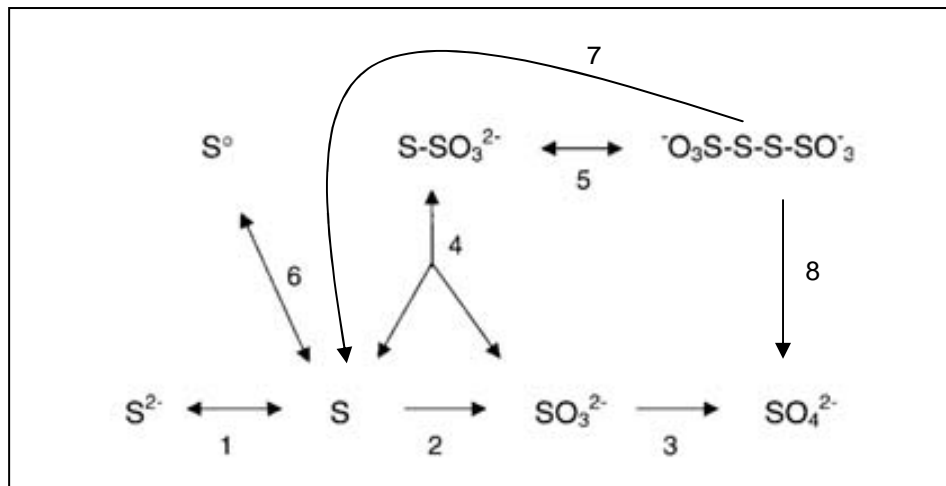
Figure 2.4. General sulfur oxidation scheme (Adapted from Suzuki et al. (1999))

The first step is the oxidation of sulfide to sulfur and sulfite (steps 1 and 2). The last oxidation step is the oxidation of sulfite to sulfate (step 3). Polysulfides and thiosulfate may be formed from the chemical reactions between elemental sulfur, sulfide and sulfite (steps 6 and 4). The biological oxidation of thiosulfate is a bit more complex. One of the pathways involves an initial cleavage so that the sulfane sulfur ($\mathbf{S}$-SO_3^{2-}) is accumulated as sulfur whereas the sulfone sulfur (S-$\mathbf{S}O_3^{2-}$) rapidly oxidizes to sulfite (step 4). Moreover, thiosulfate can be oxidized to tetrathionate and further oxidized to sulfate and to elemental sulfur (steps 7 and 8).

A part from the general schema described above, there are three basic models accepted to explain thiosulfate oxidation that have been related with the oxidation of other sulfur compounds as sulfide, elemental sulfur and polythionates.

- *Thiosulfate-branched oxidation pathway*

According to this model (Figure 2.5), HS^- is oxidized to elemental sulfur in the periplasm. The reaction is catalyzed by the enzyme sulfide:quinone oxidoreductase (SQR). Then, elemental sulfur stored in the periplasm is transported to the cytoplasm through the sulfide carrier system (SCS). Once in the cytoplasm, sulfide is oxidized to sulfite and further to sulfate through the APS pathway. Sulfate will be later excreted by the cell (Peck, 1960; Kelly, 2003). Regarding thiosulfate, the mechanism is similar to that presented in Figure 2.4 and is also a periplasmatic reaction. The production of tetrathionate is not fully known and, although is quite well defined, still some steps are not proved. *Thiobacillus denitrificans, Thiobacillus thioparus* and *Beggiatoa alba* are some of the bacteria related with this oxidation pathway (Brüser et al. 2000).
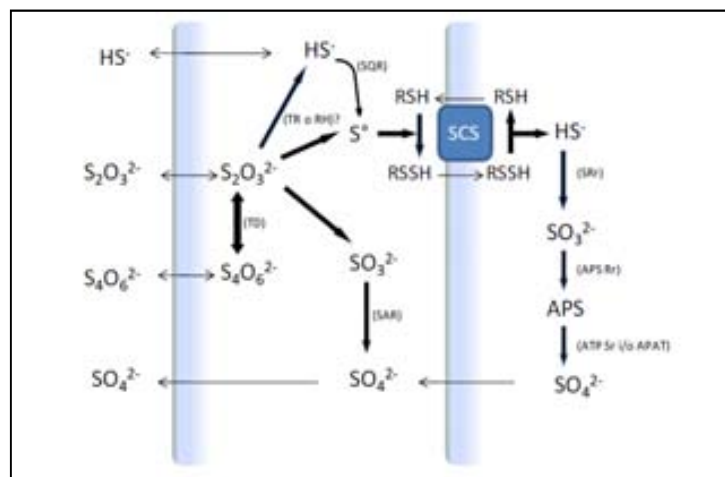
Figure 2.5. Thiosulfate-branched oxidation pathway. SCS: "sulfide carrier system" involving an unknown trans-sulfhydrylase on the periplasmatic side, a thiol/perthiol transporting system in the membrane and a heterodisulfide reductase on the cytoplasmic side. APS: adenosine-5'-phosphosulfate. SQR: sulfide:quinone oxidoreductase. SAR: sulfide:acceptor oxidoreductase. TD: thiosulfate dehydrogenase. TR: thiosulfate reductase. RH: rhodanese. SRr: inverse sulfite reductase. APS Rr: APS reverse reductase. ATP Sr: ATP reverse sulfurylase. APAT: adenylyl-sulfate:phosphate adenylyl-transferase (Adapted from Brüser et al., 2000 and Rovira, 2013).

- *Multi-enzyme-complex pathway*

This pathway was formerly described as the "PSO (*Paraccocus* Sulfur Oxidation) pathway" by Kelly et al. (1997) since the mechanism used by *Paraccocus*

pantothrophus to oxidize RSC was taken as a reference. After the complete characterization of *P. pantothrophus* enzymatic system it was recognized as the Sox system model. According to this model, thiosulfate is directly oxidized to sulfate through a 4-component protein-complex located in the periplasm by reducing the cytochrome c (Figure 2.6). Moreover, the oxidation of other RSC as sulfide, elemental sulfur and sulfite through the Sox system is also possible. The complete Sox system has been found in α-proteobacteria but in β-proteobacteria, γ-proteobacteria and Chlorobiaceae one of the Sox enzymes is not produced (sulfide deshydrogenase or soxCD), indicating that another pathway is required to oxidize the elemental sulfur to sulfate (Friedrich et al., 2005).
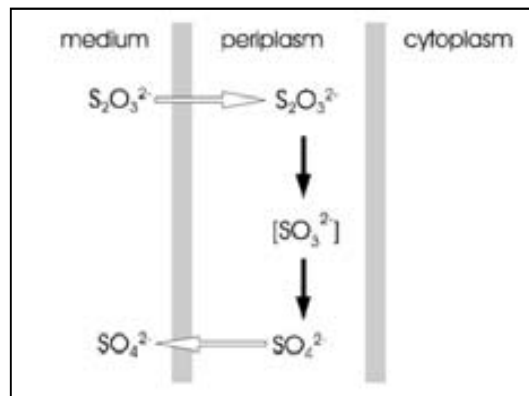
Figure 2.6. Model of the multi-enzyme-complex pathway of thiosulfate oxidation in *Paraccocus* species (Brüser et al. 2000)

- *Tetrathionate-oxidation pathway*

The first proposal of a thiosulfate oxidation via tetrathionate was made for *Thiobacillus thioparus* by Vishniac (1952). However, further investigations about the metabolism of this organism showed strong evidence against the tetrathionate pathway. Nevertheless, recent studies have confirmed the existence of thiosulfate dehydrogenase in various *Thiobacillus* species which is the responsible enzyme in the thiosulfate conversion to tetrathionate (Visser et al., 1996; Kelly et al., 1997; Suzuki, 1999). Many authors have studied tetrathionate-oxidation pathway in different organisms but the localization of the reaction has not been established yet (Lu and Kelly, 1988;

Meulenberg et al., 1993; Hallberg et al., 1996). In Figure 2.7 the tetrathionate-oxidation pathway is presented.
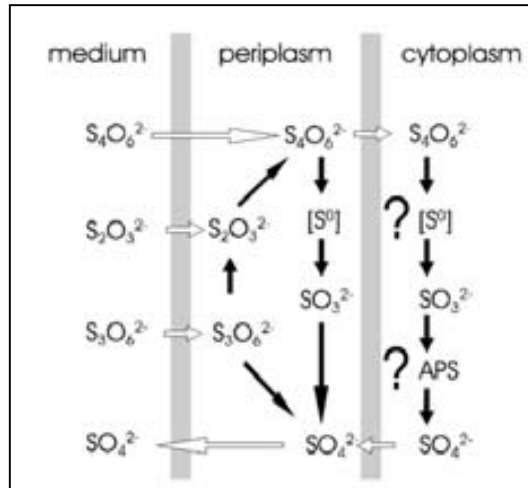
Figure 2.7. Model of the tetrathionate pathway of thiosulfate oxidation in obligate aerobic *Thiobacillus* species (Brüser et al. 2000)

As can be noted the tetrathionate oxidation pathway is highly hypothetical although several species have been related with this pathway as *Halothiobacillus neapolitanus*, *Acidithiobacillus ferroxidans* (both obligate autotrophic γ-proteobacteria) or *Acidiphilium acidophilum* (facultative autotrophic α-proteobacterium) (Kelly et al., 1997)

2.4.3. Sulfur based autotrophic denitrification

Sulfur based autotrophic denitrification is a process carried out by a group of microorganisms referred to as sulfide-oxidizing nitrate-reducing (SO-NR) bacteria which also use RSC as energy source while reducing nitrate to nitrogen gas or other nitrogenous intermediates. Denitrification is not a single-step process but a sequence of reduction steps in which NO_2^-, NO and N_2O are involved as intermediary reaction compounds. Thus, in this process the biological sulfur cycle is directly linked to the biological nitrogen cycle (Figure 2.8).
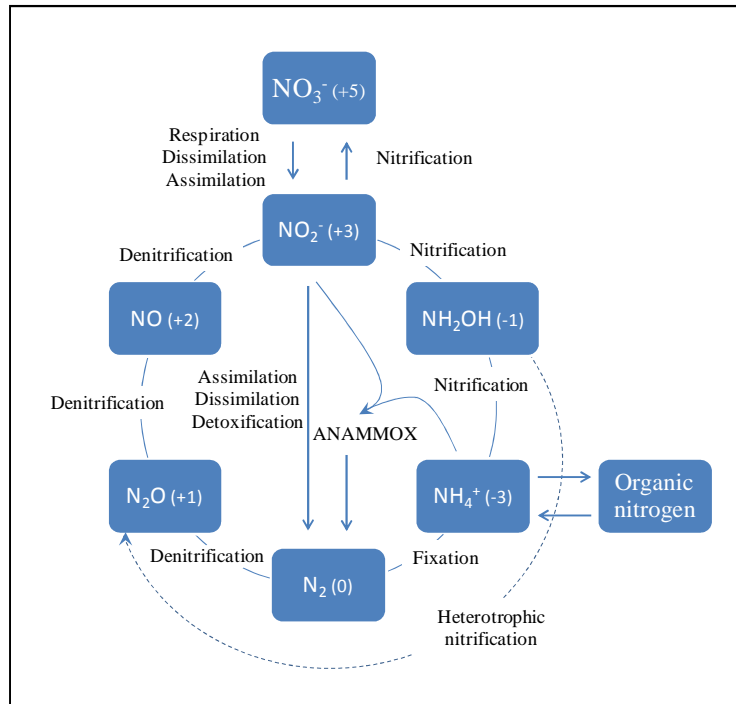
Figure 2.8. Biological nitrogen cycle (Adapted from Richardson et al. (1999))

The classical denitrification pathway is presented in Figure 2.9. As can be observed many different reductases are involved in the process. A great number of bacteria are capable of denitrifying but not all the species can denitrify completely to N_2 from nitrate since some of them have a lack of specific reductases to carry on the complete denitrification. In fact, there are organisms that do not possess one of the reductases involved in the denitrification process being capable just to reduce NO_3^- to N_2O, for example. Other organisms have a lack of nitrate reductase being nitrite dependent since they are unable to reduce NO_3^- to NO_2^- (Knowles, 1982). In the following sections some characteristics of the most important enzymes involved in denitrification process are described.

- *Nitrate reductases*

Nitrate reductases catalyze the reduction of NO_3^- to NO_2^- (Eq. 2.10). Bacteria can contain three different nitrate reductases. Two of them are located in the cytoplasmatic membrane (NAR) or the periplasm (NAP). The third nitrate reductase is used for

nitrogen assimilation in some strains and is located in the cytoplasm (NAS). Nitrate reductases require iron and molybdenum to catalyze the reaction (Richardson and Watmough, 1999).

$$NO_3^- + 2H^+ + 2e^- \rightarrow NO_2^- + H_2O \tag{2.10}$$

- *Nitrite reductases*

Nitrite reductases catalyze the reduction of nitrite to nitric oxide (NO) or to NH_4^+ and H_2O (Eqs. 2.11 and 2.12). Reduction of NO_2^- to NO is carried out by two respiratory enzymes (NirS and NirK) located in the bacterial periplasm. Reduction of NO_2^- to NH_4^+ is catalyzed by cytochrome c NIR which is also capable of reducing NO to N_2O. These enzymes also need trace metals as iron and copper to catalyze the reaction (Knowles, 1982; Richardson and Watmough, 1999). Moreover, many authors have also suggested that nitrite reductases may be inhibited by nitrite since nitrite reduction rate is negatively affected by the presence of nitrite (Korner and Zumft, 1989; Fajardo et al., 2014a).

$$NO_2^- + 2H^+ + e^- \rightarrow NO + H_2O \tag{2.11}$$
$$NO_2^- + 8H^+ + 6e^- \rightarrow NH_4^+ + 2H_2O \tag{2.12}$$

- *Nitric oxide and nitrous oxide reductases*

Bacterial nitric oxide and nitrous oxide reductases (NORs and Nos, respectively) catalyze the last two reduction reactions in denitrification (Eqs. 2.13 and 2.14).

$$2NO + 2H^+ + 2e^- \rightarrow N_2O + H_2O \tag{2.13}$$
$$N_2O + 2H^+ + 2e^- \rightarrow N_2 + H_2O \tag{2.14}$$

Both of them are copper-containing enzymes. Hendriks et al. (2000) reported that NO reduction to N_2O occurs almost instantaneously after its formation due to the toxicity of NO. After its production, N_2O can be further reduced to N_2 although Knowles (1982) reported that Nos is inhibited at low pH and is more sensitive to O_2

than other reductases being the ratio $N_2O:N_2$ obtained dependent on this parameters. Other studies have showed that N_2O is also accumulated under a deficiency of Cu, which is essential for Nos activity (Granger and Ward, 2003; Twining et al., 2007). The inhibition of nitrous oxide reductase by sulfide has been also reported by many authors (Sorensen et al., 1980; Manconi et al., 2006; Senga et al., 2006; Fajardo et al., 2014a).
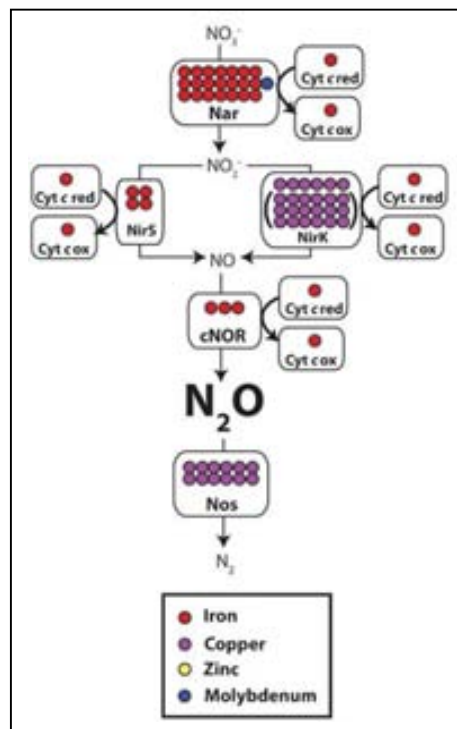
Figure 2.9. Classical denitrification pathway with the trace metals required in each of the denitrification steps by the corresponding reductases (Glass and Orphan, 2012)

2.5. RESPIROMETRIC AND TITRIMETRIC TECHNIQUES TO CHARACTERIZE S-OXIDIZING BIOMASS

Monitoring of microbial activity and development of kinetic models to describe the biological desulfurization that takes place in a BTF is highly desirable in order to design, evaluate, and optimize the process. However, the characterization of immobilized biomass is complex since biomass concentration, as well as its growth yield, is a parameter hard to measure. In this sense, respirometry and titrimetry are on-line techniques extensively used for the characterization of heterotrophic and

autotrophic suspended biomass under aerobic and anoxic conditions, especially for the characterization of activated sludge from wastewater treatment processes. Furthermore, these techniques allow obtaining the biokinetic characteristics of a microbial culture by modeling the respirometric profiles (Spanjers and Vanrolleghem, 1995; Petersen et al. 2002).
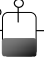
2.5.1. Respirometric technique

Respirometry is the measurement and interpretation of the biological electron acceptor consumption (usually oxygen) under well-defined experimental conditions (Spanjers et al., 1996). This technique has been demonstrated as a powerful tool to gain insight in the characterization of wastewater, to estimate kinetic and stoichiometric parameters, to monitor bioprocesses and to evaluate potential toxicity and inhibition effects over different suspended cultures, mainly in aerobic processes (Kong et al., 1996; Spanjers et al., 1996; Vanrolleghem et al., 1999; Guisasola et al., 2007; Cokgor et al., 2009). Theoretically, respirometry can be analogously applied to an anoxic process by measuring the nitrate (or nitrite) uptake rate (NUR) (Sin and Vanrolleghem, 2004). However, the lack of reliable and inexpensive on-line nitrate/nitrite sensors to monitor respirometric tests (Sin et al., 2003) makes anoxic respirometric tests tedious and more laborious than aerobic ones. Then, accurate off-line monitoring of nitrate and nitrite concentrations requires of performing several tests to properly characterize the evolution of the biological reactions under well-known and controlled environmental conditions.

Oxygen uptake rate (OUR) or NUR curves obtained from respirometric tests after the injection of substrate pulses are related with the biodegradation processes. During a respirometric test not only the starting and the ending points are observed but also how the whole process evolves. In aerobic respirometric tests, the OUR calculation is based on the dissolved oxygen (DO) balance in the respirometer which is different depending on its configuration. There are many configurations through which respirometric tests can be conducted. In Table 2.2 a summary of the possible respirometer configurations, with the corresponding oxygen mass balances, is presented. The classification of a respirometer is based on a three-letter configuration. The first letter indicates wether the oxygen measurement is performed in the gas (G) or the liquid (L) phase. The second and third letters indicate wether the gas and liquid phases are static (S) or dynamic (F),

respectively. It must be mentioned that this configuration has not been standardized for anoxic respirometries although the same configurations could be used if nitrogen gaseous compounds and/or ionic species are monitored

Table 2.2. Summary of respirometer configurations (Adapted from Spanjers et al., 1996)

			Measurement in liquid phase				Measurement in gas phase			
	Respirometric principle									
	Process	Coefficient	LSS	LFS	LSF	LFF	GSS	GFS	GSF	GFF
Liquid-phase balance	Respiration	$V_L r_o$	-1	-1	-1	-1	-1	-1	-1	-1
	Dissolved Oxygen accumulation	$d\,(V_L S_o)\,dt^{-1}$	-1	-1	-1	-1	-1	-1	-1	-1
	Liquid flow	$Q_{in}S_{o,in} - Q_{out} S_o$			1	1			1	1
	Gas exchange	$V_L K_L a\,(S_o^* - S_o)$		1		1	1	1	1	1
Gas-phase balance	Gaseous Oxygen accumulation	$d(V_G C_o)\,dt^{-1}$					-1	-1	-1	-1
	Gas flow	$F_{in}C_{o,in} - F_{out}C_o$						1		1
	Gas exchange	$V_L K_L a\,(S_o^* - S_o)$					-1	-1	-1	-1

The equipment to perform the respirometric tests generally consists of a sample container, a mixing device, pH and T controllers and one or more dissolved oxygen or nitrogenous compounds probes. Thus, respirometric tests are performed under such controlled conditions that allow characterizing other physical and chemical processes taking place simultaneously with the biological reaction. As an example, when sulfide oxidation is characterized through aerobic respirometric tests with autotrophic biomass, the stripping of substrate (H_2S) and carbon source (CO_2) occur being affected the biological activity measurement (Mora et al., 2014a; Mora et al., 2014b). For this reason it is necessary to quantify all the processes contributing the substrate or electron acceptor utilization, including the endogenous respiration (OUR_{end} or NUR_{end}). The endogenous respiration, collectively termed decay, consists of the electron acceptor consumption corresponding to the use of internally and externally stored materials by cells to sustain their integrity and the lysis, whereby cells are decomposed by external enzymes or other organisms (Young and Cowan, 2004). In Figure 2.10 the typical LFS

respirogram is presented from which the OUR_{end} as well as the overall oxygen mass transfer coefficient (K_La) can be calculated. The mass balance applied to obtain the exogenous oxygen uptake rate, i.e. the consumption directly related with the substrate biodegradation, is calculated through Eq. 2.15 for LFS respirometric tests performed at a constant volume.

$$OUR_{ex} = K_La \cdot \left[S_0^* - S_0(t) \right] - \frac{dS_0}{dt} - OUR_{end} \qquad (2.15)$$

where S_0^* is the DO saturation (mg O_2 L^{-1}) and S_0 is the DO concentration.
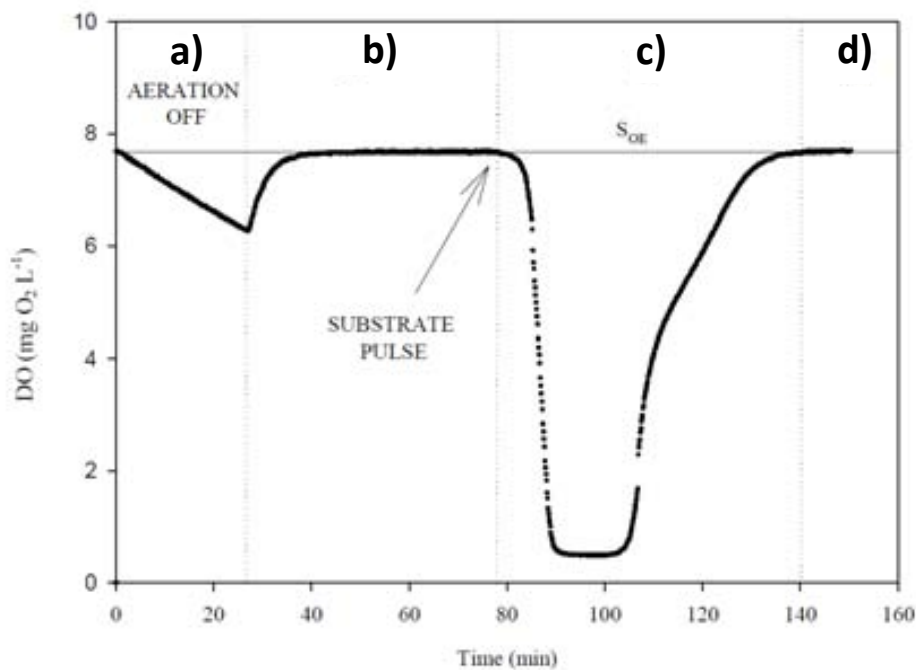
Figure 2.10. A typical LFS respirogram (Guisasola, 2005) (a) Aeration is cut off to calculate the OUR_{end} from the slope of the DO profile (b) Aeration is re-started until DO concentration reaches the initial value (S_{OE}) again. S_{OE} is the DO concentration where oxygen transfer equals OUR_{end}. From the DO profile the K_La is obtained (c) A substrate pulse is added and consequently the DO concentration decreases until substrate depletion (d) The biomass returns to endogenous conditions and DO reaches again S_{OE}.

The OUR_{ex} curves reflect the kinetics of the biodegradation process and allow the estimation of kinetic and stoichiometric parameters by direct model fitting to a respirometric curve (Jubany et al., 2005).

2.5.2. Titrimetric technique

Titrimetry is the indirect measurement of the proton production through the monitoring of the amount of base or acid dosage necessary to maintain a constant pH where pH-affecting reactions are taking place (Spanjers et al., 1996; Marcelino et al., 2009). This technique was mainly developed to monitor nitrification since this reaction has a well-known stoichiometric relation between acidity production and ammonium oxidation (Ramadori et al., 1980). Titrimetry has also been commonly used to monitor biological processes such as organic matter degradation, denitrification and phosphorous removal (Bogaert et al., 1997; Gernaey et al., 2002; Guisasola et al., 2007; Vargas et al., 2008). Apart from the biological activity, other physical or chemical processes as the stripping of CO_2 or H_2S produced due to the continuous sparging of a system with gas (air or nitrogen gas for example for aerobic or anoxic/anaerobic tests, respectively), could be quantified with this tool. Moreover, titrimetry has demonstrated to be a suitable tool for on-line monitoring of biological processes because proton production can be calculated even with highly buffered media (Vargas et al., 2008).

In particular, NUR monitoring is problematic since nitrate and nitrite measurements still have some problems associated. The need of samples pre-treatment, interferences caused by organic compounds for UV determinations, interferences caused by nitrites and signal drifting for ion selective probes are the main issues (Lynggaard-Jensen, 1999; Sin and Vanrolleghem, 2004). The possibility of using off-gas analyses or biosensors requires complex and expensive instrumentation being the titrimetric technique a reliable, cheap and simple alternative to monitor biological processes (Artiga et al., 2005; Ficara and Canziani, 2007). As an example, Gernaey et al. (1997) implemented an on-line nitrification monitoring system with a titrimetric sensor installed in an activated sludge wastewater treatment process to estimate the ammonium concentration and the nitrification rates without the need for any sampling of the reactor. Also, Ficara et al. (2007) developed a nitrate and nitrite concentrations, biomass yield and heterotrophic denitrification pH-stat monitoring system as well by using on-

line titrimetric measurements. Hence, titrimetry has also been used as an on-line reliable monitoring tool of anoxic and aerobic biological processes.

Nevertheless, although the application of titrimetric and respirometric techniques separately to characterize biological processes has been successfully performed, OUR and NUR occasionally do not provide enough information when a multi-step biological process as autotrophic denitrification with RSC oxidation occurs during a respirometric test (McMurray et al., 2004). In this situation, titrimetry coupled to respirometry can be used to uniquely identify the rate of intermediates production (Munz et al., 2009; Mora et al., 2014b) . Coupling of both techniques has also been successfully applied by other authors to study carbon source biodegradation under anoxic and aerobic conditions (Gernaey et al., 2002; Petersen et al., 2002).

2.5.3. Characterization of immobilized biomass from a desulfurizing BTF: homogeneous vs. heterogeneous respirometry

Suspended cultures of SOB have been already characterized, under anoxic and aerobic conditions, through the abovementioned respirometric and titrimetric techniques by other authors (Artiga et al., 2005; Munz et al., 2009). However, respirometry and titrimetry have not been commonly applied in recent years to study the mechanisms related with RSC oxidation by biomass obtained from desulfurizing BTFs. Frequently, kinetic and/or stoichiometric parameters have been determined through batch tests performed in sealed bottles being several experiments required to study the evolution of the biological reactions under a certain condition. Moreover, batch tests offer neither the possibility of installing sensors nor a pH control system, which are essential to monitor and preserve correctly the biological activity during an experimental test (Delhomenie et al., 2008).

In this thesis two respirometric procedures or techniques were proposed and developed to characterize the kinetics and mechanisms of biodesulfurization with immobilized biomass under well-controlled conditions, the homogeneous and the heterogeneous respirometry. The main differences between both techniques are explained below.

- *Homogeneous respirometry*

The application of homogeneous respirometry to characterize immobilized biomass implies the destruction of the biofilm since must be withdrawn from the packing material to be cultivated as a suspended culture. Then, the hydrodynamic conditions in which the biomass is cultivated and the respirometric tests performed are really different from those found in a BTF. However, once cultivated the biomass, the traditional well-known respirometric technique may be applied to study the biodegradation mechanisms and the corresponding kinetics. The main advantage of this system is the simplicity of the mathematical models used to fit the respirometric profiles. Moreover, the biomass growth yield can be experimentally calculated as well as the biomass concentration without matrix interferences since almost all the biomass is active bacteria. In chapters 5 to 8 this technique is applied under anoxic and aerobic conditions.

- *Heterogeneous respirometry*

The heterogeneous respirometry avoids the handling of the biofilm and its consequent destruction. This respirometric technique is performed in a mini-BTF which acts as a differential reactor. The concept is the same as the traditional respirometric technique, i.e. the characterization or monitoring of specific biomass activity; however, the colonized packing material is directly used without any pre-treatment. Obviously, it is also a destructive technique since the biomass concentration must be calculated after the test. The mathematical modeling associated to this technique is also complicated since additional considerations must be taken into account related with mass transfer phenomena besides many theoretical coefficients estimated. This technique is probably the most adequate to characterize SOB from desulfurizing BTF although further investigation is required to improve and standardize the technique. In chapter 9 this technique is applied under aerobic conditions.

Chapter 3

OBJECTIVES

3. OBJECTIVES

The general objective of this thesis was the characterization of S-oxidizing biomass obtained from desulfurizing biotrickling filters operated under anoxic and aerobic conditions.

Biomass concentration, biomass growth yield, stoichiometry and kinetic parameters are difficult to obtain when biomass grows attached to a packing material as a biofilm. For this reason respirometry was the main technique used to characterize the S-oxidizing biomass. The following specific objectives were proposed in order to apply this technique for each process and biomass studied:

- To develop different respirometric protocols to characterize thiosulfate, elemental sulfur and sulfide oxidation with S-oxidizing biomass obtained from aerobic and anoxic biotrickling filters, as suspended cultures or immobilized in the packing material.

- To elucidate the mechanisms involved in each of the processes studied in order to optimize the development of the corresponding kinetic models.

- To solve the stoichiometry associated to each biological reaction occurring in order to be used for the kinetic characterization.

- To characterize physical-chemical processes occurring during the biological process that could interfere in the activity monitoring (CO_2 stripping, H_2S stripping and chemical reactions).

- To propose specific kinetic expressions for each biomass characterized and conditions used (anoxic and aerobic conditions)

- To calibrate and validate the kinetic models proposed through the optimization of respirometric profiles experimentally obtained.

Chapter 4

GENERAL MATERIALS AND METHODS

4. GENERAL MATERIALS AND METHODS

4.1. DESCRIPTION OF EQUIPMENTS

The biomass used to characterize the oxidation of sulfide, thiosulfate and elemental sulfur performed in this thesis, both in aerobic and anoxic conditions, was cultivated as immobilized and suspended culture. The experimental setups used for each culture are detailed in the following sections.

4.1.1.   Biomass cultivation in continuous stirred tank reactors

Thiobacillus denitrificans pure culture and biomass obtained from different biogas desulfurizing BTFs were cultivated separately as suspended cultures in continuous stirred tank reactors (CSTR). The main elements constituting the cultivation setups were: CSTR, temperature and pH monitoring and control systems, feeding and purge pumps, flow meters and data acquisition and control software. The biomass was also cultivated using different substrates, as sulfide and thiosulfate, under aerobic and anoxic conditions. In the following sections the detailed information of each setup is presented.

- *Stirred Tank Reactors*

Three different stirred tank reactors were used in order to cultivate the biomass. In Table 4.1 the characteristics of each of the reactors are presented.

Table 4.1. Characteristics of the CSTRs used for suspended biomass cultivation

Reactor	Working volume	Construction materials		Agitation	Other characteristics
		Vessel	*Top cover*		
CSTR-1	1.3 L			Magnetic	-
CSTR-2	2.8 L	Glass	Stainless steel	Mechanic	Jacketed bottom
CSTR-3	5.0 L			Mechanic	Internal heat exchanger

- *Temperature, Oxygen and pH monitoring and control systems*

Temperature and pH were monitored and controlled continuously during biomass cultivation. For CSTR-1 and CSTR-2 both parameters were monitored through a pH

electrode with temperature probe integrated (SenTix 82, WTW, Germany) and in CSTR-2 an additional probe was also eventually used to monitor dissolve oxygen concentration (CellOx 325, WTW, Germany). Both, the electrode and the oxygen probe were connected to a bench top multimeter (Inolab Multi 740, WTW, Germany) for data monitoring. In both reactors the pH was controlled trough the automatic addition of diluted HCl and NaOH solutions with a dispensing burette (Multi-Burette 2S-D, Crison Instruments, Spain). The temperature was only controlled in CSTR-2 with an external circulating water bath (Ecoline StarEdition RE107 E100 Circulator, Lauda, USA). Regarding to CSTR-3, the temperature was also controlled with an external circulating water bath (MA Heating Immersion Circulator, Julabo, Germany). Analogously to CSTR-1 and CSTR-2, the pH was measured and controlled in CSTR-3 with a pH analyzer (pH analyzer AX400, ABB Group, Switzerland) connected to a peristaltic pump (Masterflex, Cole Parmer, The Netherlands) for HCl automatic addition.

- *Feeding and purge pumps*

Feeding of mineral medium and purge of CSTRs were performed by peristaltic pumps. For CSTR-1 and CSTR-2 the feeding of mineral medium and the purge of the reactor were performed continuously through a two-channel peristaltic pump (403U/VM2, Watson Marlow Pumps Group, UK). In the case of CSTR-3 a temporized peristaltic pump was used for all the liquid flows (Masterflex, Cole Parmer, The Netherlands).

- *Gas flow meters*

Nitrogen gas, Argon and Air were used for the reactors depending on the type of biomass cultivated. These gases were measured and controlled with glass gas flow meters GFMs (ABB Group (Switzerland) and Tecfluid (USA)).

- *Acquisition and control software*

Temperature, dissolved oxygen and pH data monitored from CSTR-1 and CSTR-2, as well as the volumes of acid and base added to control the pH, was acquired through Visual Basic or Lab Windows based software which was also in charge of acquiring data from the multimeter and controlling the pH. The summary and the schemes of each experimental setup are presented in Table 4.2 and Figure 4.1.

Table 4.2. Detailed description of the operating conditions used for biomass cultivation as suspended culture

Biomass cultivated	Setup	Origin	Operating conditions				Pumping systems			
			pH	T	Electron acceptor	Inlet gas	Substrate	Mineral medium	Sulfide[*]	Purge
Pure culture *Thiobacillus denitrificans*	CSTR-1	Culture ATCC 25259 (LGC stds, UK)	7.5	Room temperature 18–24 °C	Nitrate	N_2	$S_2O_3^{2-}$	Continuous	-	Continuous
Mixed culture	CSTR-2	Anoxic desulfurizing BTF	7.5	30 °C	Nitrate	N_2	$S_2O_3^{2-}$	Continuous	-	
	CSTR-2	Aerobic desulfurizing BTF	7.0	25 °C	Oxygen	Air	S^{2-}	Continuous	Temporized	
	CSTR-3	Anoxic desulfurizing BTF	7.5	30 °C	Nitrate	Ar	S^{2-}	Temporized	Temporized	Temporized

*for biomass cultivated with sulfide the mineral medium was fed separately from the substrate solution to avoid precipitated metallic sulfur salts

37
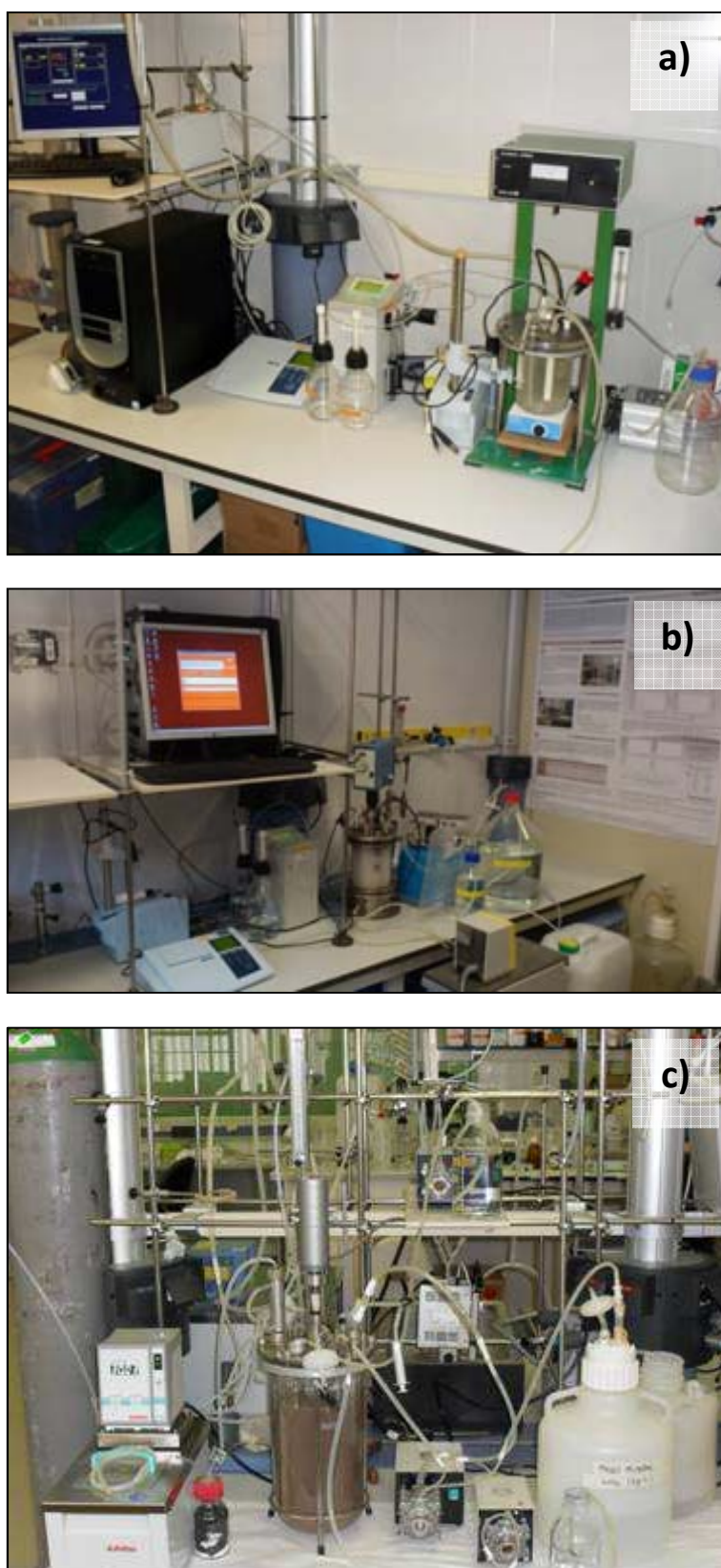
Figure 4.1. Schemes of the experimental setups to cultivate biomass in suspended conditions.
(a) CSTR-1 (b) CSTR-2 (c) CSTR-3

4.1.2. Immobilized biomass cultivation in biotrickling filters

SOB was also cultivated at room temperature in three conventional counter-currently operated BTF used for air desulfurization. In Figures 4.2 and 4.3, detailed information about the cultivation system is presented. Each BTF was randomly packed with different packing material: plastic pall ring (PR) (BTF-1), stainless steel PR (BTF-2a) and polyurethane foam (PUF) (BTF-2b). The volume packed of the main BTF (BTF-1) was 3.5 L while the remaining BTFs (BTF-2a and BTF-2b) had only a packed bed volume of 625 mL. The BTFs were connected through the liquid phase although each BTF had its own recirculation pump (DMI and DMX, Grundfos, Spain) to control the liquid trickling velocity. The pH was monitored on-line and controlled with an on/off control system based on the automatic addition of HCl and NaOH diluted solutions to the liquid in the reservoir of BTF-1.
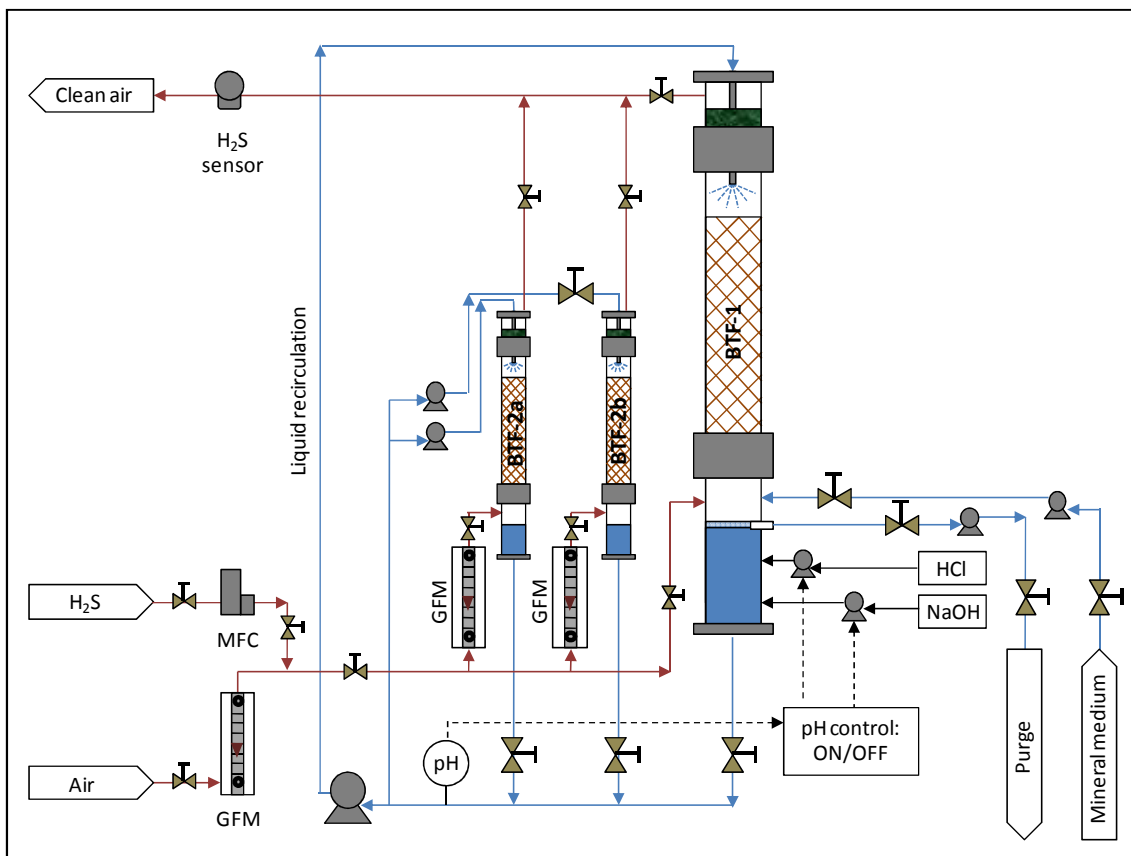
Figure 4.2. Schema of the desulfurizing BTF system

Figure 4.3. Image of the desulfurizing BTF system

The dry air flow was monitored and controlled with a glass GFM (Tecfluid, Spain) while the H_2S flow was controlled with a differential mass flow controller (MFC) (Low ΔP flow, Bronkhorst, The Netherlands). Both gas flows were mixed in the pipeline and, afterwards, the mixed flow was distributed to each BTF with different glass GFMs. By this way, the empty bed residence time and the sulfur load could be controlled for each BTF. Mineral medium was automatically pumped into the main BTF through a temporized peristaltic pump. The liquid level control system was based on overflow purge pumping.

4.1.3. Respirometric setups

The kinetic and stoichiometric characterizations of SOB were performed under anoxic and aerobic conditions with two different respirometric configurations as described in the subsequent sections.

- *Homogeneous respirometer*

The homogeneous respirometer was used when the biomass was previously suspended and cultivated in mineral medium. In Figure 4.4 the schema of the homogeneous respirometer is presented.
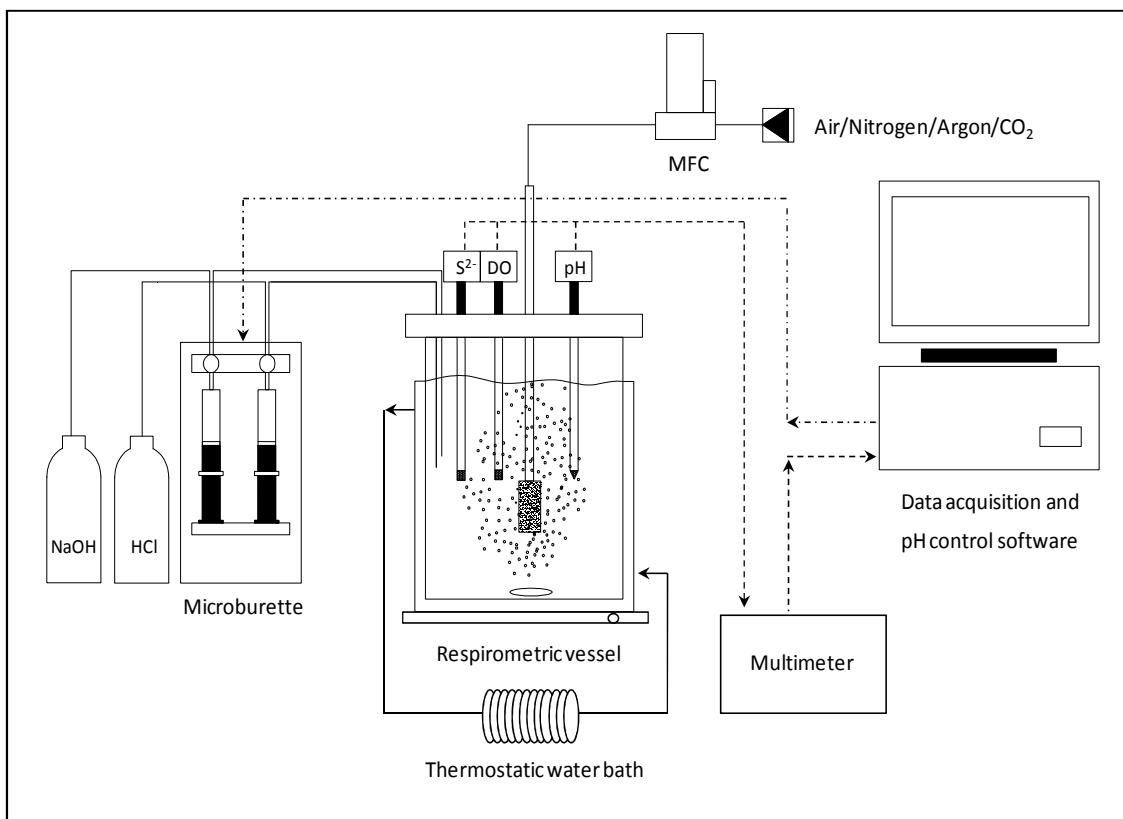
Figure 4.4. General schema of the homogeneous respirometer

The pH electrode, dissolved oxygen probe, multimeter, pH control system (control software and microburette) and MFC were the same as those specified in section 4.1.1. Dissolved sulfide concentration was eventually monitored with a sulfide ion-selective electrode (*see section 4.2.1 for detailed information about the electrode performance*). Temperature was controlled by means of a circulating thermostatic water bath (Polystat24, Fisher Scientific, Spain). Two different respirometric vessels were used depending on the kinetic study performed. In Table 4.3 further information about both vessels is detailed.

Table 4.3. Detailed characteristics of the respirometric vessels

Respirometric vessel	RV-1	RV-2
Working volume	350 mL	600 mL
Vessel material	Glass	Glass
Cover?	Stainless steel cover	No cover
Diffuser?	Stainless steel diffuser	No diffuser
Other characteristics	Jacketed vessel	Three orifices for probes and liquid phase sampling
Image		
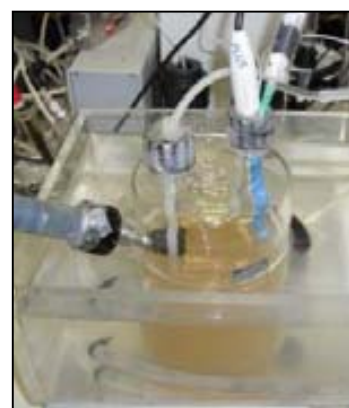
- *Heterogeneous respirometer*

The heterogeneous respirometer (HR) was used when the biomass was directly cultivated in BTF-2a and BTF-2b (Figure 4.2). In Figures 4.5 and 4.6 the schema and images of the HR are presented. The experimental system comprised a cylindrical BTF made on acrylic with 625 mL of packed bed. The main element of the HR was the differential reactor in which the cultivated packed bed obtained from the BTF was placed (Figure 4.6b). This bioreactor was operated in a counter-current mode. Therefore, the gas and liquid phases were continuously recycled with a gas compressor (gas pump 3112, Boxer, UK) and a peristaltic pump (Masterflex, Cole Parmer, The Netherlands), respectively. The pH electrode, dissolved oxygen probe, multimeter and pH control system (control software and burette) were the same as those specified in section 4.1.1. Oxygen concentration in air was measured in-line with an oxygen gas analyzer (SIDOR module OXOR-P, Sick, Germany). Dissolved oxygen concentration was also monitored in-line. Temperature was not controlled in this experimental setup.
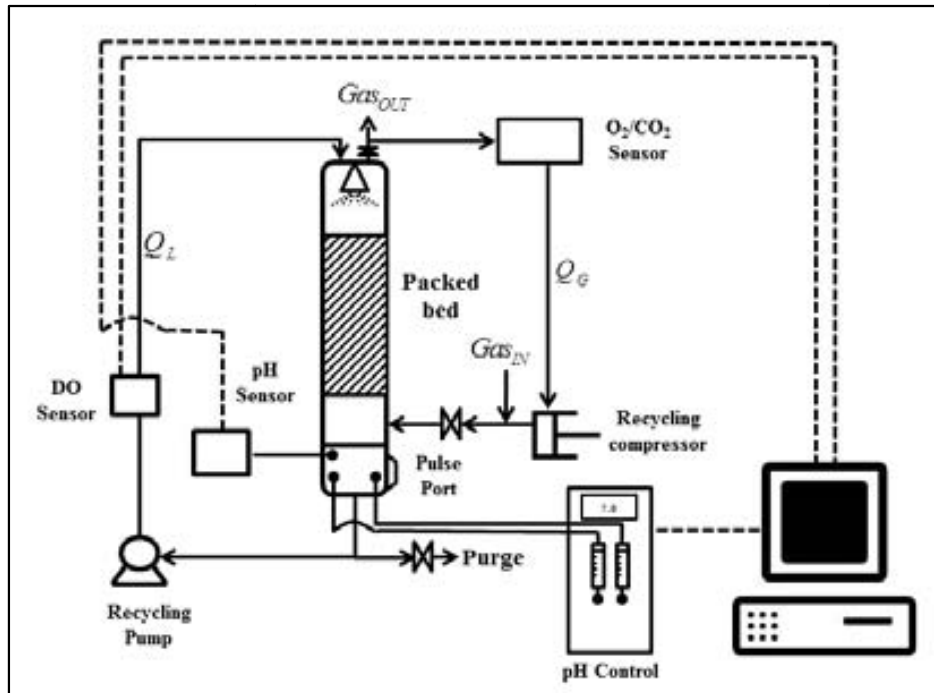
Figure 4.5. Schema of the heterogeneous respirometer.
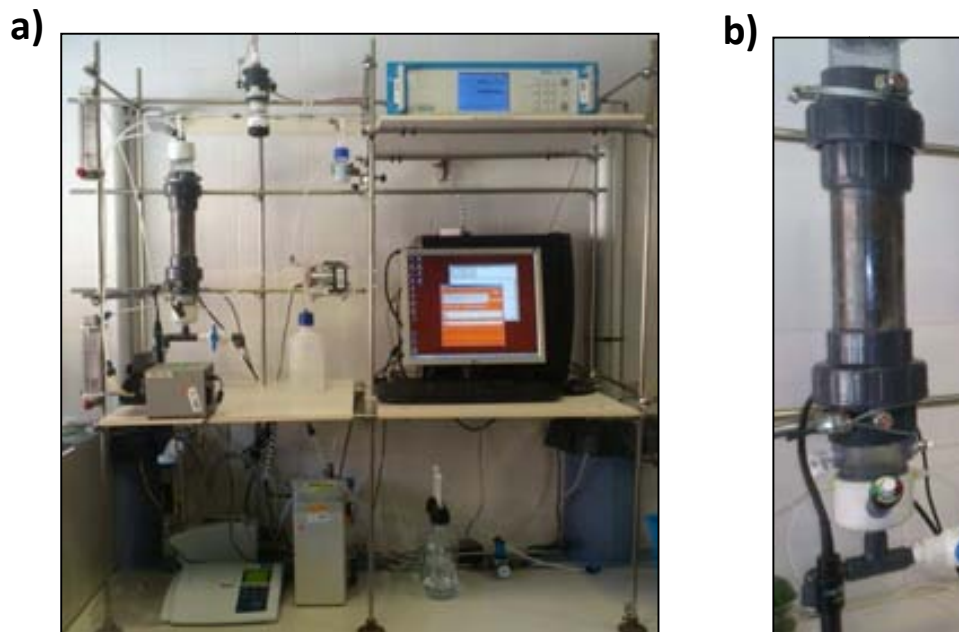
Figure 4.6. Images of the HR (a) Experimental setup (b) Differential reactor.

4.2. ANALYTICAL TECHNIQUES

4.2.1. Routine analysis and monitoring

Sampling of the liquid phase of all the reactors was required during the experimental periods in order to monitor the ionic compounds, inorganic carbon, dissolved sulfide and volatile suspended solids or optical density. These compounds were analyzed as follows:

- *Ionic compounds*

The liquid samples were filtered with a 0.22 µm cellulose filter previously to the analysis of the ionic compounds. Then, nitrite, sulfate, nitrate and thiosulfate concentrations were analyzed by ion chromatography with a suppressed conductivity detector using a Dionex ICS-2000 HPLC system with an IonPac AS18-HC column (4x250 mm - Dionex, USA).

- *Inorganic carbon*

Bicarbonate and CO_2 were used as SOB carbon source. By this way, dissolved inorganic carbon was analyzed in order to avoid carbon source limitation during all the experiments. For this analysis the sample was previously filtered with a 0.45 µm cellulose filter and then analyzed with an TIC/TOC Analyzer (Model 1020A, OI Analytical, USA) equipped with a non-dispersive infrared detector and a furnace maintained at 680 ºC.

- *Dissolved sulfide*

Dissolved sulfide was analyzed, both in the respirometric vessels and off-line, with a sulfide ion-selective electrode (VWR, USA). This electrode has its own internal reference electrode and presents a high sensitivity to S^{2-}. Thus, samples analyzed off-line must be buffered above pH 12 with an antioxidant buffer solution previously to the analysis to convert HS^- and H_2S to S^{2-}. The buffer solution contains ascorbic acid (acts as sulfide antioxidant) and EDTA (avoids interferences with metallic compounds) dissolved in NaOH (2M). This electrode also presents sensitivity and stability to HS^- in clean diluted matrices which allowed monitoring the stripping of sulfide in-situ during

abiotic tests. The electrode was connected to a bench top multimeter to monitor the concentration data (symphony, VWR, USA).

- *Volatile suspended solids (VSS)*

VSS were analyzed in order to calculate the biomass concentration, biomass growth yields and specific substrate uptake rates for the kinetic and stoichiometric characterization of SOB. Total suspended solids (TSS) and VSS were performed according to Standard Methods (APHA, 2005). By this way, an aliquot of liquid sample (V_s) was firstly filtered through a pre-weighed standard glass microfiber filter (W_1) of 0.7 µm (GF/F grade, Whatman, USA) and dried at a constant temperature of 105 ºC until constant weight. The increase of weight (W_2) represents the organic and inorganic matter in suspension in the sample. The relation between the weight increase (W_1-W_2) and the sample volume is the concentration of TSS. After this first step the sample is ignited at 550 ºC. The loss of weight represents the VSS content in the sample. The inorganic suspended material, or fixed suspended solids (FSS), is calculated from the difference between TSS and VSS.

In case of using *Thiobacillus denitrificans* the concentration of biomass was obtained from a correlation between the VSS and the optical density. Thus, a portion of culture sample was filtered through a 0.20 µm ashless cellulose pre-weighted filter (Merck Millipore, Merck, Germany) and dried at 105 ºC until constant weight. The following steps to obtain the VSS concentration were the same as explained above. The optical density of the remaining portion of culture sample was measured at 550 nm with a spectrometer. A linear correlation was calculated for VSS concentrations between 50 and 180 mg VSS L^{-1}.

4.2.2. Molecular biology analytical techniques

Molecular biology analytical techniques as DGGE (denaturing gradient gel electrophoresis) and 16S rRNA sequencing were also used to study biomass diversity preservation in two of the CSTR operations (*see Chapters 7 and 8*). In the following sections both techniques are briefly explained.

- *Denaturing gradient gel electrophoresis*

The protocol followed to separate the DNA of the biomass with a denaturing gradient gel electrophoresis was that reported in Fernandez et al. (2013). This methodology comprised basically three steps: DNA extraction from the biomass, DNA amplification and DGGE. In this thesis the sequencing of the separated DNA from DGGE was not performed since the comparison between the DNA profiles obtained from DGGE was enough to study the biomass diversity preservation. Hence, the complete DNA of the biomass was extracted using an UltraClean Soil DNA Isolation Kit (Mo Bio Laboratories Inc., USA) according to the manufacturer's instructions. The V3–V5 region of the bacterial 16S rRNA gene was PCR-amplified (amplified through polymerase chain reaction) using VELOCITY™ DNA Polymerase and primers GC-338F and 907R (Bioline, Spain). The 25 µL reaction mixtures contained 5 µL of 5X Hi-Fi Reaction Buffer (Bioline, Spain), 0.5 µL of each primer (10 µM), 2.5 µL of 10 mM dNTP mix, 2 µL of DNA, 0.75 µL of DMSO and 0.125 µL of 2 U/µL VELOCITY™ DNA polymerase® (Bioline, Spain) in 13.625 µL of DNase- and RNase-free sterilised water (Promega®, Spain). The PCR products were analyzed by electrophoresis on 1% agarose gels in 0.5X TBE buffer (100 mM Tris, 90 mM boric acid, 0.001 mM EDTA) stained with SYBR® Gold nucleic acid gel stain (Bioline, Spain) to confirm the product size and estimate the DNA concentration.

The PCR products were evaluated with DGGE using the Dcode™ Universal Mutation Detection System (BioRad, USA). The DNA samples were loaded onto 8% (w/v) polyacrylamide gels and run in 1X TAE (40 mM Tris, pH 8.0, 20 mM acetic acid, 1 mM EDTA). The polyacrylamide gels were made with a denaturing gradient from 30% to 60% (where 100% denaturant contained 7 M urea and 40% formamide). Electrophoresis was performed at 60 °C and 75 V for 17 h. After electrophoresis, the gel was stained with SYBR® Gold nucleic acid gel stain (Bioline, Spain) according to the manufacturer's instructions.

- *16S rRNA sequencing*

The 16S rRNA sequencing was performed following the methodology described in Montebello et al. (2013). The analysis comprised basically four steps: DNA extraction, DNA amplification, single strand DNA obtainment and pyrosequencing of

the genetic material. Hence, for the extraction, PowerSoil DNA Isolation Kits were used (Mo Bio Laboratories, USA) according to the manufacturer instructions. The quality and concentration of extracted DNA were checked in 2 μL of each DNA elution by spectrometry at a wavelength of 260–280 nm in a Nanodrop (Thermo Fisher Scientific, USA). A 260/280 nm ratio of 1.8 was used as quality cut-off. Then, concentrations were normalized to 20 ng μL^{-1}.

Afterwards, bacterial Tag-encoded FLX Amplicon Pyrosequencing (bTEFAP) was selected as the sequencing approach. DNA was amplified previously to the pyrosequencing procedure using a forward and reverse fusion primer (Section SM-2). Amplifications were performed in 25 μL reaction volumes with Qiagen HotStar Taq master mix (Qiagen, USA), 1 μL of each 5 μM primer, and 1 μL of template. Reactions were performed on ABI Veriti thermocyclers (Applied Biosytems, USA) under the following conditions: 95 °C for 5 min, followed by 35 cycles of 94 °C for 30 s; 54 °C for 40 s and 72 °C for 1 min, followed by one cycle of final elongation at 72 °C for 10 min.

Amplification products were visualized with gels (Life Technologies, USA). Products were then pooled equimolarly and each pool was cleaned with Diffinity RapidTip (Diffinity Genomics, USA), and size selected using Agencourt AMPure XP (BeckmanCoulter, USA) following Roche 454 protocols (454 Life Sciences, USA). Size selected pools were then quantified and 150 ng of DNA were hybridized to Dynabeads M-270 (Life Technologies, USA) to create single stranded DNA according to Roche 454 protocols. Single stranded DNA was diluted and used in PCR reactions, which were performed and subsequently enriched. Sequencing was performed on a FLX + 454 Roche platform at Research and Testing Laboratory (RTL) (Texas, USA) according to RTL protocols (RTL, 2012). Also, quality of data obtained from sequencing was evaluated and denoised and chimeras were removed from the data set at RTL.

Chapter 5

DEVELOPMENT OF AN ANOXIC RESPIROMETRIC TECHNIQUE TO CHARACTERIZE SO-NR MIXED CULTURES OBTAINED FROM DESULFURIZING BIOTRICKLING FILTERS

5. DEVELOPMENT OF AN ANOXIC RESPIROMETRIC TECHNIQUE TO CHARACTERIZE SO-NR MIXED CULTURES OBTAINED FROM DESULFURIZING BIOTRICKLING FILTERS

The main motivation of this chapter was to define a procedure for the characterization of biomass obtained from BTFs, which are the reactors most commonly operated in our research group. Since in this reactors the biomass grows attached to a packing material, the determination of kinetic parameters, stoichiometric coefficients and biomass growth yields are difficult to be obtained without the influence of other physical-chemical processes. The first approach was the development of an anoxic respirometric protocol for SO-NR characterization, which was performed with thiosulfate to simplify the protocol definition. Then, this protocol was used in this chapter and in the following chapters in order to obtain the kinetic and stoichiometric characterization of different SOB using many substrates.

Abstract

In this chapter an anoxic respirometric procedure was defined and applied to characterize a SO-NR culture obtained from an anoxic biogas desulfurizing BTF treating high loads of H_2S. Immobilized biomass extracted from the BTF was grown as a suspended culture with thiosulfate as electron donor to obtain the biomass growth yield and the consumed $S_2O_3^{2-}$-S/NO_3^--N ratio. Afterwards, respirometry was applied to describe thiosulfate oxidation under anoxic conditions. A pure culture of *Thiobacillus denitrificans* was also used as a control culture in order to validate the procedure proposed in this work to characterize the SO-NR biomass. Respirometric profiles obtained with this microbial culture showed that nitrite was formed as intermediate during nitrate reduction and revealed that no competitive inhibition appeared when both electron acceptors were present in the medium. Although final bioreaction products depended on the initial $S_2O_3^{2-}$-S/NO_3^--N ratio, such ratio did not affect thiosulfate oxidation or denitrification rates. Moreover, respirometric profiles showed that the specific nitrite uptake rate depended on the biomass characteristics being that of a SO-NR mixed culture (39.8 mg N g^{-1} VSS h^{-1}) higher than that obtained from a pure culture of *T. denitrificans* (19.7 mg N g^{-1} VSS h^{-1}).

A modified version of this chapter has been published as:

Mora, M., Guisasola, A., Gamisans, X., Gabriel, D., 2014c. Examining thiosulfate-driven autotrophic denitrification through respirometry. *Chemosphere* 113, 1-8.

5.1. INTRODUCTION

Aerobic respirometry has been reported as a proper, reliable technique for the characterization of suspended and immobilized S-oxidizing cultures (Gonzalez-Sanchez et al., 2009; Munz et al., 2009). On the contrary, anoxic respirometry has not been extensively applied and even less to characterize SO-NR cultures obtained from anoxic desulfurizing BTFs although it could provide essential information to gain insight in the mechanisms, biomass growth yield and stoichiometry of the reactions involved, thus allowing the performance optimization of desulfurizing BTFs (Mora et al., 2014a). Moreover, describing the biological oxidation of reduced sulfur compounds (such as thiosulfate, sulfide or elemental sulfur) under anoxic conditions can be complex since it involves several steps and the potential use of different electron acceptors (nitrate, nitrite). Nonetheless, these processes are often simplified considering complete nitrate-based denitrification and neglecting biomass growth (Eqs. 5.1 to 5.3).

$$S_2O_3^{2-} + 1.6NO_3^- + 0.2H_2O \quad \rightarrow \quad 2SO_4^{2-} + 0.8N_2 + 0.4H^+ \qquad (5.1)$$

$$\triangle G^0 = \text{-766 kJ mol}^{-1}$$

$$S^{2-} + 1.6NO_3^- + 1.6H^+ \quad \rightarrow \quad SO_4^{2-} + 0.8N_2 + 0.8H_2O \qquad (5.2)$$

$$\triangle G^0 = \text{-744 kJ mol}^{-1}$$

$$S^0 + 1.2NO_3^- + 0.4H_2O \quad \rightarrow \quad SO_4^{2-} + 0.6N_2 + 0.8H^+ \qquad (5.3)$$

$$\triangle G^0 = \text{-548 kJ mol}^{-1}$$

From the stated above, the aim of this chapter was to setup a procedure to characterize SO-NR microbial populations, obtained from an anoxic desulfurizing BTF, through anoxic respirometry. Thiosulfate was used as electron donor due to its easier manipulation and for being already proved to be interchangeable with H_2S in studies performed with chemolithotrophic bacteria (Stefess et al., 1996). Moreover, two different cultures (pure and mixed) were compared not only to elucidate the denitrification mechanisms between them but also to validate the procedure proposed.

On the one hand, a pure culture of *Thiobacillus denitrificans,* which is an autotrophic, facultative anaerobic bacterium capable of oxidizing several reduced sulfur compounds (e.g. sulfide or thiosulfate), was used. This microorganism was selected since it is typically found in microbial consortia of conventional BTFs, treating high loads of H_2S, under anoxic (Soreanu et al., 2008) or aerobic (Maestre et al., 2010) conditions. Also, *T. denitrificans* has been previously studied by other authors (Syed et al., 2006) being adequate to be used as a control culture. On the other hand, a SO-NR mixed culture, obtained from a pilot anoxic BTF (Montebello et al., 2012) was also used to assure the suitability of the procedure to obtain biological activities as well as growth yields. Finally, it must be pointed out that this study has also an interesting applicability on thiosulfate removal from coke oven wastewaters as well as on denitrification processes used in industrial or urban wastewater treatment plants.

5.2. MATERIALS AND METHODS

5.2.1. SO-NR biomass cultivation

Two continuous stirred tank reactors (CSTR-1 and CSTR-2, *see section 4.1.1 for detailed information*) were used to maintain the SO-NR pure and mixed cultures, under operating conditions similar to those reported as optimal (Justin and Kelly, 1978). The first reactor (CSTR-1) was inoculated with a pure culture of *T. denitrificans* (culture code 25259[TM] from ATCC, LGC standards, UK). The strain was incubated in a closed shaker, at 30 ºC, an initial pH of 7.5 and using the selective nutrient solution provided with the culture (450 T2 ATCC medium for *Thiobacillus*). Prior to inoculation, the reactor was filled with the nutrient solution and gassed with nitrogen until complete oxygen stripping. After that, the reactor was inoculated with 200 mL of the pre-culture on its exponential growth phase. The start-up of CSTR-1 consisted of a batch operation to reach the maximum biomass concentration and the entire depletion of substrate. This stage was followed by a continuous operation mode without biomass recirculation. The selective nutrient solution was pumped into the system at 0.75 mL min⁻¹. Thus, a dilution rate of 0.035 h⁻¹ was set to avoid the washout of the reactor since the maximum specific growth rate (μ_{max}) reported for these bacteria is in the range of 0.05 to 0.11 h⁻¹ (Justin and Kelly, 1978; Claus and Kutzner, 1985; Oh et al., 2000). Inlet concentrations

of substrate and electron acceptor were slightly modified from the selective nutrient solution and set at 1.5 g $S_2O_3^{2-}$-S L^{-1} and 0.5 g NO_3^--N L^{-1}, respectively. A constant nitrogen gas flow of 100 mL min^{-1} was continuously supplied to maintain anoxic conditions. The N_2 diffuser was located in the headspace of the reactor to minimize CO_2 stripping (periodic inorganic carbon monitoring confirmed the absence of carbon limitations).

The second reactor (CSTR-2) was inoculated with a mixed culture collected from a lab-scale BTF treating sulfide containing biogas under anoxic conditions (Montebello et al., 2012). The BTF was packed with open-pore PUF cubes of 8 cm^3 as packing material (Filtren TM25450, Recticel Iberica, Spain). The BTF was run for several months under steady-state conditions at neutral pH and at an empty bed residence time (EBRT) of 163 s treating biogas containing around 2000 ppm_v of H_2S (63.2 g H_2S-S m^{-3} h^{-1}). The inoculation procedure of the CSTR-2 was similar to that employed in CSTR-1. The reactor was filled with nutrient solution and gassed with nitrogen gas. The composition of the nutrient solution was the same as that used in the BTF (ATCC-1255 *Thiomicrospira denitrificans* medium) but using sodium thiosulfate as substrate, sodium bicarbonate as carbon source and a higher concentration of nitrate: $Na_2S_2O_3 \cdot 5H_2O$ (6.0 g L^{-1}), $NaHCO_3$ (2.0 g L^{-1}), KNO_3 (3.0 g L^{-1}). The inoculum was obtained by sonication of the packing material in a water bath (Branson 3510 ultrasonic cleaner, Emerson Electric, USA) at 20 ºC. Afterwards, it was transferred to the reactor and started the continuous operation. Prior incubation of the mixed culture was not necessary since the amount of biomass obtained from the packing material as well as the cellular residence time were high enough to avoid the entire washout of the biomass (1.56 g VSS L^{-1} and 55.6 h, respectively). The nitrogen gas flow used in CSTR-2 was 2 times higher than that used in CSTR-1 (200 mL min^{-1}) to keep the DO concentration under 0.2 mg L^{-1}. These conditions were set since have been reported as optimal for SO-NR biomass growth (Fajardo et al., 2014a) to avoid the loss of microbial diversity. The operation of CSTR-2 was divided in two periods. During the first period (20 weeks) the operating conditions were set as explained above. However, during the second period (2 weeks), the biomass was acclimated to nitrite by stepwise decreasing the hydraulic retention time (HRT) to 35% of its initial value, which resulted in a maximum nitrite concentration of 150 mg NO_2^--N L^{-1}.

Biomass and ionic species concentrations were daily monitored off-line, both in the reactors and in the feeding bottles, during the whole operation. The biomass growth yield ($Y_{x/s}$) for both cultures was calculated at the steady-state of both CSTR-1 and CSTR-2 according to Eq. 5.4 for each CSTR.

$$Y_{x/s} = \frac{[VSS]_{out} - [VSS]_{in}}{[S_2O_3{}^{2-}-S]_{in} - [S_2O_3{}^{2-}-S]_{out}} \qquad (5.4)$$

Where VSS_{out} and VSS_{in} are the biomass concentration (mg VSS L^{-1}) at the outlet an inlet flows of the reactor, respectively, and $S_2O_3{}^{2-}$-S_{in} and $S_2O_3{}^{2-}$-S_{out} is the thiosulfate concentration (mg $S_2O_3{}^{2-}$-S L^{-1}) at the outlet and inlet flows of the reactor, respectively.

5.2.2. Respirometric methodology development

Respirometric tests were performed with both pure and mixed cultures and thiosulfate as the electron donor. Detailed information about the respirometric setup used in this chapter is presented in section 4.1.3. Respirometric tests were carried out in RV-1. Prior to each test, biomass was collected from either CSTR-1 or CSTR-2, centrifuged at 6500 rpm and resuspended in substrate-free mineral medium. The mineral medium composition was (g L^{-1}): NO_3^--N or NO_2^--N (0.01), NH_4Cl (0.40), KH_2PO_4 (2.00), $MgSO_4 \cdot 7H_2O$ (0.40), trace metal solution (1.0 mL L^{-1} TMS for *T. denitrificans* culture or 2.0 mL L^{-1} of SL-4 for mixed culture) and adjusted to pH 7.5 with NaOH (2 M).

Once the biomass was washed and poured into the respirometer, the liquid and gas phases were gassed with N_2 to remove oxygen. After that, a pulse of a $NaHCO_3$ concentrated solution was added to obtain an initial inorganic carbon concentration of 50 mg C L^{-1}. This concentration was high enough to avoid carbon source limitation during the tests as verified with inorganic carbon analysis. The N_2 gas flow was set at 20 mL min^{-1} since previous abiotic tests showed that this flow prevented DO concentration from increasing over 0.1 mg L^{-1} in the respirometer. The N_2 flow was only introduced in the headspace of the respirometer to minimize CO_2 stripping. In each

respirometric test no substrate was added during the first 2 h inducing the biomass to an endogenous phase where the endogenous specific nitrogen uptake rate was calculated. The nitrogenous compound (nitrate/nitrite) employed as electron acceptor during the endogenous phase was the same as that used in each test.

Then, the respirometer was spiked with substrate obtaining concentrations ranging between 5 and 10 mg $S_2O_3^{2-}$-S L^{-1}. This method was applied as a "wake up" process to activate biomass enzymatic mechanisms and, therefore, to properly assess biodegradation rates in subsequent tests (Vanrolleghem et al., 1999). Respirometric tests were conducted after this minimum amount of thiosulfate was consumed.

5.2.3. Experimental tests

Table 5.1 summarizes the set of respirometric tests conducted to study the influence of the initial thiosulfate, nitrate and nitrite concentrations as well as initial $S_2O_3^{2-}$-S/NO_3^--N ratios on the biological activity. Different pulses of thiosulfate, nitrate and nitrite concentrated solutions were added to the respirometer to meet the desired ratios (in the range of 20 to 300 mg $S_2O_3^{2-}$-S L^{-1}, 0 to 60 mg NO_3^--N L^{-1} and 0 to 30 mg NO_2^--N L^{-1}, respectively). The respirometer was sampled between 10 and 100 min, depending on the time course of each test. Nitrite profiles were analyzed since its accumulation during autotrophic or heterotrophic denitrification has brought in different theories (Betlach and Tiedje, 1981; Glass and Silverstein, 1998). Maximum specific denitrification rates were calculated from the slopes of the respirometric profiles for each of the nitrogen compounds involved. Respirometric tests were conducted at different $S_2O_3^{2-}$-S/NO_3^--N ratios to study the influence of thiosulfate or nitrate limitations over nitrite production and oxidation activities.

A respirometer can be considered as a sensor and triplicates of respirometric tests were not needed (Spanjers et al., 1996). However, deviations could be assessed in terms of the standard deviation of samples analysis if required, considering 5 and 10% for ionic chromatography and VSS analysis, respectively. Such deviations were later considered to assess all rates from respirometric profiles and to analyze the S recovery in sulfur mass balances.

Table 5.1. Respirometric tests conducted with pure and mixed SO-NR cultures

Biomass	Set-Test	Acclimated to nitrite?	VSS (mg L^{-1})	Nitrite (mg N L^{-1})	Nitrate (mg N L^{-1})	Thiosulfate (mg S L^{-1})	S$_2$O$_3^{2-}$-S/NO$_3^-$-N
Pure culture	A-1	No	139	0	18	52	2.9
	A-2		186	0	16	21	1.3
	A-3		146	24	29	85	2.9
	A-4			13	17	25	1.5
Mixed culture	B-1	No	253	30	0	297	--
	B-2		193	0	60	188	3.1
	B-3 (I)	Yes	253	24	12	268	22
	B-3 (II)			20	0	211	--

5.3. RESULTS AND DISCUSSION

5.3.1.   Biomass growth yield calculation

The start up of CSTR-1 through a batch operation mode lasted 42 h and presented a lag period of 15 h (Figure 5.1). At time 120 h, a certain amount of mineral medium was added to adjust the reaction volume. During this phase, biomass concentration increased up to 200 mg VSS L^{-1}. Nitrite accumulation was not observed during the start-up of the CSTR-1. Subsequently to the batch operation, CSTR-1 was operated for 7 weeks.
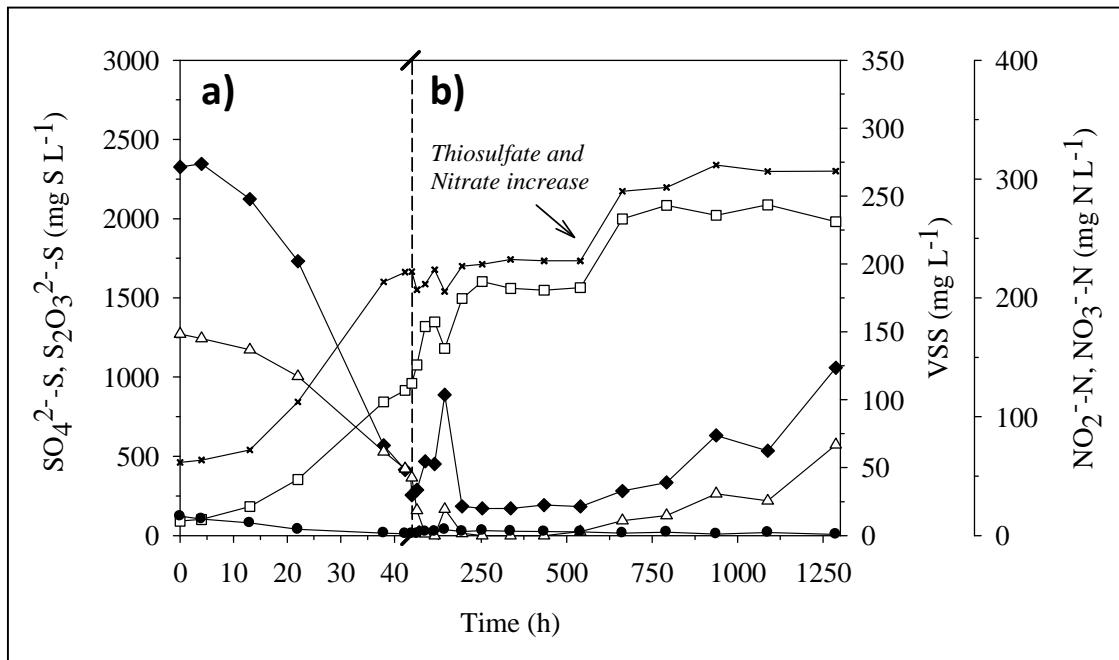
Figure 5.1. Start-up and continuous operation of the CSTR-1. (a) Batch operation mode (b) Continuous operation mode. Symbols: Thiosulfate (△), Sulfate (□), Nitrate (◆), Nitrite (●) and Biomass (✕).

The $Y_{x/s}$ was calculated using mass balances either from the exponential growth phase of the batch operation (Figure 5.1a) or from the continuous operation (Figure 5.1b between 200 and 500 h). The average value obtained was $Y_{x/s}$=0.16±0.02 g VSS g^{-1} $S_2O_3^{2-}$-S. The ratio $S_2O_3^{2-}$-S/NO_3^--N consumed was 3.23±0.10 g $S_2O_3^{2-}$-S g^{-1} NO_3^--N. After 500 h of operation, influent thiosulfate and nitrate concentrations were increased

by 60% which led to a production rate of 80 ± 3 g SO_4^{2-}-S m^{-3} h^{-1} and to a biomass concentration of 270 ± 3 mg VSS L^{-1}. Thiosulfate was accumulated during this period indicating that the maximum specific thiosulfate uptake rate was achieved.

CSTR-2 was operated for 22 weeks similarly to CSTR-1. The dilution factor applied was 0.018 h^{-1} to minimize the selectivity of the cultures according to their μ_{max}. The $Y_{x/s}$ and the $S_2O_3^{2-}$-S/NO_3^--N consumed ratio, prior to the culture acclimation to nitrite, were 0.18 ± 0.04 g VSS g^{-1} $S_2O_3^{2-}$-S and 3.73 ± 0.14 g $S_2O_3^{2-}$-S g^{-1} NO_3^--N, respectively. The latter was in agreement with those obtained by Campos et al. (2008) and Oh et al. (2000) with mixed cultures (3.82 g $S_2O_3^{2-}$-S g^{-1} NO_3^--N and 3.72 g $S_2O_3^{2-}$-S g^{-1} NO_3^--N, respectively). Interestingly, it was also observed that the $Y_{x/s}$ obtained from the culture acclimated to nitrite was the same as that obtained prior to the culture acclimation (0.18 ± 0.01 g VSS g^{-1} $S_2O_3^{2-}$-S), which confirms that acclimation of the microbial cultures did not influence the stoichiometry of the process.

The experimental $S_2O_3^{2-}$-S/NO_3^--N ratios obtained in both reactors were slightly higher than the stoichiometric value (2.86 g $S_2O_3^{2-}$-S g^{-1} NO_3^--N) from Eq. 5.1 because the fraction of electrons devoted to growth is neglected in Eq. 5.1. Fixation of CO_2 for bacterial growth implies the use of reducing equivalents from thiosulfate leading to higher $S_2O_3^{2-}$-S/NO_3^--N ratios (Timmertenhoor, 1981). This result indicates that the theoretical $S_2O_3^{2-}$-S/NO_3^--N ratio should include biomass growth to avoid the underestimation of μ_{max} from the modeling of respirometric data.

5.3.2. *Thiobacillus denitrificans* **pure culture**

Several thiosulfate concentrations and $S_2O_3^{2-}$-S/NO_3^--N ratios were tested to study the activity of *T. denitrificans* using the respirometric methodology proposed in this chapter. The specific uptake rates of thiosulfate (STUR), nitrate (SNUR) and nitrite (SNitUR) were calculated (Table 5.2) as well as the ratio between SNitUR and SNUR (α) using the respirometric profiles (Figure 5.2). Prior to each test, the endogenous specific activity was measured as 1.78 ± 0.09 mg NO_3^--N g^{-1} VSS h^{-1} which represented less than 5% of the exogenous biological activity.

Nitrite was formed as an intermediate of nitrate reduction. Several hypotheses with a high disparity about nitrite accumulation in denitrification systems have been proposed: i) delay in the induction of nitrite-reducing enzymes in the presence of nitrate,

ii) low specific utilization rate of nitrite compared to nitrate, iii) presence of a low concentration of nitrate, or iv) the S/N ratio (Krishnakumar and Manilal, 1999; Yamamoto-Ikemoto et al., 2000; Campos et al., 2008). Moreover, although nitrite-driven anoxic thiosulfate oxidation has been reported, the process stoichiometry is still usually described considering only a single-step process (Claus and Kutzner, 1985; Oh et al., 2000; Campos et al., 2008). This simplification does not describe the observed experimental nitrite profiles found herein.

Table 5.2. Specific biological activities obtained from respirometric tests

Tests	$r_{thiosulfate}$	$r_{sulfate}$	$r_{nitrate}$	$r_{nitrite}$	α	Sulfur Balance	
						$S_2O_3^{2-}$-S	SO_4^{2-}-S
	(mg S g^{-1} VSS h^{-1})		(mg N g^{-1} VSS h^{-1})			(mg S L^{-1})	
A-1	-290	302	-121	-54	0.45	52	55
A-2	-132	145	-45	-20	0.43	21	22
A-3	-153	162	-82	-19	0.23	52	50
A-4	-121	115	-63	-10	0.31	25	27
B-1	-84	85	0	-40	--	62	59
B-2	-222	199	-58	-46	0.80	188	182
B-3 (I)	-258	275	-53	-62	1.17	36	40
B-3 (II)	-137	129	0	-64	--	46	43

The experimental respirometric profiles (Figure 5.2) suggested that the initial nitrate concentration and $S_2O_3^{2-}$-S/NO_3^--N ratio were critical when predicting the final products of thiosulfate biodegradation. As an example, Figure 5.2b shows that nitrite was not depleted because thiosulfate limited the process. In this case, the initial $S_2O_3^{2-}$-S/NO_3^--N ratio (1.28 g $S_2O_3^{2-}$-S g^{-1} NO_3^--N) resulted in an incomplete denitritation. On the other hand, Figure 5.2a shows that nitrate and thiosulfate were completely depleted as well as most of the nitrite produced was consumed when the initial $S_2O_3^{2-}$-S/NO_3^--N ratio was 2.9 g $S_2O_3^{2-}$-S g^{-1} NO_3-N. In this case, a temporary nitrite accumulation up to 10 mg N-NO_2^- L^{-1} did not produce any inhibitory effect since a similar α was found in test A-1 and A-2 (Table 5.2). Moreover, a 2.4-fold higher thiosulfate oxidation rate was obtained at thiosulfate concentrations over 50 mg $S_2O_3^{2-}$-S L^{-1} indicating that STUR were positively affected by the substrate concentration.
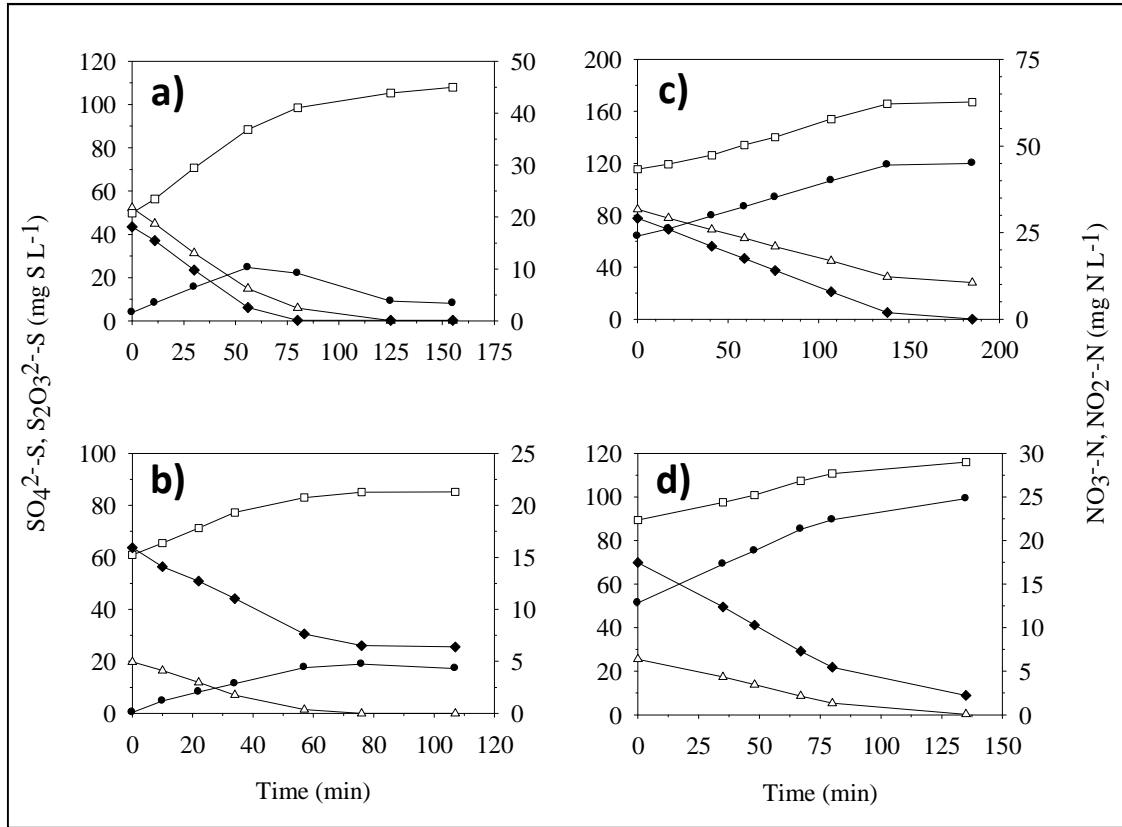
Figure 5.2. Respirometric profiles obtained from thiosulfate oxidation with a pure culture of *T. denitrificans*. (a) Test A-1 (b) Test A-2 (c) Test A-3 (d) Test A-4. Symbols: Thiosulfate ($\triangle$), Sulfate ($\square$), Nitrate ($\blacklozenge$), Nitrite ($\bullet$).

In test A-3 (Figure 5.2c) a high initial nitrite concentration of about 25 mg NO_2^--N L^{-1} (corresponding to $6.61 \cdot 10^{-3}$ mg HNO_2 L^{-1} at pH = 7.5) was used. Nitrite concentrations up to 45 mg NO_2^--N L^{-1} were reached in this test. Figure 5.2c shows that denitrification inhibition by nitrite occurred since the STUR decreased almost a 50% with respect to test A-1. In addition, as shown in Table 5.2, SNitUR was lower than that obtained in the other cases, indicating that denitritation was also affected by the nitrite presence. Likewise, Figure 5.2d shows a similar behavior in terms of nitrite inhibition in test A-4 confirming that nitrite inhibition was produced over both denitritation and denitratation processes. It was found that STUR was not affected by substrate limitations at concentrations over 20 mg $S_2O_3^{2-}$-S L^{-1}, which was slightly lower than the half-saturation constant value obtained by Artiga et al. (2005) (32 mg $S_2O_3^{2-}$-S L^{-1}) with a SO-NR mixed culture. Finally, taking into account the standard deviation of experimental data, sulfur mass balance deviations below 7% (Table 5.2) in all

experiments showed that production of elemental sulfur under these conditions was negligible since thiosulfate degradation was in agreement with sulfate production.

5.3.3 SO-NR mixed culture

Three respirometric tests were conducted with the mixed culture (B-1, B-2 and B-3) (Figure 5.3) and several specific activities were calculated (Table 5.2). In all the cases, the initial thiosulfate concentration was high enough to avoid substrate limiting conditions. Moreover, test B-3 was performed once the SO-NR mixed culture was acclimated to nitrite.

Test B-1 (Figure 5.3a) performed with the non-acclimated biomass to nitrite and with nitrite as electron acceptor presented a SNitUR of 39.8 ± 2.0 mg NO_2^--N g^{-1} VSS h^{-1} at an initial nitrite concentration of 30 mg NO_2^--N L^{-1}. Such SNitUR was 2-fold that obtained with the pure culture of *T. denitrificans* (Test A-3), in which the initial nitrite concentration was 24 mg NO_2^--N L^{-1}. The presence of more active nitrite-reducing bacteria in the mixed culture, an inhibition by nitrite or a highest concentration of thiosulfate lead to such different SNitUR. Moreover, this mixed culture presented high nitrite affinity since the change of the nitrite reduction rate only occurred at a concentration of about 0.5 mg NO_2^--N L^{-1}. The $S_2O_3^{2-}$-S/NO_2^--N ratio consumed during the test was 2.17 g $S_2O_3^{2-}$-S g^{-1} NO_2^--N.

Test B-2 (Figure 5.3b) was conducted with nitrate as electron acceptor. As shown in Table 5.2, SNitUR was very similar to that obtained in experiment B-1 which means, on the one hand, that there was no competitive inhibition when nitrate was present in the medium and, on the other hand, that nitrite concentrations up to 30 mg NO_2^--N L^{-1} did not produce inhibition by nitrite. This result slightly differed from that obtained with the pure culture. As shown in Table 5.2, tests A-3 and A-4 demonstrate that nitrite negatively affected denitritation at concentrations over 10 mg NO_2^--N L^{-1}. Probably, a larger microbial diversity of the mixed culture as well as the exposure of the mixed culture to certain nitrite peaks in the BTF produced a higher nitrite tolerance. In addition, SNUR and STUR were lower than those obtained with the pure culture indicating that the mixed culture had a lower thiosulfate oxidation capacity than the pure culture. However, this fact allowed nitrite not being accumulated to inhibitory

concentrations during the test. Artiga et al. (2005) obtained a similar SNUR of 51.04 ± 9.24 mg NO_3^--N g^{-1} VSS h^{-1} using thiosulfate oxidizing denitrifying sludge.
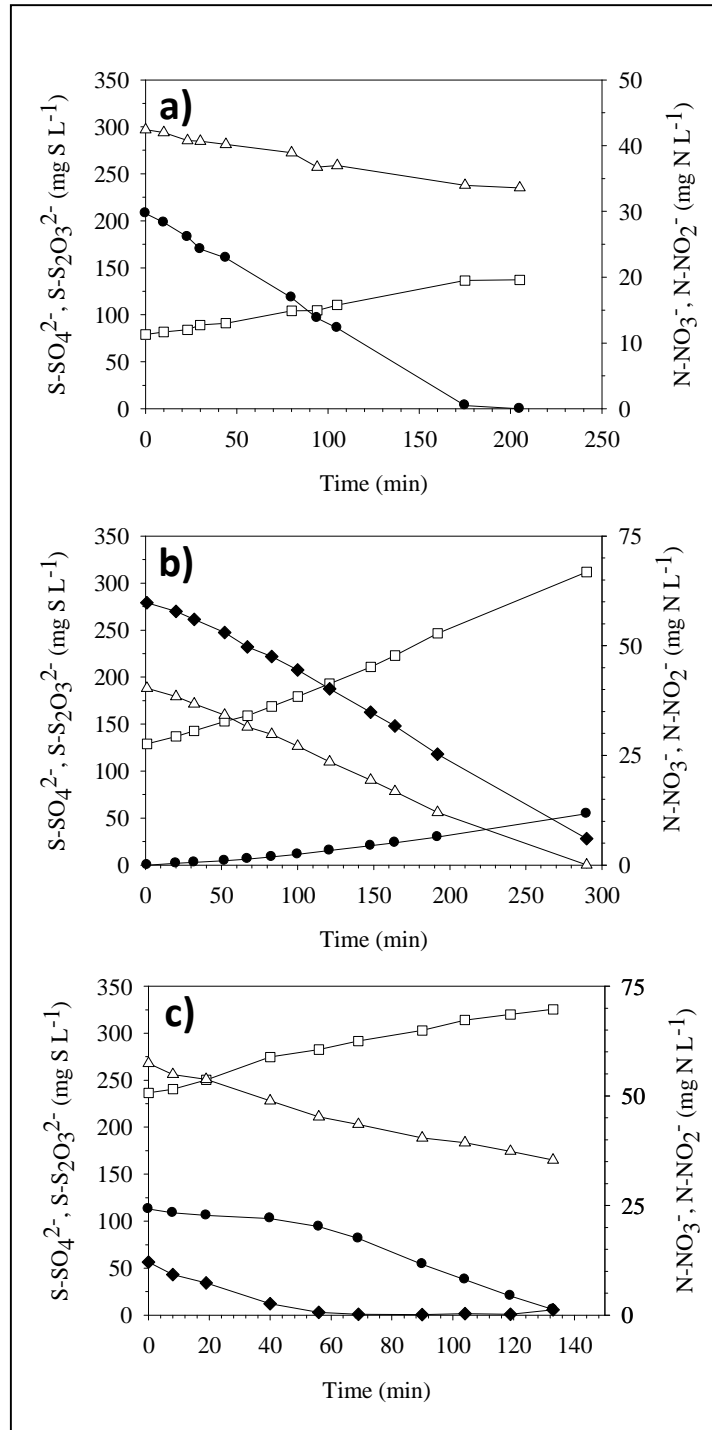
Figure 5.3. Respirometric tests performed with the SO-NR mixed culture. (a) Test B-1 (b) Test B-2 (c) Test B-3 divided in two stages: B-3 (I) (t<60 min) and B-3 (II) (t>60 min). Symbols: Thiosulfate ($\triangle$), Sulfate ($\square$), Nitrate ($\blacklozenge$), Nitrite ($\bullet$).

Test B-3 (Figure 5.3c) was performed once the mixed culture was acclimated to nitrite. A SNitUR of 63.2 ± 0.7 mg NO_2^--N g^{-1} VSS h^{-1} was calculated, which was a 37% higher than that obtained with non-acclimated autotrophic biomass. Furthermore, it was observed that the SNitUR of the mixed culture did not change during the test even if both electron acceptors were present in the medium. This behavior had been also observed with the *T. denitrificans* pure culture. Thus, the improvement of denitrification from nitrite was quantitatively evaluated using the respirometry with the mixed culture before and after its acclimation.

5.4. CONCLUSIONS

Respirometric experiments performed under different initial $S_2O_3^{2-}$-S/NO_3^--N ratios and using different electron acceptors showed that the thiosulfate oxidation rate was influenced by the electron acceptor used and also inhibited by nitrite at concentration over 25 mg N L^{-1} ($6.61\cdot10^{-3}$ mg HNO_2 L^{-1} at pH=7.5). The final products obtained were affected by the initial thiosulfate to nitrate ratio employed being nitrite completely depleted when the $S_2O_3^{2-}$-S/NO_3^--N ratio was over 0.80 mol $S_2O_3^{2-}$-S mol^{-1} NO_3^--N. Nitrite accumulation did not depend on the initial $S_2O_3^{2-}$-S/NO_3^--N ratio but on the initial nitrate concentration and on biomass characteristics, being more active the denitritation rate of the mixed culture obtained from the anoxic BTF rather than that of the *T. denitrificans* pure culture. No competitive inhibition between nitrate and nitrite was detected during the respirometric tests when both were present in the medium. Acclimation of the mixed culture to 150 mg NO_2^--N L^{-1} resulted in a denitritation rate a 37% higher than that of non-acclimated biomass.

Finally, it was concluded that the procedure developed in this chapter to characterize mixed cultures obtained from desulfurizing BTFs was successfully applied and allowed studying denitrification mechanisms as well as estimating the biological activities.

Chapter 6

COUPLING RESPIROMETRY AND TITRIMETRY TO INVESTIGATE THE KINETICS OF THIOSULFATE-DRIVEN AUTOTROPHIC DENITRIFICATION AND THE EFFECT OF NITRITE ACCLIMATION

6. COUPLING RESPIROMETRY AND TITRIMETRY TO INVESTIGATE THE STOICHIOMETRY AND KINETICS OF THIOSULFATE-DRIVEN AUTOTROPHIC DENITRIFICATION AND THE EFFECT OF NITRITE ACCLIMATION

The motivation of this chapter was to gain knowledge about autotrophic denitrification mechanisms and the kinetics of the process by using the procedure developed in the previous chapter. Then, the anoxic respirometry would allow obtaining several kinetic parameters. Since nitrite is an intermediate in the denitrification process, that could affect negatively the operation of a reactor if accumulated in the liquid phase, nitrite inhibition and potential acclimation to nitrite were analyzed. A complementary biomass activity monitoring technique such as titrimetry was used. This technique coupled to respirometry helped to obtain the stoichiometry corresponding to the process particularly with the biomass to be characterized. This fact is quite interesting since kinetic parameters could be especially different if the stoichiometry is obtained from literature or solved from the biomass growth yield.

Abstract

Anoxic respirometry coupled to kinetics modeling of respirometric profiles was the methodology used to study the two-step denitrification associated to thiosulfate oxidation with SO-NR biomass acclimated and non-acclimated to nitrite. Previously to the kinetic characterization of the microbial culture, the stoichiometry of two-step denitrification reaction was solved by coupling respirometric and titrimetric profiles. Regarding the kinetic modeling, autotrophic denitritation was initially studied with a non-acclimated SO-NR culture to confirm that nitrite reduction kinetics could be described through a Haldane-type equation. Afterwards, a kinetic model describing the two-step denitrification ($NO_3^- \rightarrow NO_2^- \rightarrow N_2$) was calibrated and validated through the estimation of several kinetic parameters from the fitting of experimental respirometric profiles obtained using either nitrate or nitrite as electron acceptors for both acclimated and non-acclimated biomass. The Fisher Information Matrix method was used to obtain the confidence intervals and also to evaluate the sensitivity and the identifiability in model calibration of each kinetic parameter estimated.

A modified version of this chapter has been published as:

M. Mora, L.R. López, X. Gamisans, D. Gabriel, 2014b. Coupling respirometry and titrimetry for the characterization of the biological activity of a SO-NR consortium, *Chem. Eng. J.* 251, 111-115.

and accepted for publication as:

M. Mora, A.D. Dorado, X. Gamisans, D. Gabriel, 2015. Investigating the kinetics of autotrophic denitrification with thiosulfate: modeling the denitritation mechanisms and the effect of the acclimation of SO-NR cultures to nitrite. *Chem. Eng. J.* 262, 235-241.

6.1. INTRODUCTION

Few studies have reported the single application of respirometry in order to study thiosulfate (Mora et al., 2014c) and sulfide oxidation (Mora et al., 2014a) mechanisms related to denitrification by SO-NR biomass obtained from BTFs. However, the stoichiometric coefficients used and the kinetic parameters obtained in both cases were significantly different. This means that the use of some kinetic or stoichiometric data reported in literature for SO-NR biomass entails an inaccurate characterization of a specific biomass since the experimental conditions as well as the microbial diversity of biomass are hardly the same. For this reason, previously to the modeling of a respirometric profile, it is necessary to obtain the stoichiometry of the process, considering the $Y_{x/s}$ associated, besides including the specific degradation mechanisms associated to the corresponding microbial culture in the kinetic model.

Modeling of two-step denitrification associated to thiosulfate oxidation has not been reported previously. However, the need of using two-step denitrification equations ($NO_3^- \rightarrow NO_2^- \rightarrow N_2$) for a proper description of these processes has already been reported (An et al., 2010). Some authors have used single-substrate kinetic models taking into account microbial growth rates associated only to a single pollutant biodegradation (Monod, Haldane and other kinetic equations) (Delhomenie et al., 2008; Cai et al., 2013) to describe biological processes. A drawback of single-substrate kinetic models is the disability to describe the potential limitations of other species such as nutrients or the electron acceptor. Also, models based on single-substrates can hardly describe the formation of multiple end-products in complex biological processes such as biological denitrification and desulfurization processes (Klok et al., 2013). For this reason, a multi-substrate model has to be proposed to describe the two-step denitrification since both electron acceptors (nitrate and nitrite) are implicated in the process. Moreover, the confidence intervals of the kinetic parameters are not commonly assessed even if they are as important as the estimation of the parameters themselves. The Fisher Information Matrix (FIM) method is a proven tool that accurately provides confidence intervals for kinetic parameters. This method is based on the calculation of the covariance matrix inverse, which is directly associated to the uncertainty of the model parameters estimated and the quantity and quality of the experimental data. Many authors have successfully used this mathematical method to evaluate the reliability of

the parameters estimated both in wastewater and in polluted gas treatment processes (Guisasola et al., 2006; Dorado et al., 2008). The FIM method allows evaluating the sensitivities of the parameters and the quality of estimations.

Therefore, the aim of this chapter was to show the potential of coupling respirometry and titrimetry as a tool to obtain information about the biological activity of a SO-NR mixed culture obtained from an anoxic BTF. The combination of both techniques in a single test allowed obtaining stoichiometric coefficients of simultaneous reactions ($NO_3^-\rightarrow NO_2^-\rightarrow N_2$) as well as calculating biological activities and biomass-substrate yields of the two-step autotrophic denitrification using thiosulfate as electron donor. Moreover, the kinetic parameters of the autotrophic denitrification mechanisms based on thiosulfate oxidation were determined. The effect of culture acclimation to nitrite was also investigated and evaluated in this chapter through the changes in the kinetic parameters, which are directly related with the operating conditions of the reactor in which the biomass was grown and the history of the culture. The acclimation of the biomass to nitrite was also proposed to face nitrite inhibition problems in denitrifying reactors.

6.2. MATERIALS AND METHODS

6.2.1.   SO-NR biomass

The SO-NR biomass used in this chapter was obtained from an anoxic biogas desulfurizing BTF at different operation times (175 d and 325 d of operation) (Montebello et al., 2012). The first sampling of the biomass from the BTF (175 d) was used to inoculate CSTR-2 (*see sections 4.1.1 and 5.2.1 for detailed information*). Once assessed the steady state, the study of denitritation kinetics was performed using the SO-NR biomass cultured in the CSTR (Operation A). This biomass was then discarded for further studies. The second sample of biomass obtained from the BTF (325 d) was cultured also in the CSTR-2 (Operation B) during 22 weeks, without nitrite accumulation, for assessing the two-step denitrification process. Later, the biomass was acclimated to nitrite 2 weeks before the end of the CSTR operation by decreasing stepwise the hydraulic retention time. A detailed description of the start-up and Operation B are described in Chapter 5 (*see sections 5.2.1 and 5.3.1*).

6.2.2.   Respirometric and titrimetric tests

Two sets of respirometric tests were performed with the biomass cultured in the CSTR in order to evaluate the denitrification kinetics associated to thiosulfate oxidation (Table 6.1). Respirometric tests were carried out in RV-1 (*see section 4.1.3*). During the first set of tests (Set A) nitrite was used as the electron acceptor in order to define the kinetic model describing denitritation. The second set (Set B) was performed to study the stoichiometry and kinetics of the whole denitrification process and to assess the impact of biomass acclimation to nitrite. Biomass used in set A and B had the same origin (anoxic desulfurizing BTF) but were collected and cultivated in different periods of time (*see section 6.2.1 – Operation A and B of the CSTR*). Thus, impact of biomass acclimation was only assessed with biomass from set B before and after biomass acclimation to nitrite. Moreover, the use of thiosulfate allowed studying denitrification and nitrite acclimation clearly since the effects of many additional reduced sulfur compounds reactions were avoided. It would not be the case of sulfide since elemental sulfur can be formed as an intermediary product affecting consequently the denitrification rates (Mora et al., 2014a).

Table 6.1. Respirometric tests performed to study the stoichiometry and kinetics of thiosulfate oxidation under anoxic conditions by SO-NR biomass acclimated and non-acclimated no nitrite

Set-Test	CSTR Operation	Acclimated to nitrite?	Nitrite (mg N L^{-1})	Nitrate (mg N L^{-1})	Thiosulfate (mg S L^{-1})
A-1			103	0	124
A-2	A	No	10.7	0	322
A-3			29.7	0	297
B-1		Yes	20.8	1	328
B-2	B	Yes	0	0	269
B-3		Yes	24.2	12.1	268
B-4		No	1	53.1	160

*Biomass concentration ≈ 250 mg SSV L^{-1}

To obtain the respirometric profiles a certain volume of the biomass cultured in the CSTR was previously washed and poured into the respirometer. Subsequently,

known pulses of thiosulfate, nitrate and nitrite were added to the respirometer after overcoming both the endogenous and the wake up phases. The continuous sampling of the system allowed monitoring the concentration of the species involved in the process, which enables the estimation of the corresponding kinetic parameters by modeling the respirometric profiles. The protocol used for biomass preparation prior to the anoxic respirometric tests as well as the set up of the respirometer and the procedure to obtain the respirometric profiles were previously optimized and properly described in Chapter 5 (*see section 5.2.2*).

It must be mentioned that tests B-1, B-2 and B-3 presented in Table 6.1 were performed sequentially during the same single test and used to calculate the stoichiometry of thiosulfate-driven two-step denitrification. As can be observed, in test B-1 a pulse of nitrite and thiosulfate was added. Test B-2 was initiated after depletion of the electron acceptor. No pulses were added in test B-2 in order to study the CO_2 stripping process without the influence of the biological reactions. In test B-3 both nitrate and nitrite were simultaneously added with thiosulfate.

6.2.3. Proton production rate

Titrimetric measurements calculated according to Eq. 6.1 during the test served to calculate the total proton production rate (HPR_t) as the first derivative of the proton production (HP) (Eq. 6.2). The HPR_t is the sum of the contribution of the two processes occurring together during the respirometric tests: 1) the biological activity (HPR_b) and 2) the stripping of the carbon source (HPR_s) (Eq. 6.3).

$$HP = C_{base}V_{base} - C_{acid}V_{acid} \qquad (6.1)$$

$$HPR = d(HP)/dt \qquad (6.2)$$

$$HPR_t = HPR_b + HPR_s \qquad (6.3)$$

Therefore, to estimate the HPR_b, and subsequently the stoichiometric coefficients of the simultaneous reactions ($NO_3^- \rightarrow NO_2^- \rightarrow N_2$), is necessary to previously define accurately the stripping process hence determining the contribution of HPR_s to HPR_t.

Several abiotic tests using titrimetry were carried out to determine the K_La (*data not shown*) for the respirometer used in this study. The operational conditions employed were the same as those used during the respirometric assay. The test was started with the addition of a known pulse of a concentrated $NaHCO_3$ solution (70 mg C L^{-1}) in order to monitor and analyze the CO_2 stripping. The experimental HP was then calculated based on the volume of acid and base added to maintain a constant pH. To obtain the modeled HP, a mathematical model reported elsewhere (Ficara et al., 2003; Mora et al., 2014b) was used to properly estimate the mass transfer coefficient K_La. The calibrated K_La was also validated during test B-2 since no biological reactions were taking place during this period.

6.3. MODEL DEVELOPMENT

According to literature (Soto et al., 2007), nitrate reduction could be represented by a Monod-type equation while nitrite reduction can be described by Haldane-type kinetics. The accumulation of nitrite has also been reported as a kinetic affecting factor which could depend of the pH (Furumai et al., 1996), the S/N ratio used (Manconi et al., 2007; An et al., 2010) or the competition for each electron acceptor (nitrite or nitrate) (Krishnakumar and Manilal, 1999) among others. In this case none of these considerations were included in the kinetic model since in a previous study (Mora et al., 2014c) it was observed that the factor affecting the progress of this process for a constant pH was the denitratation and denitritation kinetics, being this fact related with the biomass present in the culture.

6.3.1.   Stoichiometry of thiosulfate-driven autotrophic denitrification

Stoichiometric coefficients are necessary to properly characterize the kinetics of a microbial population since biomass growth yields have a strong influence on the relation between all the species implicated in the biological process. In this chapter stoichiometric coefficients were estimated by using a combination of the data obtained both from respirometric and titrimetric measurements corresponding to tests B-1, B-2 and B-3. Three equations were proposed to describe the biological denitrification process (Eqs. 6.4 to 6.6). The corresponding mass, charge and reduction degree balances were derived. The experimental ratios $HPR_b/NitUR$ and HPR_b/NUR obtained

from the respirometric test were used to solve Eqs. 6.5 and 6.6 according to Roels (Roels, 1983). The stoichiometry of the global reaction was obtained from the sum of Eqs. 6.5 and 6.6. A typical biomass composition of $C_5H_7NO_2$ was assumed as well as the utilization of NH_4^+ as the nitrogen source for biomass growth.

- *Global reaction*

$$\textbf{\textit{a1}}\ S_2O_3^{2-} + \textbf{\textit{b1}}\ NO_3^- + \textbf{\textit{c1}}\ CO_2 + \textbf{\textit{d1}}\ HCO_3^- + \textbf{\textit{e1}}\ NH_4^+ + \textbf{\textit{f1}}\ H_2O \rightarrow$$

$$\textbf{\textit{x1}}\ C_5H_7O_2N + \textbf{\textit{g1}}\ N_2 + \textbf{\textit{h1}}\ H^+ + \textbf{\textit{i1}}\ SO_4^{2-} \tag{6.4}$$

- *Two-step denitrification reactions*

$$\textbf{\textit{a2}}\ S_2O_3^{2-} + \textbf{\textit{b2}}\ NO_3^- + \textbf{\textit{c2}}\ CO_2 + \textbf{\textit{d2}}\ HCO_3^- + \textbf{\textit{e2}}\ NH_4^+ + \textbf{\textit{f2}}\ H_2O \rightarrow$$

$$\textbf{\textit{x2}}\ C_5H_7O_2N + \textbf{\textit{g2}}\ NO_2^- + \textbf{\textit{h2}}\ H^+ + \textbf{\textit{i2}}\ SO_4^{2-} \tag{6.5}$$

$$\textbf{\textit{a3}}\ S_2O_3^{2-} + \textbf{\textit{b3}}\ NO_2^- + \textbf{\textit{c3}}\ CO_2 + \textbf{\textit{d3}}\ HCO_3^- + \textbf{\textit{e3}}\ NH_4^+ + \textbf{\textit{f3}}\ H^+ \rightarrow$$

$$\textbf{\textit{x3}}\ C_5H_7O_2N + \textbf{\textit{g3}}\ N_2 + \textbf{\textit{h3}}\ H_2O + \textbf{\textit{i3}}\ SO_4^{2-} \tag{6.6}$$
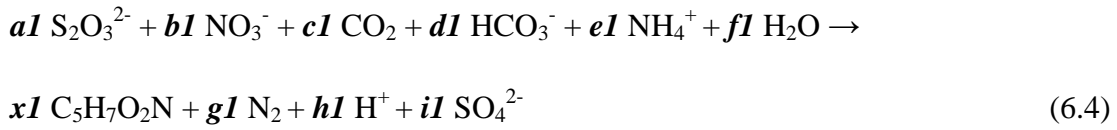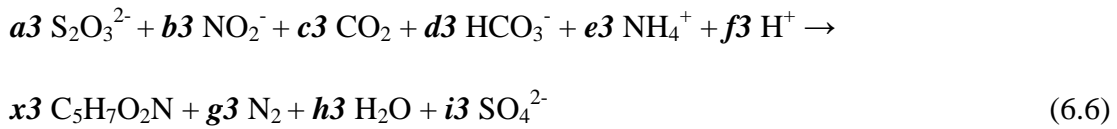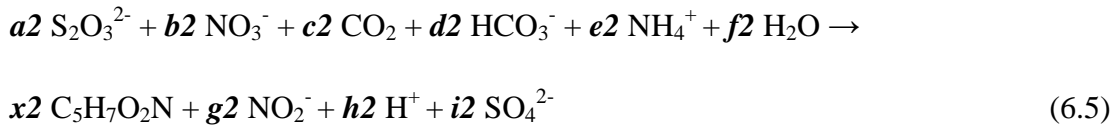
From these coefficients the biomass growth yield related to substrate ($Y_{X/S}$) or any electron acceptor ($Y_{X/Nit}$ and $Y_{X/N}$) and also the ratio between the species involved in the process can be calculated. It must be mentioned that, in previous works, in contrast with the present study, two-step denitrification have not been considered since nitrite was not observed during the respirometric assays (Mora et al., 2014a).

6.3.2. Modeling nitrite reduction

Nitrogen gas was the final product considered from nitrite reduction (Eq. 6.6). Several kinetic models have been previously proposed to describe denitritation (Almeida et al., 1995; Wild et al., 1995; Glass et al., 1997; Soto et al., 2007; Estuardo et al., 2008). Often, accumulation of nitrite during denitrification and the consequent

inhibition has been considered in such models (Betlach and Tiedje, 1981; Krishnakumar and Manilal, 1999). In this study the inhibition caused by nitrite on nitrite reduction was studied and described by a Haldane-type equation (Eq. 6.7) according to respirometric tests performed in Set A as discussed later.

$$r_{denitritation} = r_{max} \frac{Nit}{K_{Nit} + Nit + \frac{Nit2}{K_{i,Nit}}} \tag{6.7}$$

Where $r_{denitritation}$ and r_{max} are the specific and the maximum specific denitritation rates (mg NO_2^--N g^{-1} VSS h^{-1}), respectively; Nit is the nitrite concentration (mg NO_2^--N L^{-1}); K_{Nit} is the half-saturation coefficient for nitrite (mg NO_2^--N L^{-1}); and $K_{i,Nit}$ is the nitrite inhibition constant (mg NO_2^--N L^{-1}).

In addition to the Haldane-type term for nitrite, the set of differential equations describing mass balances for nitrite and thiosulfate consumption, sulfate production and biomass growth (Eqs. 6.8 to 6.11) as well as a Monod-type term to describe thiosulfate oxidation were considered. No elemental sulfur accumulation was included in the model since, as previously referenced (Furumai et al., 1996; Campos et al., 2008; Mora et al., 2014c), thiosulfate oxidation under anoxic conditions produced directly sulfate as the final product.

$$\frac{dNit}{dt} = -\frac{1}{Y_{X/Nit}} \cdot \mu_{max,Nit} \cdot X \cdot \frac{S}{K_S + S} \cdot \frac{Nit}{K_{Nit} + Nit + \frac{Nit2}{K_{i,Nit}}} \tag{6.8}$$

$$\frac{dS}{dt} = \frac{1}{Y_{Nit/S}} \cdot \frac{dNit}{dt} \tag{6.9}$$

$$\frac{dSO}{dt} = -\frac{dS}{dt} \tag{6.10}$$

$$\frac{dX}{dt} = \mu_{max,Nit} \cdot X \cdot \frac{S}{K_S + S} \cdot \frac{Nit}{K_{Nit} + Nit + \frac{Nit^2}{K_{i,Nit}}} \tag{6.11}$$

where S is the concentration of thiosulfate (mg $S_2O_3^{2-}$-S L^{-1}); SO is the concentration of sulfate (mg SO_4^{2-}-S L^{-1}); X is the biomass concentration experimentally quantified as VSS concentration (mg VSS L^{-1}); $\mu_{max,Nit}$ is the maximum specific growth rate of the biomass using nitrite as the electron acceptor (h^{-1}); K_s is the half-saturation coefficient for thiosulfate (mg $S_2O_3^{2-}$-S L^{-1}); and $Y_{X/Nit}$ and $Y_{Nit/S}$ are the stoichiometric biomass growth yield related to nitrite (mg VSS mg^{-1} N) and the nitrite to thiosulfate ratio (mg N mg^{-1} S), respectively.

6.3.3. Modeling two-step denitrification

The denitrification process has been previously characterized through several kinetic equations combining non-competitive inhibition between denitrification intermediates and simple Monod equations (Wild et al., 1995; Soto et al., 2007). In this chapter, a two-step denitrification mechanism associated to thiosulfate oxidation (experimental tests corresponding to set B) was modeled considering rate limitation caused by nitrate and inhibition caused by nitrite over denitritation. Moreover, no competition between the electron acceptors has been taken into account neither the influence of the initial $S_2O_3^{2-}$-S/NO_3^--N ratio on denitrification mechanisms since in previous results none of these phenomena were observed (Mora et al., 2014c). Simulation of the respirometric profiles was performed by taking into account Eqs. 6.8 to 6.11 and the differential equations corresponding to nitrate consumption (Eqs. 6.12 - 6.14).

$$\frac{dN}{dt} = -\frac{1}{Y_{X/N}} \cdot \mu_{max,N} \cdot X \cdot \frac{S}{K_S + S} \cdot \frac{N}{K_N + N} \tag{6.12}$$

$$\frac{d[S]}{dt} = \frac{1}{Y_{Nit/S}} \cdot \frac{d[Nit]}{dt} + \frac{1}{Y_{N/S}} \cdot \frac{d[N]}{dt} \tag{6.13}$$

$$\frac{d[X]}{dt} = \mu_{max,N} \cdot X \cdot \frac{[S]}{K_S + [S]} \cdot \frac{[N]}{K_N + [N]} \tag{6.14}$$

where N is the concentration of nitrate (mg NO_3^--N L^{-1}), $\mu_{max,N}$ is the maximum specific growth rate of the biomass using nitrate as the electron acceptor (h^{-1}), K_N is the half-saturation coefficient for nitrate (mg NO_3^--N L^{-1}) and $Y_{X/N}$ and $Y_{N/S}$ are the stoichiometric biomass growth yield related to nitrate (mg VSS mg^{-1} N) and the NO_3^--N/$S_2O_3^{2-}$-S ratio (mg N mg^{-1} S), respectively.

6.3.4. Parameters estimation

Maximum specific growth rates, half-saturation constants and inhibition constants were estimated as well as the respirometric profiles were simulated by means of MATLAB 7.7 (Mathworks, Natik, MA). The differential equations presented above (Eqs. 6.8 - 6.14) were solved using a variable step Runge-Kutta method (*ode45*) and the parameter estimation was carried out by using unconstrained non-linear optimization (*fminsearch*). In this case, the fitting of the experimental data to model predictions uniquely considers the electron acceptors (nitrite and nitrate) and it is based on seeking the minimum value of the objective function (Eq. 6.15). This function is defined as the norm of the differences between the predicted values of the mathematical model and the experimental data:

$$F = \sqrt{\sum_{i=1}^{n} \left[y_{exp,i} - y_{\theta,i} \right]^2} \qquad (6.15)$$

Where n is the number of experimental data, $y_{\theta,i}$ is the predicted value with the kinetic parameters to estimate (θ) and $y_{exp,i}$ is the value experimentally measured.

6.3.5.   Fisher Information Matrix

The confidence intervals of the estimated parameters were assessed through the Fisher Information Matrix mathematical method. The FIM summarizes the quantity and quality of information obtained in each experiment because it considers the output sensitivity functions and the measurement errors of an experimental data (i.e. accuracy of an experiment). When white measurement noise (i.e. independent and normally distributed with zero mean) and no model mismatch, no data autocorrelation and uncorrelated errors can be assumed, the inverse of the FIM provides the lower bound of the parameter estimation error covariance matrix, which can be used for assessing the estimation uncertainty of the optimal estimated parameters. Moreover, since output sensitivities of parameters are calculated using a model, the FIM also depends on the model structure (Mehra, 1974; Dochain and Vanrolleghem, 2001; Guisasola et al., 2006; Dorado et al., 2008).

6.4. RESULTS AND DISCUSSION

6.4.1.   Stoichiometric coefficients

Experimental respirometric and titrimetric profiles obtained from test B-1, B-2 and B-3 to calculate the stoichiometric coefficients of two-step denitrification are presented in Figure 6.1. It can be observed that in period I, as well as in period IIIb after nitrate depletion, nitrite was the single electron acceptor. Therefore, nitrite reduction was coupled with thiosulfate oxidation. From these periods a NitUR of 0.394 ± 0.001 mmol NO_2^- h^{-1}, a SUR_{Nit} (thiosulfate uptake rate associated to nitrite reduction) of 0.189 ± 0.004 mmol $S_2O_3^{2-}$ h^{-1} and a $NitUR/SUR_{Nit}$ ratio of 2.08 ± 0.04 mol NO_2^-/mol

$S_2O_3^{2-}$ were calculated (Table 6.2). Elemental sulfur production was not detected since SUR was similar to the sulfate production rate. Thus, the sulfur mass balance was accomplished.
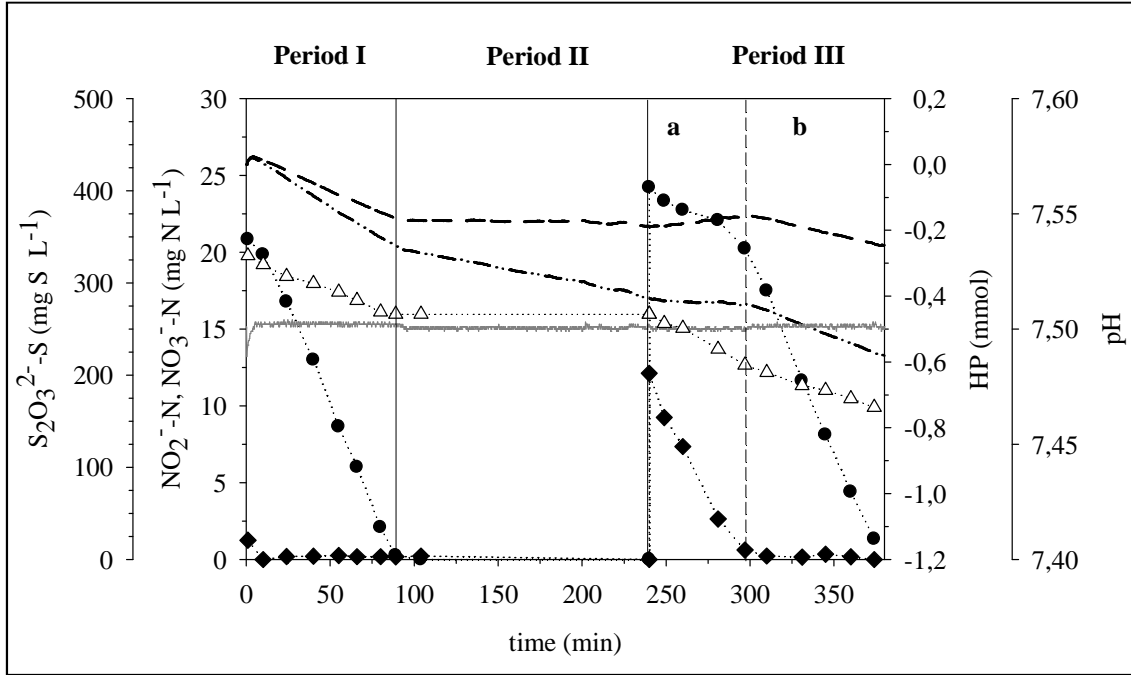
Figure 6.1. Respirometric and titrimetric test performed to calculate the stoichiometric coefficients. (Period I) Test B-1, (Period II) Test B-2, (Period III) Test B-3 divided in two stages (a) Nitrate and nitrite as electron acceptors (b) Uniquely nitrite as electron acceptor. Symbols: Thiosulfate ($\triangle$), Nitrate ($\blacklozenge$), Nitrite ($\bullet$). Lines: pH (grey solid line), HP_b (dashed line), HP_t (dot-dashed line).

Table 6.2. Experimental HPR and nitrite, nitrate and thiosulfate uptake rates obtained from the respirometric profiles

| Test | Period | NitUR | NUR | SUR_{Nit} | SUR_N | HPR_{Nit} |
		(mmol N h^{-1})		(mmol $S_2O_3^{2-}$ h^{-1})		(mmol H^+ h^{-1})
B-1	**I**	0.395	--	0.185	--	0.131
B-3	**IIIa**	0.402	0.343	0.194	0.130	0.074
B-3	**IIIb**	0.393	--	0.192	--	0.070

During period I, the HPR_b observed was almost twice the HPR_b corresponding to period IIIb. Slight differences between the experimental HPR_s and the predicted HPR_s were observed during the first 100 minutes in the abiotic test (*data not shown*) since,

under non-equilibrium conditions (period I), a higher difference between CO_2 concentrations in the liquid phase and in the headspace ($CO_2 = 0$ mg C L^{-1}) produced a higher CO_2 stripping. A larger effectiveness of the CO_2 mass transfer to the gas phase during period I explained the differences observed. Consequently, the K_La was underestimated during period I compared to periods II and III. Thus, the HPR_b used to calculate the $HPR_b/NitUR$ ratio (0.178 mol H^+/mol NO_2^-) was that obtained in period IIIb. The stoichiometry of the denitrification from nitrite, using CO_2 and HCO_3^- as carbon sources and considering the associated biomass growth was estimated (Eq. 6.16) with data from period III.
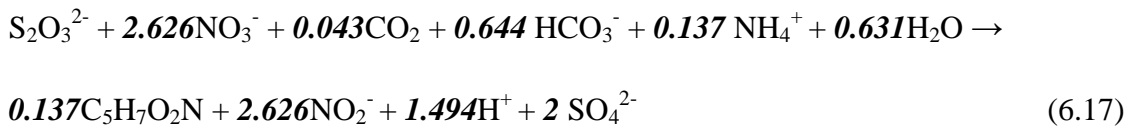
$$S_2O_3^{2-} + \textbf{\textit{2.070}}NO_2^- + \textbf{\textit{0.028}}CO_2 + \textbf{\textit{0.419}}HCO_3^- + \textbf{\textit{0.089}}NH_4^+ + \textbf{\textit{0.400}}H^+ \rightarrow$$

$$\textbf{\textit{0.089}}\ C_5H_7O_2N + \textbf{\textit{1.035}}\ N_2 + \textbf{\textit{0.275}}\ H_2O + \textbf{\textit{2}}\ SO_4^{2-} \tag{6.16}$$
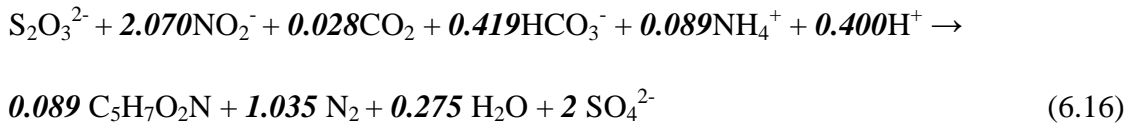
In period II the stripping of CO_2 was the unique process taking place. The HPR_s was equivalent to the observed HPR_t. Thus, the flat HPR_b profile served to validate the CO_2 stripping model and the K_La estimation resulting in a K_La of 0.475 h^{-1}. The K_La estimated was between one and two orders of magnitude lower than other K_La reported in systems where air was sparged in the liquid phase (Ficara et al., 2003). Therefore, the stripping of CO_2 is minimized when nitrogen is sparged in the headspace of the respirometer since turbulence in the liquid, and hence gas-liquid mass transfer, is reduced compared to air bubbling. Minimal carbon source stripping avoids not only its limitation during the respirometric test but also a lower interference in the observed HP (Tora et al., 2010). In consequence, increased sensitivity and reliability are obtained from titrimetric data.

In period IIIa, nitrate and nitrite were simultaneously used as electron acceptors. It was observed that NitUR was higher than NUR since nitrite was consumed during nitrate reduction. Many authors have reported that nitrite reduction is the slower step of the denitrification process, which causes the accumulation of nitrite (Betlach and Tiedje, 1981; Campos et al., 2008). However, the CSTR containing the SO-NR culture was operated at a lower residence time causing an incomplete denitrification and,

subsequently, the acclimation of biomass to nitrite (*see Chapter 5 for detailed information*). Furthermore, similar NitURs were obtained during the whole period III regardless of the presence of nitrate in the medium. Based on this observation, the stoichiometry of nitrate reduction reaction (Eq. 6.17) was solved by using the stoichiometric ratio NitUR/SUR$_{Nit}$, previously obtained from period IIIb, and calculating the SUR related uniquely to the nitrate reduction rate through Eq. (6.18) (SUR$_N$ = 0.130 mmol $S_2O_3^{2-}$ h^{-1}).

$$S_2O_3^{2-} + \textbf{\textit{2.626}}NO_3^- + \textbf{\textit{0.043}}CO_2 + \textbf{\textit{0.644}}\ HCO_3^- + \textbf{\textit{0.137}}\ NH_4^+ + \textbf{\textit{0.631}}H_2O \rightarrow$$

$$\textbf{\textit{0.137}}C_5H_7O_2N + \textbf{\textit{2.626}}NO_2^- + \textbf{\textit{1.494}}H^+ + \textbf{\textit{2}}\ SO_4^{2-} \quad\quad\quad (6.17)$$

$$SUR_N = SUR_{(period\ IIIa)} - NitUR_{(period\ IIIa)} / [NitUR / SUR_{Nit}]_{(period\ IIIb)} \quad\quad (6.18)$$

As a result, the corresponding NUR/SUR$_N$ and HPR$_b$/NUR ratios were determined (2.626 mol $S_2O_3^{2-}$/mol NO_3^- and 0.569 mol H^+/mol NO_3^-, respectively) and the two-step denitrification with thiosulfate oxidation was completely defined. The $Y_{x/s}$ for each electron acceptor used were obtained from the stoichiometric coefficients as well as the yield associated to the complete denitrification (Eq. 6.19).

$$S_2O_3^{2-} + \textbf{\textit{1.16}}NO_3^- + \textbf{\textit{0.035}}CO_2 + \textbf{\textit{0.519}}\ HCO_3^- + \textbf{\textit{0.110}}\ NH_4^+ + \textbf{\textit{0.124}}H_2O \rightarrow$$

$$\textbf{\textit{0.110}}C_5H_7O_2N + \textbf{\textit{0.578}}N_2 + \textbf{\textit{0.435}}\ H^+ + \textbf{\textit{2}}\ SO_4^{2-} \quad\quad\quad (6.19)$$
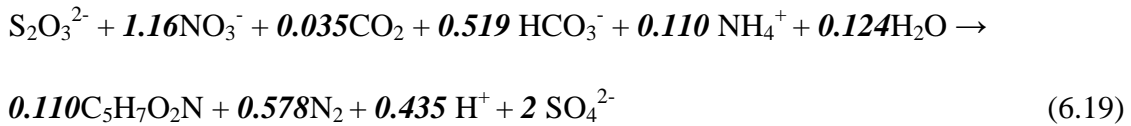
A $Y_{x/s}$ of 0.111 g VSS/g $S_2O_3^{2-}$ was calculated, which was similar to that obtained by Mora et al. (2014c) for the complete denitrification associated to thiosulfate oxidation of a suspended SO-NR mixed culture in a CSTR (0.101 g VSS/g $S_2O_3^2$). Campos et al. (2008) and Artiga et al. (2005) also obtained comparable yields with SOB (0.103 g VSS/g $S_2O_3^{2-}$ and 0.107 g VSS/g $S_2O_3^{2-}$, respectively), which were

slightly higher than that reported by Oh et al. (2000) (0.082 g dry weight/g $S_2O_3^{2-}$). In addition, it was found in literature (Yavuz et al., 2007) that the biomass yield associated to sulfide oxidation under anoxic conditions was equivalent to that obtained using thiosulfate as substrate. However, in terms of nitrate requirements both electron donors are not comparable since the N/S ratio (g NO_3^--N g^{-1} S) necessary to oxidize sulfide (0.612 g NO_3^--N/g S) is 2.4 times that required to oxidize thiosulfate (0.254 g NO_3^--N/g $S_2O_3^{2-}$-S).

It was also observed that the biomass growth from nitrite was about 20% lower compared with the biomass yield corresponding to the complete denitrification (Eq. 6.19). This result differs from that obtained by Timmer-ten Hoor (1981) with pure sulfide-oxidizing cultures who reported similar biomass yields regardless the electron acceptor used. This bibliographic value was applied in Mora et al. (2014c) to solve the two-step denitrification stoichiometry. Thus, the biomass yield related to partial denitrification was underestimated in Mora et al. (2014c) for the same SO-NR mixed culture used in this chapter. Hence, the use of titrimetric data in a single respirometric test per electron acceptor allowed solving both reactions by reducing the degrees of freedom of the system with no additional experimental tests.

6.4.2. Denitritation kinetics

From the experiments performed in Set A with a SO-NR culture not-acclimated to nitrite (Table 6.1) three respirometric profiles were obtained at different initial nitrite concentrations (Figure 6.2, a-c). From the slopes of nitrite concentration profiles many NitURs were calculated for different nitrite concentrations and plotted as a function of the nitrite concentration in Figure 6.2d a Haldane-type equation (Eq. 6.7) was properly fitted to the experimental kinetic profile (Figure 6.2d) to estimate r_{max}, K_{Nit} and $K_{i,Nit}$ (Table 6.3). The $\mu_{max,Nit}$ (Eq. 6.8) was also calibrated using the respirometric test A-2 (Figure 6.2b) since a sensitivity analysis showed that the predicted nitrite concentration was more influenced by variations of $\mu_{max,Nit}$ in test A-2 than in tests A-1 and A-3. The half-saturation coefficient for thiosulfate (K_S) was not calibrated since the concentration used almost in all respirometric tests was always above 120 mg $S_2O_3^{2-}$-S L^{-1}, which is much higher than the K_S reported in literature. A K_S of 32.4 mg $S_2O_3^{2-}$-S L^{-1} reported in Artiga et al. (2005) for a thiosulfate-oxidizing nitrate-reducing culture was used. As shown in Figure 6.2 (a, c), the denitritation profiles, as well as the corresponding

thiosulfate oxidation associated, were satisfactorily described through the Haldane-type equation previously calibrated with the kinetic profile (Figure 6.2d) and the test A-2 (Figure 6.2b). Literature regarding kinetics of bacterial growth with thiosulfate using nitrite as the electron acceptor is very limited and prior to the present work no data for biokinetic parameters were reported. However, Fajardo et al. (2014a) obtained a maximum specific uptake rate of 3.7 mg NO_2^--N g^{-1} VSS h^{-1} using nitrite as electron acceptor with SOB cultivated in a sequencing batch reactor. This rate was almost 15 times lower than that obtained in the present work (54.1 mg N g^{-1} VSS h^{-1}) indicating that the cultures cannot be compared and that specific tests must be performed for each microbial culture to properly assess its kinetic parameters.
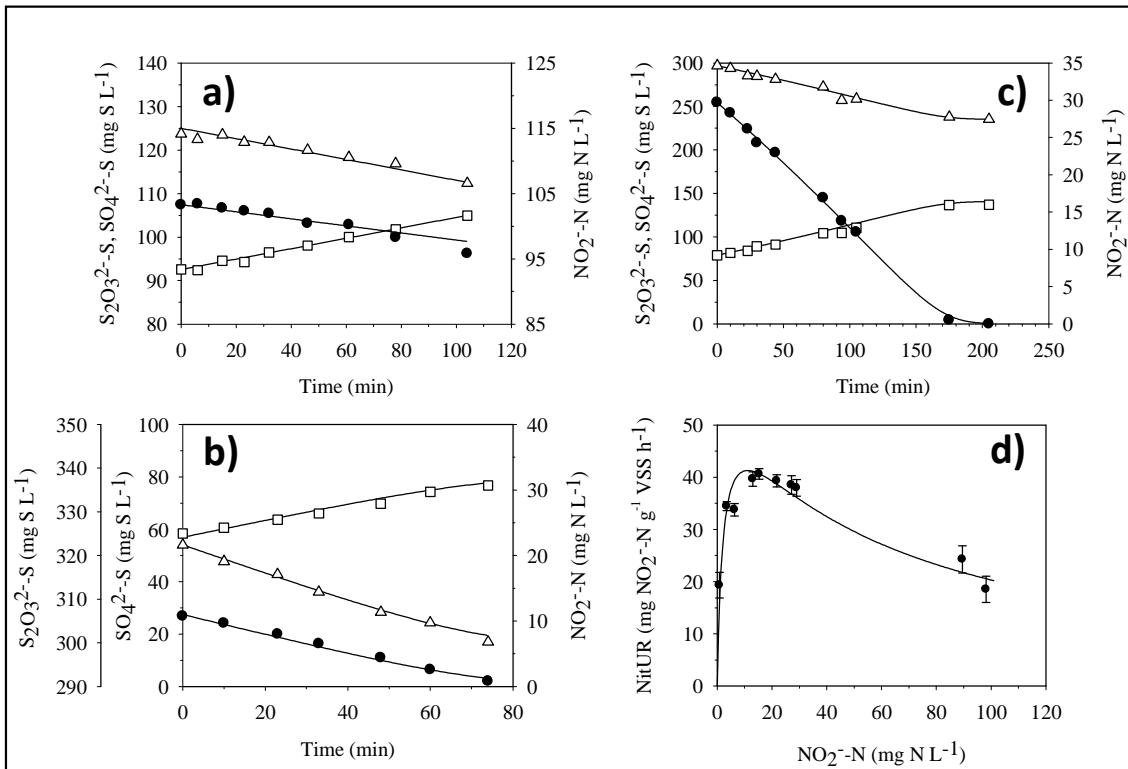
Figure 6.2. Experimental respirometric profiles and model predictions obtained with experiments performed in Set A. (a) Test A-1 performed at a high nitrite inhibiting concentration of 100 mg NO_2^--N L^{-1} (b) Test A-2 performed with 10 mg NO_2^--N L^{-1} (c) Test A-3 performed with 30 mg NO_2^--N L^{-1} and best fitted with $\mu_{max,Nit}$ (d) Experimental profile corresponding to the NitUR obtained from the previous respirometric tests at different nitrite concentrations and Haldane model prediction for the calibration of r_{max}, K_{Nit} and $K_{i,Nit}$. Symbols: Thiosulfate ($\triangle$), Sulfate ($\square$), Nitrate ($\blacklozenge$), Nitrite and NitUR ($\bullet$). Modeled data (solid line)

Table 6.3 shows the confidence intervals in the estimation of each parameter obtained through the FIM method. As can be observed, a maximum confidence interval of 0.34% was determined for K_{Nit} indicating that the high sensitivity of all kinetic parameters at these concentration ranges guarantees the parameter identifiability during model calibration (i.e. the possibility in giving an unique value of each parameter in the model). Such low confidence intervals indicate both the use of an accurate measurement technique as well as a correct experimental design that satisfactorily described the experimental behavior with the kinetic model proposed. The estimated $\mu_{max,Nit}$ was slightly lower than the dilution rate set in the reactor (0.018 h^{-1}). This result reveals that the utilization of nitrite as electron acceptor in the CSTR would have caused the wash out of biomass.

Table 6.3. Denitritation kinetic parameters obtained after model calibration and estimation of the confidence interval by means of the FIM mathematical method.

	μ_{max} (h^{-1})	r_{max} (mg N g^{-1} VSS h^{-1})	K_{Nit} (mg NO_2^--N L^{-1})	$K_{i,Nit}$
Value	0.0167	58.3	2.32	54.1
Confidence interval (%)	[0.0167] (0.0321)	[58.2 – 58.4] (0.1092)	[2.31 – 2.33] (0.3386)	[54.0 – 54.2] (0.2660)

6.4.3. Calibration of two-step denitrification model

Experiments corresponding to Set B (Table 6.1) were performed with the biomass cultured in the CSTR during Operation B. In Set B, tests with biomass acclimated and non-acclimated to nitrite were carried out to completely calibrate the two-step denitrification model and to determine the influence of biomass acclimation to nitrite over SO-NR thiosulfate-based denitrification kinetics. Calibration of the two-step denitrification kinetic model was performed with tests B-1 and B-3 with acclimated biomass. Once kinetics corresponding to nitrate reduction had been obtained, the denitritation parameters were estimated with experimental data from test B-4 for the non-acclimated biomass.

- *Biomass acclimated to nitrite*

Similarly to the non-acclimated biomass test in set A, kinetic parameters related to denitritation ($\mu_{max,Nit}$, K_{Nit} and $K_{i,Nit}$) with the biomass acclimated to nitrite were estimated (Table 6.4) from respirometric test B-1 using a Haldane-type equation (Eq. 6.7) which was confirmed above (*see section 6.4.2*) that is adequate to describe denitritation. Figure 6.3a shows that the model satisfactorily fits the experimental data over again even if larger confidence intervals than those obtained through the nitrite uptake rate profile for the non-acclimated biomass (*see section 6.4.2*) were obtained. In this case a nitrite uptake rate profile could not be performed since no experimental data was available at nitrite inhibiting concentrations. Still results were considered satisfactory since none of the confidence intervals exceed a 5% of deviation. As expected, a higher confidence interval was found for K_{Nit} since the nitrite concentration range in the tests was not the most suitable for its estimation. Nonetheless, results indicate that the compilation of several nitrite uptake rates from respirometric tests performed under different conditions is very helpful to properly fit a kinetic equation to the experimental data even if inhibition concentrations were not achieved. It is worth mentioning that a fair comparison of inhibition constants from Table 6.3 and Table 6.4 for the non-acclimated and acclimated biomass, respectively, was not possible since both microbial populations were different as indicated by the differences in their maximum specific growth rates.

Regarding the calibration of nitrate reduction, kinetic parameters previously estimated from test B-1 were used to estimate $\mu_{max,N}$, K_N and K_S. A K_S of 16.1±0.04 mg S-$S_2O_3^{2-}$ L^{-1} was obtained, which was slightly different from that reported by Artiga et al. (2005), indicating that the use of the parameter reported in literature for concentrations up to 120 mg $S_2O_3^{2-}$-S L^{-1} lead to more than 10% error in model predictions. The $\mu_{max,N}$ obtained (0.0269±0.0001 h^{-1}) was very low compared with those reported for SO-NR biomass (0.05 – 0.2 h^{-1}) (Claus and Kutzner, 1985; Oh et al., 2000) probably because the biomass was obtained from a desulfurizing BTF. In such biofilm-based reactors, biomass is not naturally selected because of its growth rate but for the resistance and acclimation to specific operating conditions. The estimated K_N indicates

that nitrate would not be limiting the reaction at concentrations above 20 mg NO_3^--N L^{-1} since this value allows reaching a 95% of the maximum reaction rate.
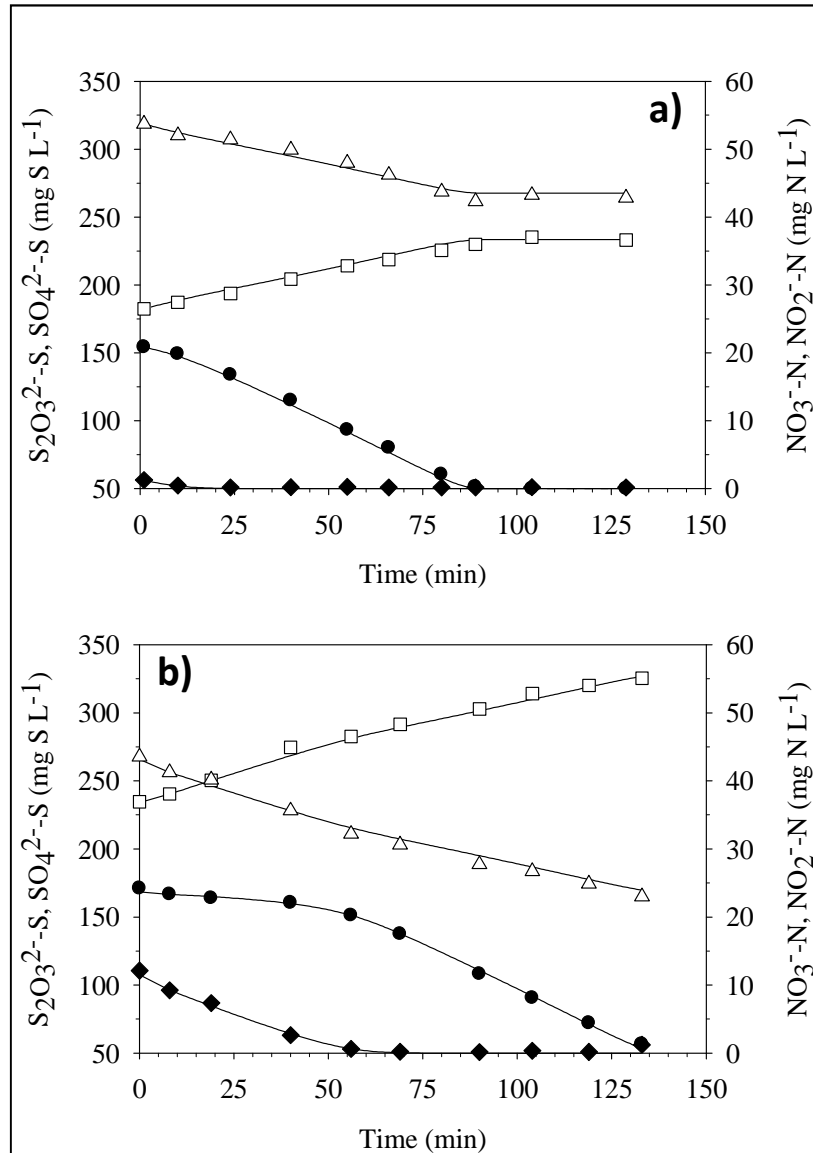
Figure 6.3. Respirometric profiles obtained with SO-NR biomass acclimated to nitrite. (a) Test B-1 performed uniquely with nitrite as electron acceptor (b) Test B-3 performed with nitrate and nitrite as electron acceptors. Symbols: Thiosulfate ($\triangle$), Sulfate ($\square$), Nitrate ($\blacklozenge$), Nitrite ($\bullet$). Modeled data (solid line)

Biomass acclimated to nitrite presented high denitritation rates since no accumulation of nitrite was observed in test B-3 (Figure 6.3b). This fact avoids the inhibition caused by nitrite over thiosulfate oxidation under anoxic conditions and

allows using high concentrations of nitrate in the biofilter without limiting the reaction rate. Therefore, biomass acclimation to nitrite can be favorably implemented in those processes in which denitritation is lower than denitratation causing nitrite accumulation and, consequently, an efficiency drop due to an inhibiting situation.

Table 6.4. Two-step denitrification kinetic parameters after model calibration and estimation of confidence intervals through the FIM method with biomass acclimated to nitrite.

Parameter	Units	Value	% error	Confidence interval
$\mu_{max,N}$	h^{-1}	0.0269	0.602	[0.0267 – 0.0270]
K_S	mg $S_2O_3^{2-}$-S L^{-1}	16.1	0.244	[16.1 – 16.2]
K_N	mg NO_3^--N L^{-1}	0.846	3.81	[0.814 – 0.878]
$\mu_{max,Nit}$	h^{-1}	0.0283	0.607	[0.0281 – 0.0285]
K_{Nit}	mg NO_2^--N L^{-1}	0.428	4.16	[0.410 – 0.446]
$K_{i,Nit}$	mg NO_2^--N L^{-1}	75.2	3.27	[72.8 – 77.7]

- *Biomass non-acclimated to nitrite*

Test B-4 (Figure 6.4) was performed with the same biomass used in tests B-1 and B-3 previously to the acclimation period to nitrite to uniquely assess the effect of nitrite acclimation in the estimation of the kinetic parameters of the denitritation mechanism. In this test (B-4), the denitritation model was calibrated by using the kinetic parameters corresponding to nitrate reduction obtained from the model calibration performed with test B-3. These parameters were used on the basis that nitrite acclimation affected uniquely to denitritation. As shown in Figure 6.4, the calibrated kinetic model accurately described the experimental data corresponding to the two-step denitrification associated to thiosulfate oxidation. The biomass concentration profile was also predicted considering the growth yields obtained from the stoichiometry ($Y_{X/N}$ and $Y_{X/Nit}$) and also a 100% of active biomass. As can be observed, the biomass concentration increased by 15% from its initial value. This biomass growth was considered to not overestimate the kinetic parameters. In Table 6.5 the estimated

parameters and the corresponding confidence intervals are presented for the non-acclimated biomass.
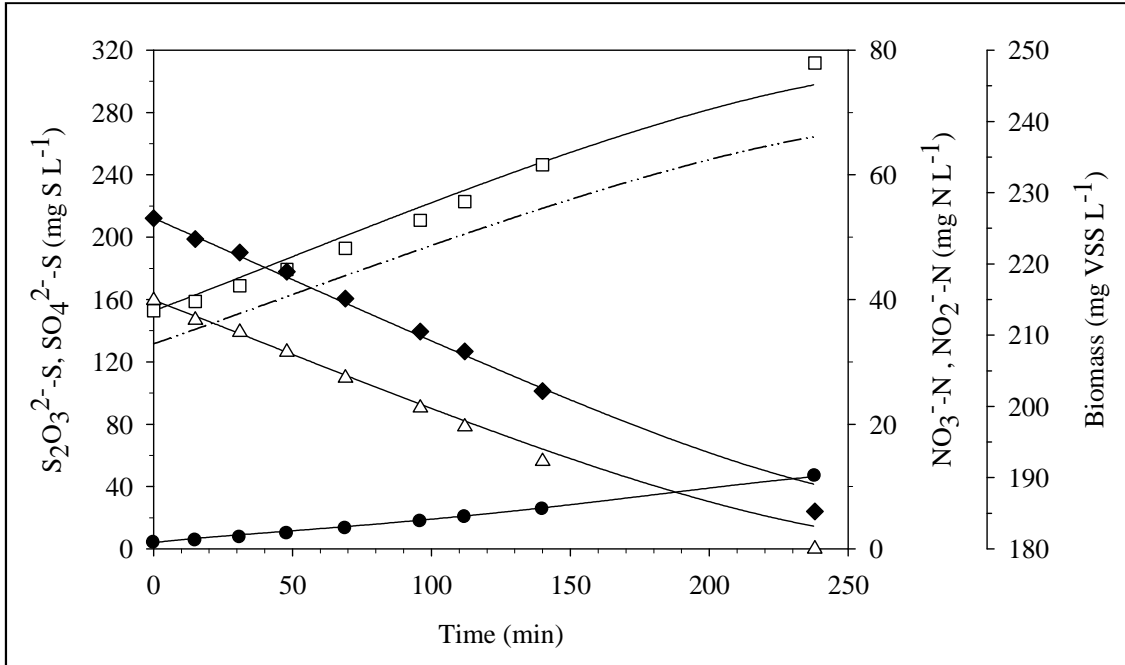
Figure 6.4. Respirometric profile obtained from test B-4 with SO-NR biomass non-acclimated to nitrite. Symbols: Thiosulfate ($\triangle$), Sulfate ($\square$), Nitrate ($\blacklozenge$), Nitrite ($\bullet$). Modeled data (solid line), modeled biomass (dash dot line)

Table 6.5. Denitritation kinetic parameters for non-acclimated biomass. Confidence interval from the application of the FIM mathematical method

	μ_{max} (h^{-1})	K_{Nit} $(mg\ NO_2^-\text{-}N\ L^{-1})$	$K_{i,Nit}$ $(mg\ NO_2^-\text{-}N\ L^{-1})$
Value	0.0257	0.590	11.5
Confidence interval	[0.0253 – 0.0261]	[0.546 – 0.635]	[11.1 – 11.9]
(%)	(1.68)	(7.54)	(3.57)

6.4.4. Kinetic evaluation of biomass nitrite acclimation

Comparison of the parameters in Table 6.4 and Table 6.5 indicates that biomass acclimation to nitrite improved characteristics related to the nitrite inhibition effect. In terms of growth both microbial cultures presented a similar maximum specific growth rate indicating that microbial cultures did not changed before and after acclimation. However, the inhibition constant for the acclimated biomass (75.2±2.5 mg N L^{-1}) was almost 7-fold that obtained with the non-acclimated biomass (11.5±0.4 mg N L^{-1}) meaning that the acclimated biomass shows lower degree of nitrite inhibition. Concerning biomass affinity to nitrite, similar half-saturation constants were estimated although the K_{Nit} was slightly lower for the acclimated biomass. This result was somehow expected since the biomass was acclimated by reducing stepwise the dilution rate being accumulated the nitrite until reaching concentrations of about 150 mg NO_2^--N L^{-1}. In this sense the biomass was forced to grow at this elevated concentration being the influence of the half-saturation constant negligible and, consequently, not affected by the acclimation. This results lead to confirm that the culture presented a high resistance to nitrite accumulation, since the $\mu_{max,Nit}$ was almost maintained, but also a high resilience (Cabrol et al., 2012) since the concentration of nitrite decreased after reaching the maximum concentration although maintaining a lower HRT (*data not shown*).

As expected, the parameters obtained in set B were different from those previously obtained in set A (*see sections 6.4.2 and 6.4.3*) since the biomass was obtained at different operation times of the BTF. The kinetic parameters reported in Mora et al. (2014a) using SO-NR biomass from the same anoxic desulfurizing BTF were also different from those estimated in this study since the biomass was obtained 1 year later. These results remark the importance of the biomass history and the effect of operating conditions fluctuations over culture characteristics and kinetic behavior.

Finally, in this calibration the uncertainties for all the parameters were slightly higher than those obtained in previous calibrations for denitritation and two-step denitrification biomass acclimated to nitrite (Tables 6.3 and 6.4) but specially the uncertainty associated to K_{Nit} and $K_{i,Nit}$. It is worthy to mention that the confidence intervals assessed through the FIM method could be reduced by increasing the quantity of experimental data measured, which can be considered relatively low in these

experiments. Even so, all kinetic parameters were identifiable on the basis of respiration tests indicating that the conditions selected to calibrate the model were especially suitable.

6.5. CONCLUSIONS

From the results obtained in this chapter it can be concluded that the two-step denitrification associated to thiosulfate oxidation was successfully described with the stoichiometry calculated and the kinetic model proposed and calibrated herein, which has not been previously reported in other studies. The calibration of the model allowed the experimental data fitting as well as the prediction of the biomass growth associated, which was necessary to properly estimate the kinetic parameters.

Denitritation was satisfactorily described through a Haldane equation with the SO-NR cultures acclimated and non-acclimated to nitrite. The effect of nitrite acclimation was also evaluated and it was confirmed that the biomass presented high resistance and resilience to nitrite concentrations up to 150 mg N L^{-1}.

Terms related to non-competitive inhibition between nitrate and nitrite were excluded since this behavior was not observed with the SO-NR culture studied. In addition, the kinetic parameters estimated presented a high sensitivity to model predictions since small confidence intervals were assessed with the FIM method.

Results obtained in this chapter also provide complementary information to the research related with the simultaneous desulfurization and denitrification of liquid effluents, the biochemical studies of SO-NR microbial populations and also about the mathematical modeling of biological denitrification processes.

Chapter 7

**KINETIC AND STOICHIOMETRIC
CHARACTERIZATION OF ANOXIC SULFIDE
OXIDATION BY SO-NR MIXED CULTURES OBTAINED
FROM ANOXIC BIOTRICKLING FILTERS**

7. KINETIC AND STOICHIOMETRIC CHARACTERIZATION OF ANOXIC SULFIDE OXIDATION BY SO-NR MIXED CULTURES OBTAINED FROM ANOXIC BIOTRICKLING FILTERS

In this chapter sulfide would finally be used to study desulfurization mechanisms, since thiosulfate was used in previous chapters to better develop the anoxic respirometry protocol, but also to study clearly denitrification without the interference of another intermediate species. In this case, the study was mainly focused in calibrating a kinetic model to be included in the general model describing the biotrickling filter from which the biomass was withdrawn. Moreover, molecular biology techniques were additionally applied in order to verify preservation of the biomass during the whole characterization process since this analysis was not already included in previous studies.

Abstract

Monitoring the biological activity in BTFs is difficult since it implies estimating biomass concentration and its growth yield, which can hardly be measured in immobilized biomass systems. In this study, the characterization of a sulfide-oxidizing nitrate-reducing biomass obtained from an anoxic BTF was performed through the application of respirometric and titrimetric techniques. Previously, the biomass was maintained in a continuous stirred tank reactor under steady-state conditions resulting in a growth yield of 0.328 ± 0.045 g VSS g^{-1} S. To properly assess biological activity in respirometric tests, abiotic assays were conducted to characterize the stripping of CO_2 and sulfide. The global mass transfer coefficient for both processes was estimated. Subsequently, different respirometric tests were performed: 1) to solve the stoichiometry related to the autotrophic denitrification of sulfide using either nitrate or nitrite as electron acceptors, 2) to evaluate the inhibition caused by nitrite and sulfide on sulfide oxidation, and 3) to propose, calibrate and validate a kinetic model considering both electron acceptors in the overall anoxic biodesulfurization process. The kinetic model considered a Haldane-type equation to describe sulfide and nitrite inhibitions, a non-competitive inhibition to reflect the effect of sulfide on the elemental sulfur oxidation besides single-step denitrification since no nitrite was produced during the biological assays.

A modified version of this chapter has been published as:

M. Mora, M. Fernández, J.M. Gómez, D. Cantero, J. Lafuente, X. Gamisans, D.
Gabriel, 2014a. Kinetic and stoichiometric characterization of anoxic sulfide
oxidation by SO-NR cultures from anoxic biotrickling filters, *Appl. Microbiol.
Biotechnol.* 1-11.

7.1. INTRODUCTION

Development of mathematical models is necessary to design and optimize the biological H_2S removal process. Particularly, accurate microbial kinetic data is needed in these general models for a proper prediction of the biological activity and, consequently, to properly assess the local and overall performance of such heterogeneous, plug flow-type reactors (Martin et al., 2002). However, as mentioned in previous chapters, the characterization of autotrophic SO-NR biomass from a desulfurizing BTF implies estimating the biomass concentration and the growth yield coefficient, parameters that can hardly be measured in-situ when using immobilized biomass. In addition, several physical and chemical processes related with mass transfer phenomena and ionic equilibriums take place simultaneously in the BTF (López et al. 2013), which increases the uncertainty of model parameters estimation.

In this study, the characterization of a SO-NR mixed culture, obtained from a BTF operated under anoxic conditions was performed by using respirometric and titrimetric techniques and the methodology proposed in Chapter 5. Sulfide oxidation mechanisms associated to denitrification are proposed and, in addition, $Y_{x/s}$ and kinetic parameters are defined and estimated for the calibration and validation of a microbial kinetic model. Inhibition of nitrite was also studied as an intermediate of the denitrification process that could have detrimental effects on the overall reaction when denitritation is the limiting step (McMurray et al., 2004).

7.2. MATERIALS AND METHODS

7.2.1.   S-oxidizing biomass

The SO-NR mixed culture used in this study was collected from a pilot-scale anoxic BTF (0.17 m^3 working volume) treating biogas under anoxic conditions containing an average inlet H_2S concentration of about 4500 ppm_v (Almengló et al. 2013). The BTF was packed with open-pore PUF cubes and operated during several months at pH 7.4.

The SO-NR biomass was withdrawn from the packing material and suspended in 500 mL of nutrient solution to subsequently inoculate a sterilized reactor (CSTR-3, *see section 4.1.1*). A modified ATCC-1255 *Thiomicrospira denitrificans* nutrient solution was used for the biomass growth without thiosulfate and with a higher concentration of bicarbonate and nitrate: $NaHCO_3$ (2 g L^{-1}) and KNO_3 (3 g L^{-1}). Previously to the inoculation, CSTR-3 was filled with nutrient solution (4.2 L) and gassed with Argon to remove oxygen. Afterwards, the suspended biomass was transferred to CSTR-3 and the operation was started-up in fed-batch mode by continuously supplying 5.37 mL h^{-1} of a dissolved sulfide solution (8 g $Na_2S \cdot 9H_2O$-S L^{-1}), which corresponds to a loading rate of 8.6 g S m^{-3} reactor h^{-1}. During this stage substrate inhibition did not occurred and the biomass was acclimated to operate as a suspended culture. Once nitrate was almost depleted, operation as CSTR without biomass recirculation was set during 3 weeks to maintain the SO-NR biomass under steady-state conditions. During this phase the reactor was fed with 46.2 mL h^{-1} of nutrient solution thus obtaining a dilution rate of 0.01 h^{-1}, which was low enough to avoid the washout of the biomass. Aliquots were withdrawn for respirometric tests as described in the next section. The headspace of CSTR-3 was continuously gassed with Argon (100 mL min^{-1}) to operate under anoxic conditions. The liquid phase was daily sampled to analyze nitrite, nitrate, sulfate, sulfide and VSS (*see section 4.2.1*). Moreover, biomass samples were weekly taken from the reactor to verify the microbial diversity preservation by DGGE (*see section 4.2.1*). The $Y_{x/s}$ was also calculated at steady-state conditions according to Eq. 7.1.

$$Y_{x/s} = \frac{[VSS]_{out} - [VSS]_{in}}{[SO_4^{2-}-S]_{in} - [SO_4^{2-}-S]_{out}} \qquad (7.1)$$

Where VSS_{out} and VSS_{in} are the biomass concentrations (mg VSS L^{-1}) at the outlet an inlet flows of the reactor, respectively, and SO_4^{2-}-S_{in} and SO_4^{2-}-S_{out} are the inlet and outlet sulfate concentrations (mg SO_4^{2-}-S L^{-1}), respectively.

7.2.2. Respirometric tests

A set of biotic tests (Table 7.1) were performed at 30 ºC and a pH value of 7.5 in RV-2 (*see section 4.1.3*) with SO-NR biomass obtained from CSTR-3 following the methodology proposed in Chapter 5 (see section 5.2.2). An Argon flow of 50 mL min^{-1} was sparged to the headspace of the respirometer in order to minimize the carbon source and sulfide stripping whereas maintaining anoxic conditions. Tests I-1, I-2, S-1 and S-2 were used to calibrate the kinetics of the process while test S-3 was used in order to validate the kinetic model (Table 7.1). Nitrite and sulfide inhibitions were firstly studied in tests I-1 and I-2 by adding sequential pulses of the species to the respirometer and estimating the specific uptake rate in each pulse. Afterwards, tests S-1 and S-2 were conducted to study separately the two-step sulfide oxidation with each electron acceptor. Finally, model validation in experiment S-3 was performed with the single addition of nitrate as electron acceptor.

Table 7.1. Biotic tests conducted to calibrate and validate the kinetics of sulfide oxidation in anoxic conditions

Test	Process	Nitrite (mg N L^{-1})	Nitrate (mg N L^{-1})	Sulfide (mg S L^{-1})
I-1	Nitrite inhibition	1.5-95	0	3.5-15
I-2	Sulfide inhibition	3.5-15	0	1.5-110
S-1	Sulfide oxidation	0	35	30
S-2	Sulfide oxidation	20	0	13
S-3	Sulfide oxidation	0	40	10

7.2.3. Carbon source and substrate stripping

To study the biological mechanisms and kinetics of a SO-NR microbial population in a respirometer is essential to previously characterize the physical and chemical processes that take place simultaneously to the biological processes. In this particular case, anoxic respirometric assays must be performed using a continuous inert gas flow, thus implying the stripping of both the volatile substrate and the carbon

source. The characterization of CO_2 and H_2S stripping processes was made through several abiotic tests conducted previously to the biological studies. The conditions and the mineral medium used to perform the abiotic tests were those used in the biotic tests. On the one hand, H_2S stripping was characterized with three different initial sulfide concentrations (3.2, 12 and 40 mg S^{2-} L^{-1}). Eqs. 7.2 and 7.3, corresponding to the mass balance and chemical equilibriums of H_2S (Gonzalez-Sanchez et al., 2009), were used to estimate the global mass transfer coefficient K_La by curve fitting of experimental profiles of dissolved sulfide to Eq. 7.3 by means of MATLAB 7.7 (Mathworks, Natik, MA).

$$\frac{dH_2S}{dt} = \frac{V_L}{V_G} \cdot K_La_{H_2S} \cdot \left[\left(\frac{S_{H_2S}}{1+10^{[pH-pk1]}+10^{[2\cdot pH-(pk_1+pk_2)]}} \right) - \frac{H_2S_{(g)}}{He} \right] - \left(\frac{F_{Ar}}{V_G} \cdot H_2S_{(g)} \right) \qquad (7.2)$$

$$\frac{dS_{H_2S}}{dt} = -\left[1+10^{[pH-pk1]}+10^{[2\cdot pH-(pk_1+pk_2)]} \right] \cdot K_La_{H_2S} \cdot \left[\left(\frac{S_{H_2S}}{1+10^{[pH-pk1]}+10^{[2\cdot pH-(pk_1+pk_2)]}} \right) - \frac{H_2S_{(g)}}{He} \right] \qquad (7.3)$$

Where V_L and V_G are the liquid and gas volumes in the respirometer (L), S_{H2S} is the dissolved sulfide concentration (mM), He is the dimensionless Henry's law constant, pka_1 and pka_2 are the logarithmic values of the acid dissociation constants and F_{ar} is the Argon flow (L h^{-1}). On the other hand, a titrimetric test was conducted following the methodology proposed in Lopez et al. (2013) to characterize CO_2 stripping. By this way, an initial pulse of 50 mg C L^{-1} was added to investigate whether such carbon concentration would limit the reaction rate during respirometric tests.

7.2.4. Kinetic model

Two different kinetic equations were proposed to describe the experimental respirometric profiles obtained using nitrate and nitrite as electron acceptors. The kinetic model proposed for H_2S and elemental sulfur oxidation associated to nitrate reduction is presented through Eqs. 7.4 and 7.5. For sulfide oxidation, a Haldane-type term was proposed to describe substrate inhibition by sulfide while nitrate reduction followed a Monod-type kinetic equation. For elemental sulfur oxidation, a Monod-type

term was considered for both elemental sulfur and nitrate. However, a non-competitive inhibition term was included to investigate the effect of sulfide on elemental sulfur oxidation.

$$r_{N,1} = \frac{1}{Y_{(X/S^{2-})_N}} \cdot \frac{\mu_{max_1,N} \cdot S^{2-}}{K_{S^{2-}} + S^{2-} + \frac{\left(S^{2-}\right)^2}{K_{is}}} \cdot \frac{N}{K_N + N} \cdot X \tag{7.4}$$

$$r_{N,2} = \frac{1}{Y_{(X/S^0)_N}} \cdot \frac{\mu_{max_2,N} \cdot S^0}{K_{S^0} + S^0} \cdot \frac{N}{K_N + N} \cdot \frac{K}{K + S^{2-}} \cdot X \tag{7.5}$$

Where $\mu_{max1,N}$ and $\mu_{max2,N}$ are the maximum specific uptake rates for sulfide and sulfur oxidation (h^{-1}), respectively, K_{S2-}, k_{S0} and K_N are the affinity constants for the substrates (sulfide and sulfur) and nitrate (mg L^{-1}), K_{is} is the sulfide inhibition constant (mg S L^{-1}), K is the inhibition constant for elemental sulfur oxidation (mg S L^{-1}), X is the biomass concentration (mg VSS L^{-1}), $Y_{(x/s)N}$ is the biomass growth yield using nitrate as electron acceptor (g X g^{-1} substrate) and S^{2-}, S^0 and N are sulfide, elemental sulfur and nitrate concentrations, respectively (mg S L^{-1} or mg NO_3^--N L^{-1}).

Since some authors have found that equivalent reactions occur with nitrite as an intermediate of the denitrification process with sulfide and elemental sulfur (An et al., 2010; Dogan et al., 2012), Eqs. 7.6 and 7.7 have been defined to describe denitritation with sulfide and elemental sulfur, respectively. Also, a Haldane-type inhibition term for nitrite has been considered for substrate inhibition. Maximum specific growth rates, half-saturation constants and inhibition constants were determined by curve fitting to respirometric profiles by means of MATLAB 7.7 (Mathworks, Natik, MA).

$$r_{Nit,1} = \frac{1}{Y_{(X/S^{2-})_{Nit}}} \cdot \frac{\mu_{max_1,Nit} \cdot S^{2-}}{K_{S^{2-}} + S^{2-} + \frac{(S^{2-})^2}{K_{is}}} \cdot \frac{Nit}{K_{Nit} + Nit + \frac{(Nit)^2}{K_{iNit}}} \cdot X \qquad (7.6)$$

$$r_{Nit,2} = \frac{1}{Y_{(X/S^0)_{Nit}}} \cdot \frac{\mu_{max_2,Nit} \cdot S^0}{K_{S0} + S^0} \cdot \frac{Nit}{K_{Nit} + Nit + \frac{(Nit)^2}{K_{iNit}}} \cdot \frac{K}{K + S^{2-}} \cdot X \qquad (7.7)$$

Where $\mu_{max1,Nit}$ and $\mu_{max2,Nit}$ are the maximum specific uptake rates for sulfide and elemental sulfur oxidation (h^{-1}), respectively, K_{Nit} and K_{iNit} are the affinity and the inhibition constant for nitrite (mg N L^{-1}), respectively, $Y_{(x/s)Nit}$ is the biomass growth yield using nitrite as electron acceptor (g X g^{-1} substrate) and Nit is the nitrite concentration (mg N L^{-1}).

7.3. RESULTS AND DISCUSSION

7.3.1. Assessment of the SO-NR cultivation in a CSTR

Biomass withdrawn from the anoxic BTF was successfully grown in a fermenter as a suspended culture (Figure 7.1a). During the first stage of the operation (65h of fed-batch operation) the biomass was gradually consuming the nitrate to oxidize the sulfide to sulfate while being acclimated to suspended conditions. After the fed-batch operation, the continuous operation was started being the biomass progressively washed from the reactor until reaching the steady state after 350h of operation. Nitrite was neither observed during the fed-batch nor during the continuous operations indicating that sulfide and nitrate were consumed in stoichiometric ratio and that neither the denitritation nor the elemental sulfur oxidation was limited at a dilution rate of 0.01 h^{-1}. A maximum 6% of elemental sulfur was detected probably due to nitrate limitation which was maintained under 15 mg N L^{-1} during almost the whole continuous operation although arriving occasionally to concentrations under 1 mg N L^{-1}. The dilution rate set (0.01 h^{-1}) avoided the biomass and diversity washout. The latter was verified with

DGGE analysis which showed that most of the species detected in the inoculum were preserved during reactor operation as CSTR (Figure 7.1b). This result indicates that the immobilized SO-NR mixed culture from the BTF was well acclimated to suspended culture conditions. In addition, a pure culture of *Thiobacillus denitrificans* DSM 12475 was also analyzed since this has been commonly reported as a typical bacteria in anoxic BTFs (Soreanu et al., 2008). However, no coincidence was found between SO-NR mixed culture species lanes and the abovementioned pure culture lane.
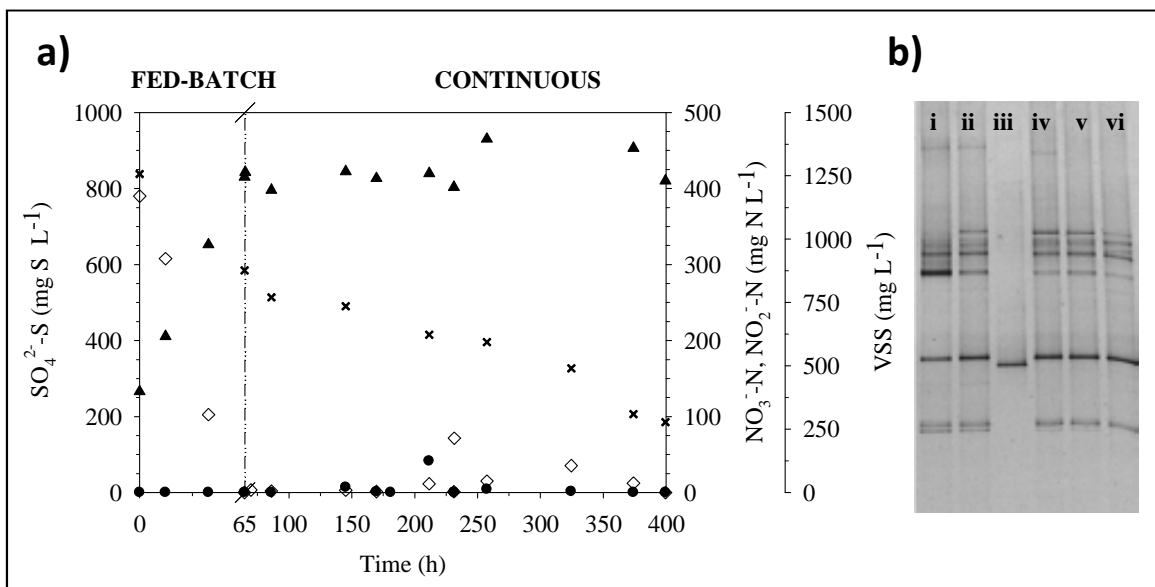

Figure 7.1. (a) Operation of the CSTR until steady state condition **(b)** DGGE fingerprinting (i) 21 days of operation (ii) 15 days of operation (iii) *Thiobacillus denitrificans* pure culture (iv) Three times of the hydraulic retention time (HRT) (v) Two times of the HRT (vi) Inoculation. Symbols: Sulfate (▲), Nitrate (◇), Biomass (✕) and Nitrite (●).

An $Y_{x/s}$ of 0.328±0.045 g VSS g^{-1} S was calculated after 350 h of operation when steady-state conditions were reached (Figure 7.1a). Considering the $Y_{x/s}$ calculated, the stoichiometry of the overall oxidation reaction was obtained (Eq. 7.8) by solving the mass and charge balances according to Roels (1983), assuming $C_5H_7O_2N$ as typical biomass composition (Heijnen, 2002) and NH_4^+ as the nitrogen source.

$$HS^- + 1.23\ NO_3^- + 0.573\ H^+ + 0.438\ HCO_3^- + 0.027\ CO_2 + 0.093\ NH_4^+ + \rightarrow$$

$$0.093\ C_5H_7O_2N + 0.866\ H_2O + 0.614\ N_2 + SO_4^{2-} \tag{7.8}$$
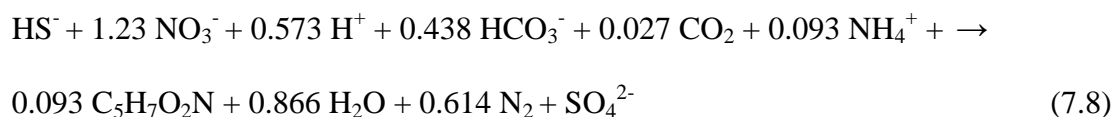
The S/N ratio calculated from the global reaction stoichiometry (Eq. 7.8) (0.813 mol HS^- mol^{-1} NO_3^-) was different compared to S/N ratios in the range of 0.56 and 0.75 g VSS g^{-1} S obtained by other authors for the complete oxidation to sulfate (Vaiopoulou et al., 2005; Cardoso et al., 2006; Yavuz et al., 2007) but similar to that proposed by Campos et al. (2008) (0.842 mol S mol^{-1} NO_3^-). This result indicates that stoichiometric coefficients, which are essential to characterize a microbial culture, should be solved for each specific biomass in order to accurately estimate the corresponding kinetic coefficients as previously concluded in previous chapters (*see Chapter 6*).

7.3.2. Characterization of sulfide and CO_2 stripping

The titrimetric test performed per triplicate to characterize the CO_2 stripping process as well as the modeled profile and the predicted TIC evolution, are shown in Figure 7.2b. A K_La of 0.840±0.186 h^{-1} was found to accurately fit the experimental data with the CO_2 stripping model. This value was very low if compared with those of liquid bubbled systems, which helped to minimize the carbon source stripping (López et al., 2013). This result is also reflected in the TIC profile (Figure 7.2b), where a 40% of the initial concentration is lost after 600 min of experiment, confirming that no carbon source limitation nor slowed respirometric rates would appear during biotic tests.

Regarding sulfide stripping, it can be observed that model prediction accurately fitted the experimental data (Figure 7.2a). An average K_La of 0.739±0.171 h^{-1} was calculated taking into account the estimations of the three different concentrations tested. This result indicated that the stripping of sulfide was also minimized since González-Sánchez et al. (2009) obtained a value of 1.2 h^{-1} for a similar respirometric system when the liquid was bubbled into the liquid phase with an air flow of 18 mL min^{-1}. As expected, K_La values obtained for CO_2 and H_2S using an Argon flow of 50 mL min^{-1} were similar since this parameter depends on the hydrodynamics of the system being practically not influenced by the characteristics of the species in diluted solutions for similar diffusion coefficients.
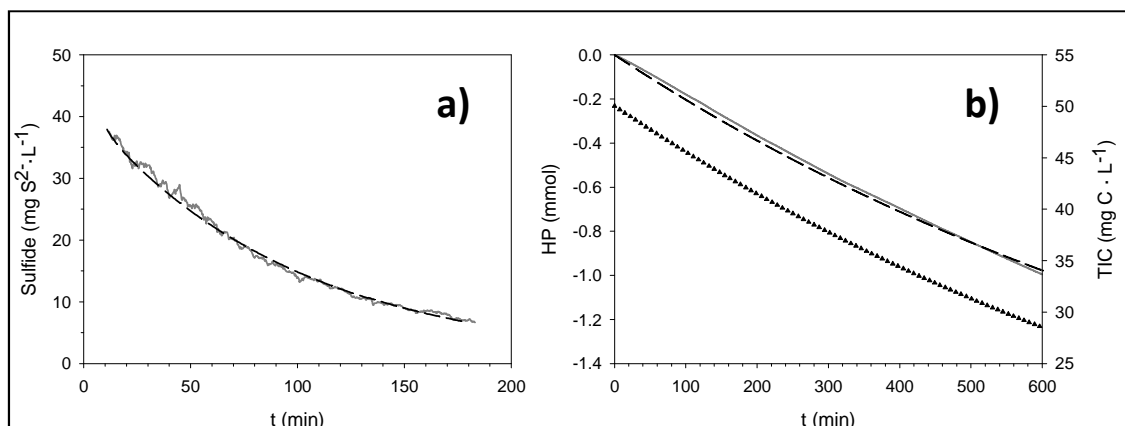
Figure 7.2. Abiotic stripping tests profiles. (a) Sulfide stripping test performed with 1.5 mM S^{2-} (b) CO_2 stripping characterization. Experimental data (solid line), Model data (dashed line) and TIC predicted profile (symbol).

7.3.3.   Kinetic analysis of sulfide and nitrite inhibitions

As already known, nitrite is an intermediate in the denitrification process ($NO_3^- \rightarrow NO_2^- \rightarrow N_2$) being accumulated when denitritation is the rate limiting step. In this research, although nitrite accumulation was not observed during the respirometric tests, the nitrite effect was studied since many authors have reported inhibition caused by nitrite over denitrification (Soto et al., 2007; Fajardo et al., 2014) and, consequently, on desulfurization. Sulfide inhibition on desulfurization has already been reported (Reyes-Avila et al., 2004; Cardoso et al., 2006; Gonzalez-Sanchez et al., 2009) but there is a lack of knowledge on kinetic inhibition parameters being necessary further investigation. In this chapter the inhibition kinetics caused by the presence of these compounds were modeled through a Haldane-type expression using the experimental data obtained from tests I-1 and I-2. From Figure 7.3 it can be observed that denitritation as well as sulfide oxidation was well described with the Haldane model confirming the existence of both inhibitions.

105
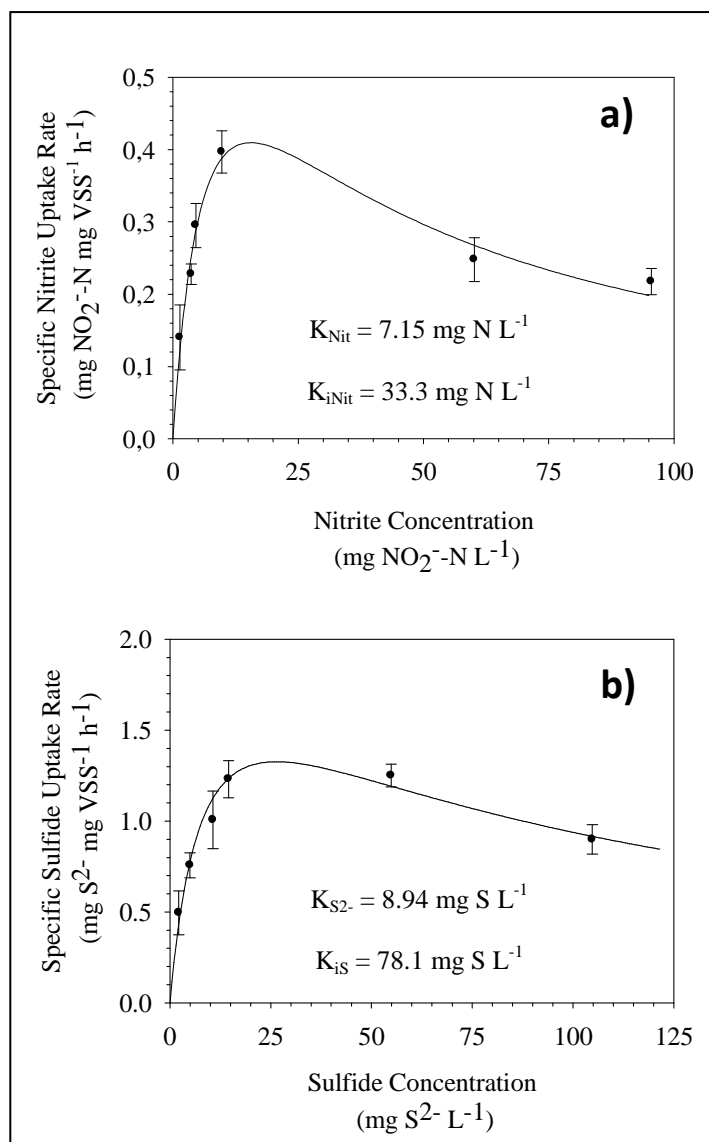
Figure 7.3. Haldane-type kinetics modeling (a) Nitrite inhibition (b) Sulfide inhibition. Experimental data (symbol) and Model data (solid line).

On the one hand, kinetic coefficients obtained for nitrite inhibition were in agreement with those reported by Fajardo et al. (2014) (K_{Nit}=10.7 mg N L^{-1} and $K_{i,Nit}$=34.7 mg N L^{-1}) for autotrophic denitrifying biomass who also observed less than a 40% of nitrite reduction at concentration over 80 mg NO_2^--N L^{-1}. Other authors have also reported satisfactory description of nitrite inhibition considering different kinetic models (Wild et al., 1995; Soto et al., 2007), which indicates that nitrite inhibition mechanisms require to be further investigated. On the other hand, kinetic coefficients obtained from the sulfide inhibition test (I-2) were especially higher (K_s=8.94 mg S L^{-1}

and K_{is}=78.1 mg S L^{-1}) than those obtained by Gonzalez-Sanchez et al. (2009) for aerobic desulfurizing cultures (K_s=0.032 mg S L^{-1} and K_{is}=32.48 mg S L^{-1}). This indicates that the biomass developed in the anoxic BTF presented less activity at significantly higher sulfide concentrations ($S^{2-} < 22.5$ mg S L^{-1}). Conversely, the anoxic biomass was less inhibited by sulfide. This result was obtained probably because the anoxic BTF was operating at both high empty bed residence time and sulfide concentration. Results also confirm that inhibitory limits, and consequently the inhibition constants estimated, largely depend on the exposure and acclimation of microbial cultures to their environment and must be determined case-by-case.

7.3.4. Sulfide oxidation using nitrate as the electron acceptor

Experimental respirometric data corresponding to the sulfide oxidation test performed with nitrate (S-1) is presented in Figure 7.4a. As can be observed, sulfide was initially oxidized to elemental sulfur since sulfate concentration remained almost constant during the first 20 minutes. Moreover, as mentioned above, nitrite was not detected during the experiment being the partial denitrification of nitrate not considered in this particular case. From these results the stoichiometry of the two-step sulfide oxidation associated to denitratation was solved (Eqs. 7.9 and 7.10) using the overall biological reaction previously solved (Eq. 7.8) and the nitrate to sulfate ratio obtained from the last 20 minutes of the respirometric test (N/S=0.35) in which the unique reaction taking place was the oxidation of elemental sulfur.

$$HS^- + 0.350\ NO_3^- + 1.40\ H^+ + 0.059\ HCO_3^- + 0.004\ CO_2 + 0.013\ NH_4^+ \rightarrow$$

$$0.013\ C_5H_7O_2N + 1.21\ H_2O + 0.175\ N_2 + S^0 \tag{7.9}$$

$$S^0 + 0.876\ NO_3^- + 0.343\ H_2O + 0.379\ HCO_3^- + 0.023\ CO_2 + 0.080\ NH_4^+ \rightarrow$$

$$0.080\ C_5H_7O_2N + 0.824\ H^+ + 0.44\ N_2 + SO_4^{2-} \tag{7.10}$$
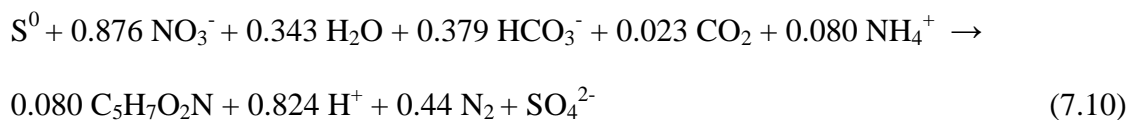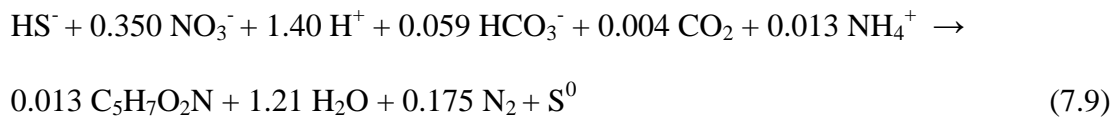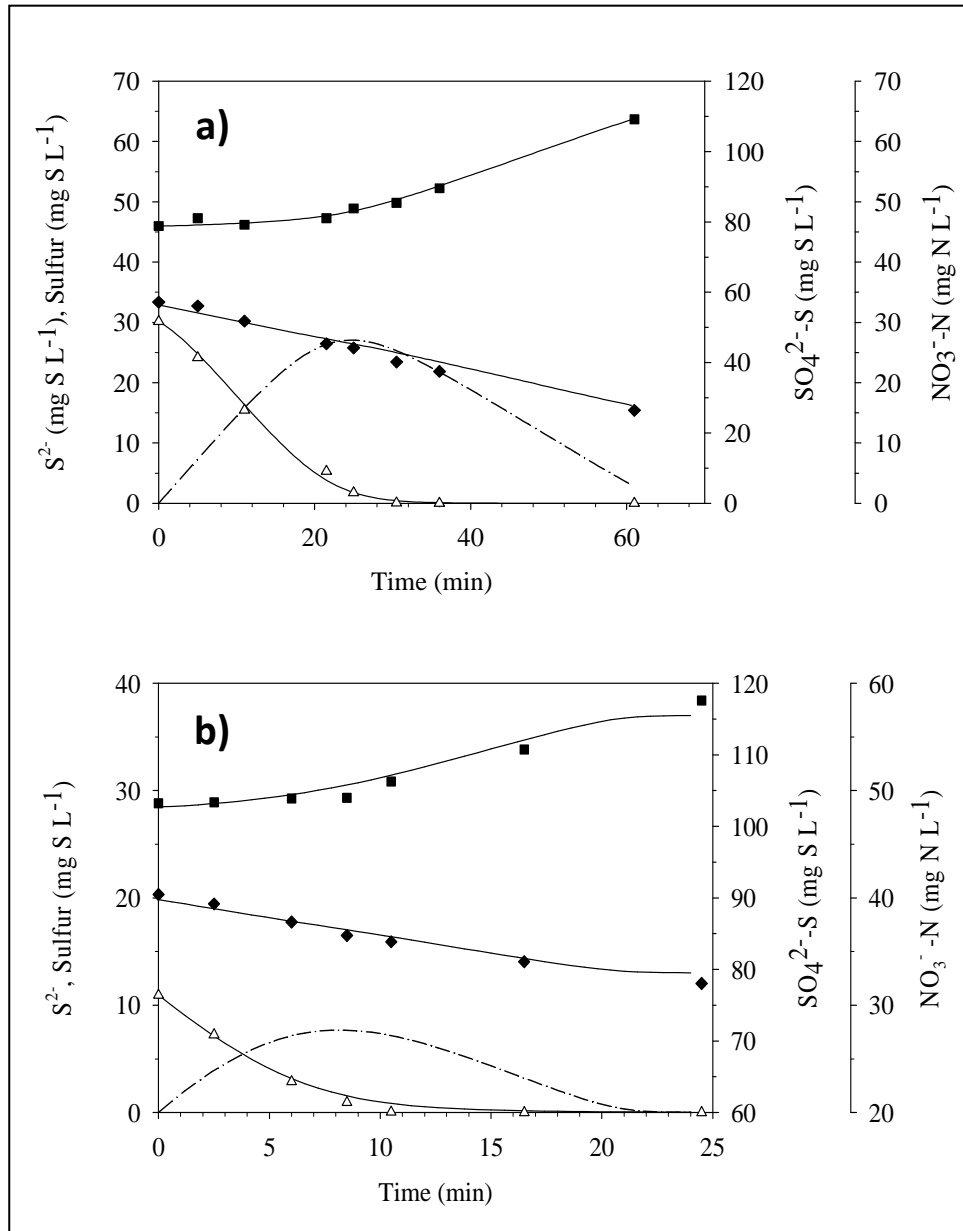
Figure 7.4. Kinetic modeling of sulfide oxidation using nitrate as electron acceptor (Tests S-1 and S-3). (a) Model calibration (b) Model validation. Sulfate (■), Nitrate (◆), Sulfide (△), Elemental sulfur (dot line), Model data (solid line).

In Figure 7.4a the predicted profiles and experimental data for all species, including the expected profile for elemental sulfur, are shown. Haldane kinetic parameters obtained previously (Figure 7.3) and the affinity constant related to nitrate

108

(K_N = 1.30 mg N L^{-1}) reported by Artiga et al. (2005) were used to estimate the remaining parameters ($\mu_{max1,N}$, $\mu_{max2,N}$, K and k_{S0}) for experiment S-1. As can be observed, a satisfactory prediction of the experimental data was obtained with the model calibration. The estimated parameters (Table 7.2) were used to validate the kinetic model with the experimental data obtained from test S-3, which is presented in Figure 7.4b. Again, the model calibrated in experiment S-1 effectively predicted the experimental profiles of experiment S-3 performed at a different S/N ratio.

From the respirometric profile of test S-1 it was confirmed that nitrite was not accumulated as an intermediate of denitrification thus indicating that the denitritation rate was not a limiting step. Furthermore, nitrite reduction was neither influenced by an excess of nitrate nor by sulfide under 30 mg S L^{-1}. Some authors have associated nitrite accumulation with a sulfide limitation (Manconi et al., 2007) although according to McMurray et al. (2004) products arising from stepwise denitrification depend mainly on the bacterial community, their environmental conditions and the availability of the carbon source. For this reason, the stoichiometry of a biological process must be previously adapted and solved for each microbial culture to accurately describe the biodegradation mechanisms. In this chapter the calculated stoichiometric coefficients corresponding to the two-step sulfide oxidation using nitrate as electron acceptor were different from those thermodynamically calculated by other authors (Kleerebezem and Mendez, 2002; Yavuz et al., 2007). This result indicates that the use of experimental data is necessary in order to obtain specific coefficients. Otherwise, some kinetic parameters such as the specific growth rates could be under or over estimated. Moreover, the stoichiometry in this study does not consider the partial denitrification since the SO-NR culture had a high denitritation activity.

Regarding sulfide oxidation, elemental sulfur was not oxidized until sulfide was almost depleted (K=3.04 mg S L^{-1}), which indicates the existence of a non-competitive inhibition of sulfide over the elemental sulfur oxidation rate. This observation is in agreement with that observed by An et al. (2010). Nonetheless, Can-Dogan et al. (2010) observed the formation of elemental sulfur under nitrate limiting conditions and suggested that the end product of sulfide oxidation depended on the ratio of the nitrogen source to sulfide. Manconi et al. (2007) neither observed inhibition by sulfide over elemental sulfur oxidation with SO-NR mixed cultures but detected a milky appearance
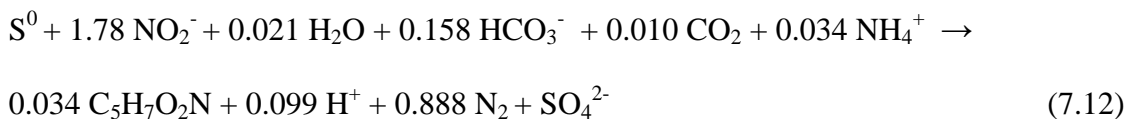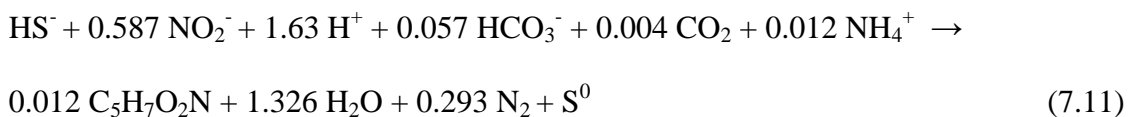
of the reactor during sulfide-excess operating conditions, which does not agree with the results obtained in this chapter. This leads again to conclude that anoxic sulfide oxidation mechanisms depended mainly on the microbial community composition and its acclimation to different substrates.

The stoichiometry solved to express the two-step sulfide oxidation with nitrate combined with the kinetic model proposed satisfactorily described the respirometric profile obtained from test S-1 and S-3. In the literature few comparable studies providing the kinetic characterization of autotrophic denitrification using sulfide as electron donor have been found. An et al. (2010) reported μ_{max} values ranging from 0.08 to 0.17 h^{-1} using a mixed culture from the water treatment of oil industry which were similar to those obtained in this study (Table 7.2). Gadekar et al. (2006) also reported a μ_{max} of 0.36 h^{-1} with a pure culture of *Thiomicrospira sp.*. In any case, Figure 7.4b shows that the model was satisfactorily validated with test S-3, which was performed at different sulfide concentration from that used in test S-1, indicating that the kinetic data estimated from the calibration was able to adequately describe the sulfide oxidation under anoxic conditions.

7.3.5. Sulfide oxidation using nitrite as the electron acceptor

In the case of nitrite, thermodynamically calculated biomass growth yields reported by Dogan et al. (2012) were used in order to solve the total reaction stoichiometry (Eqs. 7.11 - 7.13) since the CSTR was not operated with this electron acceptor.

- *Two-step sulfide oxidation*

$HS^- + 0.587\ NO_2^- + 1.63\ H^+ + 0.057\ HCO_3^- + 0.004\ CO_2 + 0.012\ NH_4^+ \rightarrow$

$0.012\ C_5H_7O_2N + 1.326\ H_2O + 0.293\ N_2 + S^0$ $\qquad\qquad$ (7.11)

$S^0 + 1.78\ NO_2^- + 0.021\ H_2O + 0.158\ HCO_3^- + 0.010\ CO_2 + 0.034\ NH_4^+ \rightarrow$

$0.034\ C_5H_7O_2N + 0.099\ H^+ + 0.888\ N_2 + SO_4^{2-}$ $\qquad\qquad$ (7.12)

- Overall sulfide oxidation

$HS^- + 2.36\ NO_2^- + 1.53\ H^+ + 0.215\ HCO_3^- + 0.013\ CO_2 + 0.046\ NH_4^+ \rightarrow$

$0.046\ C_5H_7O_2N + 1.30\ H_2O + 1.18\ N_2 + SO_4^{2-}$ (7.13)
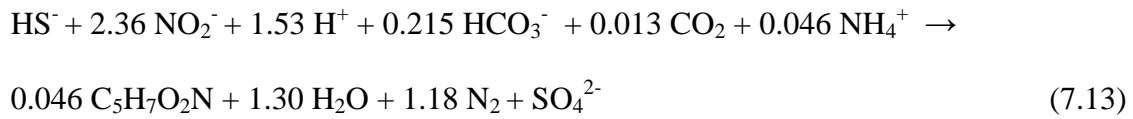
As shown in Figure 7.5, the kinetic model together with the calculated stoichiometric coefficients properly described the respirometric profile corresponding to test S-2, which was performed uniquely with nitrite as electron acceptor.
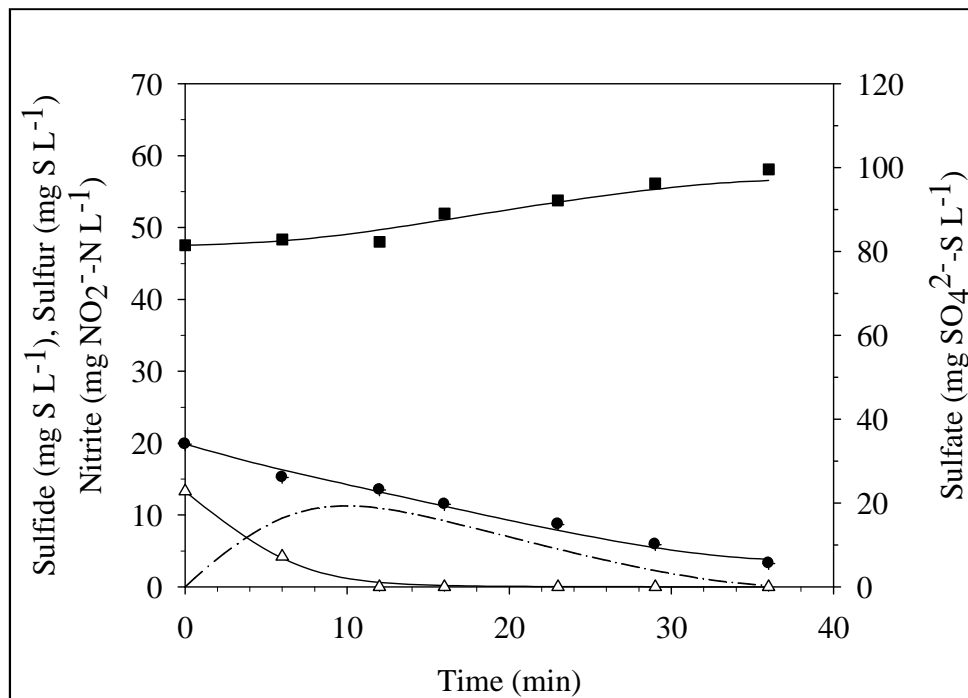
Figure 7.5. Kinetic modeling of sulfide oxidation using nitrite as electron acceptor (Test S-2). Sulfate (■), Nitrite (●), Sulfide (△), Elemental sulfur (dot line) and Model data (solid line).

From the fitting of the experimental data, the maximum specific growth rates corresponding to each of the process considered ($\mu_{max1,Nit}$, $\mu_{max2,Nit}$) (Eqs. 7.11 and 7.12) were estimated (Table 7.2). It was observed that the kinetic parameters were noticeably different from those found from test S-1 for each electron acceptor used. Parameters estimated by curve fitting to experimental data in test S-2 served to satisfactorily predict

the experimental profiles. However, since thermodynamically calculated stoichiometric coefficients were used the maximum specific growth rates $\mu_{max1,Nit}$ and $\mu_{max2,Nit}$ were less accurately estimated. However, less biomass was produced per mol of sulfide even if the desulfurizing activity with nitrite was comparable to that obtained using nitrate under non-inhibiting concentrations. These findings are in agreement with Dogan et al. (2012) who proposed the use of nitrite as an advantageous option in order to reduce the biomass production as well as to improve the sulfide oxidation rates. A direct consequence of such finding is that the use of non-inhibiting concentrations of nitrite in an anoxic desulfurizing BTF could minimize or even avoid the clogging of the trickling bed due to an excessive biomass growth as well as to enhance the elimination capacity of the system.

Table 7.2. Biokinetic parameters determined from the fitting of the experimental respirometric profiles with the kinetic models proposed (T=30ºC; pH=7.5)

Coefficients	Values	Units
$\mu_{max\,1,N}$	0.125	h^{-1}
$\mu_{max\,2,N}$	0.218	h^{-1}
$\mu_{max\,1,Nit}$	0.187	h^{-1}
$\mu_{max\,2,Nit}$	0.093	h^{-1}
K_{Nit}	7.15	mg N L^{-1}
$K_{i,Nit}$	33.3	mg N L^{-1}
$K_{S^{2-}}$	8.94	mg S L^{-1}
$K_{i,S^{2-}}$	78.1	mg S L^{-1}
K_{S^0}	0.609	mg S L^{-1}
K	3.04	mg S L^{-1}

7.4. CONCLUSIONS

Overall, results obtained in this chapter demonstrated that respirometry and titrimetry can effectively be applied to investigate the mechanisms and kinetics of anoxic desulfurization. The complete kinetic model proposed satisfactorily fitted the experimental respirometric profiles. The model considered the inhibition caused by nitrite and sulfide over the biological process (substrate inhibition kinetic) as well as the non-competitive inhibition caused by sulfide on elemental sulfur oxidation since sulfate production was not observed until sulfide was almost depleted. Moreover, the partial denitrification of nitrate was not observed indicating that the microbial community had a high denitritating activity. Kinetic parameters were accurately estimated and validated being a future challenge the optimization of the BTF operation by incorporating the kinetic model in the general model describing the desulfurization under anoxic conditions.

Chapter 8

APPLICATION OF LFS RESPIROMETRY TO CHARACTERIZE SULFIDE, ELEMENTAL SULFUR AND THIOSULFATE OXIDATION KINETICS AND STOICHIOMETRY BY SOB

8. APPLICATION OF LFS RESPIROMETRY TO CHARACTERIZE SULFIDE, ELEMENTAL SULFUR AND THIOSULFATE OXIDATION KINETICS AND STOICHIOMETRY BY SOB

In this chapter the well-known LFS respirometry was applied in order to perform the kinetic characterization of aerobic biomass obtained from a desulfurizing biotrickling filter. This research was especially interesting since many studies have been performed to characterize the kinetics of S-oxidizing biomass but there is not a clear agreement about desulfurization mechanisms at neutral conditions. Then, to increase the knowledge, the oxidation mechanisms were studied besides the stoichiometry solved and kinetics estimated. It was also interesting to study the chemical oxidation of sulfide in the presence of oxygen which has been reported as a very reactive species even in the absence of catalyzers. Moreover, since model parameters and some degradation mechanisms are specific of each culture, the pyrosequencing technique was applied in order to know more about the bacterial diversity of the biomass.
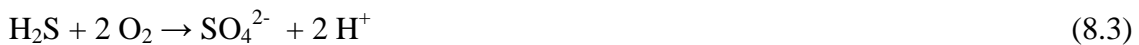
Abstract

LFS respirometry has been used in this chapter to find out which are the mechanisms implicated in aerobic biological sulfide oxidation. Other physical-chemical phenomena, such as stripping or chemical oxidation of sulfide, were characterized since they might cause interference over the biological activity measurement. The global mass transfer coefficient for sulfide and the kinetic parameters corresponding to the chemical oxidation of sulfide with oxygen were estimated. A biodegradation mechanism was proposed besides the stoichiometry of the process solved. A kinetic model describing each of the reactions occurring during sulfide oxidation was calibrated and validated. No product selectivity was found related to the O_2/S ratio available in the medium. Moreover, it was found that sulfide was preferentially consumed and oxidized to elemental sulfur even though an excess of oxygen was present in the medium. The shrinking particle equation was included in the kinetic model to describe elemental sulfur oxidation since the oxygen profile could not be described with a simple Monod equation. The high sensitivity associated to oxygen monitoring allowed selecting the equation that better described elemental sulfur oxidation although further investigation is required in order to improve the fitting of the experimental dissolved oxygen profiles.

A modified version of this chapter is being prepared for publication as :

8.1. INTRODUCTION

Desulfurization of biogas under aerobic conditions using biotrickling filters has been demonstrated as an efficient and environmentally friendly technique to upgrade biogas. The problem is that, although air is currently used as the most economical source electron acceptor to oxidize sulfide from biogas, it cannot be added in large amounts since dilutes biogas and it is dangerous due to its explosiveness. Then, when high loads of sulfide are treated, elemental sulfur, which is the intermediate compound of the oxidation reaction, is produced and accumulated inside the packed bed as a consequence of oxygen transfer limitation (Fortuny et al., 2008; Rodriguez et al., 2014) (Eqs. 8.1 to 8.3). This fact causes operation problems such as pressure drop increase due to reactor clogging. For this reason, a general mathematical model describing desulfurization in a biotrickling filter is necessary in order to both, gain knowledge and to optimize the process. Once the model is developed many control strategies could be applied in order to obtain the best operating conditions to avoid elemental sulfur accumulation (Almenglo et al., 2013). In this sense, mathematical models describing the kinetics of sulfur oxidizing bacteria obtained from a desulfurizing biotrickling filter are especially desirable to be developed and calibrated. Once the kinetics have been determined, they can be incorporated in the above mentioned general model since the bacterial activity is one of the most important processes occurring in these systems.

$$H_2S + 0.5\ O_2 \rightarrow S^0 + H_2O \tag{8.1}$$

$$S^0 + 1.5\ O_2 + H_2O \rightarrow SO_4^{2-} + 2\ H^+ \tag{8.2}$$

$$H_2S + 2\ O_2 \rightarrow SO_4^{2-} + 2\ H^+ \tag{8.3}$$

The characterization of different types of biomass has been successfully performed through LFS respirometric techniques due to the high sensitivity associated to dissolved oxygen monitoring (Spanjers et al., 1996; Jubany et al., 2005). In BTFs, the S-oxidizing biomass to be characterized is not suspended in a liquid phase but immobilized on the packing material of an aerobic desulfurizing biotrickling filter. The main disadvantage

of the immobilized biomass is that, the biomass growth yield, as well as the biomass concentration, sulfide oxidation mechanisms and desulfurizing activity, is difficult to obtain if the biomass is not grown as a suspended culture. Gonzalez-Sanchez et al. (2009) already applied LFS respirometry to characterize S-oxidizing immobilized biomass. Other authors have reported respirometric techniques using directly the packing material with immobilized biomass (Delhomenie et al., 2008). The problem with these techniques is that the conditions are not perfectly controlled (pH, homogeneity, active fraction of biomass and nutrients recirculation among others. LFS respirometry allows overcoming these problems and the only factor to be considered (in order to use the kinetics in a biofiltration model) is the correction needed for the active fraction and the biomass concentration to represent the immobilized biomass.

The kinetic description of sulfide oxidation is not that obvious. In fact, many authors have reported the characterization of suspended SOB but there is not a clear agreement about the kinetics describing sulfide oxidation and elemental sulfur production and consumption. Some authors have considered just Monod or Haldane equations to describe limitation or inhibition caused by sulfide over sulfide oxidation, respectively (Roosta et al., 2011; Mora et al., 2014a). More complex kinetic models related to the physiology of S-oxidizing biomass have also been reported (Klok et al., 2013). Regarding to elemental sulfur oxidation, kinetic models considering Monod equation or half or zero-order equations have also been reported (Koenig and Liu, 2001; Munz et al., 2009; Roosta et al., 2011; Mora et al., 2014a). As mentioned above, there is not a standard mathematical model to describe this biological process. Then, the main objective of this chapter was to develop, calibrate and validate a kinetic model for the aerobic biological sulfide oxidation. The model should take into account all the mechanisms involved in the process, in order to be subsequently used in a general model describing aerobic desulfurization in a biotrickling filter.

8.2. MATERIALS AND METHODS

8.2.1.   SOB cultivation and biomass growth yield calculation

An integrated sample of biomass was extracted from a lab-scale aerobic desulfurizing BTF. The bioreactor had been treating 2000 ppm$_v$ of H$_2$S during 1 year at

room temperature and pH 7.0. The BTF was packed with plastic pall rings (3 L of packing material) and was divided into three sections. From each section 3 pieces of packing material with biofilm attached were collected and washed in 500 mL of mineral medium with the following composition (g L^{-1}): NaHCO$_3$ (3.5); NH$_4$Cl (1); KH$_2$PO$_4$ (0.12); K$_2$HPO$_4$ (0.15); CaCl$_2$ (0.02); MgSO$_4$·7H$_2$O (0.2); and trace elements, 1 mL L^{-1} (Fortuny et al., 2008). Afterwards, the mineral medium with the suspended biomass was used to inoculate a sterilized reactor (CSTR-2, *see section 4.1.1*) which was operated as a continuous reactor without biomass recirculation.

Mineral medium and dissolved sulfide were fed separately to avoid reactions between sulfide and the metallic species contained in the mineral medium (trace elements). A flow of 7.9 mL h^{-1} of sulfide solution (10 g S-Na$_2$S·9H$_2$O L^{-1}) was supplied during the whole operation which corresponds to a loading rate of 27.5 g S m^{-3} reactor h^{-1}. A total flow of 42.5 mL h^{-1} was supplied thus obtaining a dilution rate of 0.015 h^{-1}. An air flow of 20 L h^{-1} was also supplied through a diffuser located at the bottom of the reactor in order to promote the complete oxidation of sulfide. The biomass was cultivated during almost 4 weeks. After steady-state conditions were reached, aliquots of the suspended culture were withdrawn for respirometric tests as described in the next section.

The liquid phase was daily sampled to analyze sulfate, thiosulfate, sulfide and volatile suspended solids (*see section 4.2.1*). Moreover, biomass samples from the inoculum as well as at the steady-state were taken from the reactor to verify microbial diversity preservation by a pyrosequencing analysis (*see section 4.2.1*). The Y$_{x/s}$ was also calculated at steady-state according to Eq. 7.1.

8.2.2. Characterization of H$_2$S stripping and chemical oxidation

H$_2$S stripping and chemical oxidation processes were characterized through several abiotic tests conducted in the respirometer previously to biotic tests. Dissolved sulfide concentration was continuously monitored in all assays.

The stripping of sulfide was characterized using nitrogen gas to avoid any chemical oxidation of sulfide that could contribute to its consumption. The conditions and the mineral medium used to perform the abiotic tests were those used in biotic tests.

Thus, a buffered mineral medium (50 mM P-Phosphate) with NH_4Cl (100 mg L^{-1}), $MgSO_4 \cdot 7H_2O$ (20 mg L^{-1}), $CaCl_2$ (2 mg L^{-1}) and without carbon source neither trace elements solution was used for the stripping tests. It must be mentioned that the presence of metallic compounds that catalyze chemical sulfide oxidation (Obrien and Birkner, 1977; Buisman et al., 1990) must be avoided during respirometric tests. Two different initial sulfide concentrations (15 and 30 mg S^{2-} L^{-1}) at different gas flows (15, 50 and 100 mL min^{-1}) were tested for H_2S stripping characterization. Eqs. 7.2 and 7.3, corresponding to the mass balance and chemical equilibriums of H_2S (*see section 7.2.3*) were used to estimate the global mass transfer coefficient (K_La) by curve fitting of experimental profiles of dissolved sulfide to Eq. 7.3.

Chemical sulfide oxidation tests were performed by using an air flow of 50 mL min^{-1} and a sulfide concentration of 30 mg S L^{-1}. Thiosulfate and sulfate were monitored during the test in order to find out which product was being produced by chemical reaction.

8.2.3. LFS respirometric tests

LFS respirometric technique was used in order to study the mechanisms of sulfide oxidation in aerobic conditions and to obtain the corresponding kinetic parameters. This technique consists of monitoring the dissolved oxygen concentration when a pulse of substrate is added to the respirometric vessel while air is continuously diffused in the liquid phase. At the end of the test the initial dissolved oxygen concentration is recovered, once the substrate has been completely depleted.

Two biotic tests (Table 8.1) were performed at 25 ºC and at pH 7.0 in RV-1 (*see section 4.1.3*) with S-oxidizing biomass obtained from CSTR-2 following the methodology proposed in Chapter 5. The difference in this case was that the liquid phase with the suspended biomass was continuously bubbled with 50 mL min^{-1} of air with 2% (v/v) of CO_2. By this way, the carbon source concentration was not limiting the sulfide oxidation rates as verified through total inorganic carbon analysis. Tests C-1 to C-4 corresponded to 4 consecutive substrate pulses performed in the same single respirometric test and were used to calibrate the kinetics of the process. Test V-1 corresponded to a substrate pulse performed in a different respirometric test and used in order to validate the kinetic model (Table 8.1). In each test the pulse of substrate was

added once the oxygen concentration was almost recovered from the previous test. At the beginning of each respirometric test, when the biomass was under endogenous conditions, the endogenous oxygen uptake rate, as well as the $K_L a$ for oxygen, was calculated (*see section 2.5*).

Table 8.1. Biotic tests conducted to calibrate the kinetics of sulfide oxidation in anoxic conditions

Test	Process	Sulfide (mg S L^{-1})	Air Flow (mL min^{-1})	Biomass (mg VSS L^{-1})
C-1		3.5	50	155
C-2	Calibration	10.5	50	155
C-3		23	50	155
C-4		36	50	155
V-1	Validation	25	15	260

8.3. MODEL DEVELOPMENT

The model was developed once studied the mechanism of sulfide oxidation from the respirometric tests. In this case it must be mentioned that thiosulfate and elemental sulfur were observed as intermediates in sulfide oxidation. In the following sections all the processes considered are described in detail.

8.3.1. Sulfide biological oxidation

Sulfide oxidation to elemental sulfur and thiosulfate was described through Eq. 8.4. As can be observed, a Haldane equation was considered to describe substrate inhibition caused by sulfide over sulfide oxidation. A term describing the decrease of sulfide oxidation rate due to the accumulation of intracellular elemental sulfur was also considered in the kinetic model. Finally the limitation of oxygen was described with a Monod-type kinetics.

$$r_{S^{2-}} = \frac{1}{Y_{X/S^{2-}}} \cdot \mu_{max} \cdot \frac{S^{2-}}{K_{S^{2-}} + S^{2-} + \frac{\left(S^{2-}\right)^2}{K_{is}}} \cdot \left[1 - \left(\frac{f_{S0}}{f_{max}}\right)^{\alpha}\right] \cdot \frac{DO}{K_O + DO} \cdot X \qquad (8.4)$$

where μ_{max} is the maximum specific growth rate (h^{-1}), K_{s2-} and K_O are the affinity constants for sulfide and oxygen, respectively (mg L^{-1}), K_{is} is the sulfide inhibition constant (mg S L^{-1}), f_{S0} is the ratio of intracellular elemental sulfur stored to biomass (mg S mg^{-1} VSS), f_{max} is the maximum ratio of intracellular elemental sulfur stored to biomass (mg S mg^{-1} VSS), X is the biomass concentration (mg VSS L^{-1}), $Y_{x/s2-}$ is the biomass growth yield using sulfide as substrate (g VSS g^{-1} S) and S^{2-} and DO are sulfide and dissolved oxygen concentrations, respectively (mg S L^{-1} or mg O_2 L^{-1}).

8.3.2. Thiosulfate production and biodegradation

Thiosulfate was produced as an intermediate compound during sulfide oxidation probably from a chemical oxidation between reaction intermediates in the periplasmatic space of the cells. Eq. 8.5 has been used to describe the rate of this process (r_{TS_p}) while Eq. 8.6 has been used to describe the biological oxidation of thiosulfate (r_{TS}). In this case the thiosulfate limitation has also been considered with Monod-type kinetics.

$$r_{TS\_p} = k_{TS\_p} \cdot \left(S^{2-}\right)^{\beta} \qquad (8.5)$$

$$r_{TS} = \frac{1}{Y_{X/TS}} \cdot \mu_{max} \cdot \eta_{TS} \cdot \frac{TS}{K_{TS} + TS} \cdot \frac{DO}{K_O + DO} \cdot X \qquad (8.6)$$

Where k_{TS_p} is the kinetic constant for thiosulfate production under biotic conditions, β is a constant (dimensionless), η_{TS} is an energetic correction factor to describe growth on thiosulfate, TS is thiosulfate concentration (mg S L^{-1}), K_{TS} is the affinity constant for thiosulfate consumption (mg S L^{-1}) and $Y_{X/TS}$ is the biomass growth yield using thiosulfate as substrate (g VSS g^{-1} S).

8.3.3. Elemental sulfur biological oxidation

Elemental sulfur is the most important intermediate during biological sulfide oxidation. In Eq. 8.7 the reaction rate equation that describes the biodegradation of this compound is presented. As found in previous chapters (*see section 7.3)*, elemental sulfur was degraded once the sulfide is almost depleted. For this reason a non-competitive inhibition term was used in order to describe the substrate switch. Moreover, elemental sulfur biodegradation kinetics was described using a shrinking particle model analogous to that used for PHB biodegradation modeling (Tamis et al., 2014).

$$r_{S0} = \frac{1}{Y_{X/S0}} \cdot \mu_{max} \cdot k_{S0} \cdot \left(f_{S0}\right)^{2/3} \cdot \frac{K}{K + S^{2-}} \cdot \frac{DO}{K_O + DO} \cdot X \tag{8.7}$$

Where k_{S0} is the shrinking kinetic constant for elemental sulfur (mg $VSS^{2/3}$ $mg^{-2/3}$ S), K is the substrate switch constant (mg S L^{-1}) and $Y_{X/S0}$ is the biomass growth yield using elemental sulfur as substrate (mg VSS mg^{-1} S). It must be mentioned that k_{S0} value takes into account the energetic correction factor to describe growth on elemental sulfur, which is equivalent to η_{TS}.

8.3.4. Oxygen uptake rate

The oxygen was modeled taking into account sulfide, thiosulfate, elemental sulfur biodegradation and the corresponding stoichiometric coefficients from the biological reactions. Eq. 8.8 is the general equation used to describe the specific oxygen uptake rate (SOUR) in a LFS respirometer.

$$SOUR = \frac{1}{X} \cdot \left[K_L a_{O_2} \cdot (DO^* - DO) - OUR_{ex} - OUR_{end}\right] \tag{8.8}$$

Where $K_L a_{O2}$ is the global mass transfer coefficient for oxygen (min^{-1}), DO* and DO are the equilibrium and the dissolved oxygen concentration (mg O_2 L^{-1}),

respectively, OUR_{ex} and OUR_{end} are the exogenous and endogenous oxygen uptake rates (mg O_2 L^{-1} min^{-1}).

8.3.5. Parameters estimation

Kinetic parameters were estimated following the procedure described in section 6.4.4 but using a weighted least squares objective function (G) (Eq. 8.9) since the number of experimental points and the magnitude of the variables considered for the optimization were especially different:

$$G\,(\theta) = w_1 \cdot norm([SS]_{exp} - [SS]_{model}\,(\theta)) + w_2 \cdot norm([DO]_{exp} - [DO]_{model}\,(\theta)) +$$
$$w_3 \cdot norm([SO]_{exp} - [SO]_{model}\,(\theta)) \qquad (8.9)$$

Where θ is the model parameter to be estimated through minimization, w_i are the weighting coefficients used for each one of the data sets included in the objective function and norm is the Euclidean norm of a vector. As an example, the calculation of the weighting coefficient w_1 is exposed in Eq. 8.10.

$$w_1 = \frac{\sum_1^i [SO]_{i,1}}{i} \cdot \left[\frac{\sum_1^j [SS]_{j,1}}{j} \right]^{-1} \cdot j^{-1} \qquad (8.10)$$

Where $[SO]_{i,1}$ is the sulfate concentrations column vector with i elements and $[SS]_{j,1}$ is the sulfide concentrations column vector with j elements. As mentioned in previous chapters, all calculations were implemented in MATLAB 7.7 (Mathworks, Natik, MA) using the function *ode45* to solve the numerical differentiation formulas, the function *fminsearch* (unconstrained nonlinear optimization method) to minimize the fitting error between the experimental and model data, and also the function interp1 (cubic spline polynomial interpolation algorithm) to interpolate the modeling results for sulfide, sulfate, dissolved oxygen and OUR at different experimental sampling times.

RESULTS AND DISCUSSION

8.3.6.   Assessment of SOB cultivation in a CSTR

The operation of the CSTR in which the SOB was cultivated is presented in Figure 8.1. It was observed that the steady state was reached after 12 d of operation. A biomass growth yield of 0.258 ± 0.025 mg VSS mg^{-1} S (0.073 mol VSS mol^{-1} S), corresponding to complete sulfide oxidation, was calculated during the steady-state (15-18 d). This value was similar to that obtained by Nelson et al. (1986a) (0.247 mg VSS mg^{-1} S) or Kelly et al. (1982) (0.213 mg VSS mg^{-1} S) for sulfide oxidizing bacteria as *Beggiatoa sp.* and *Thiobacillus sp.,* respectively.
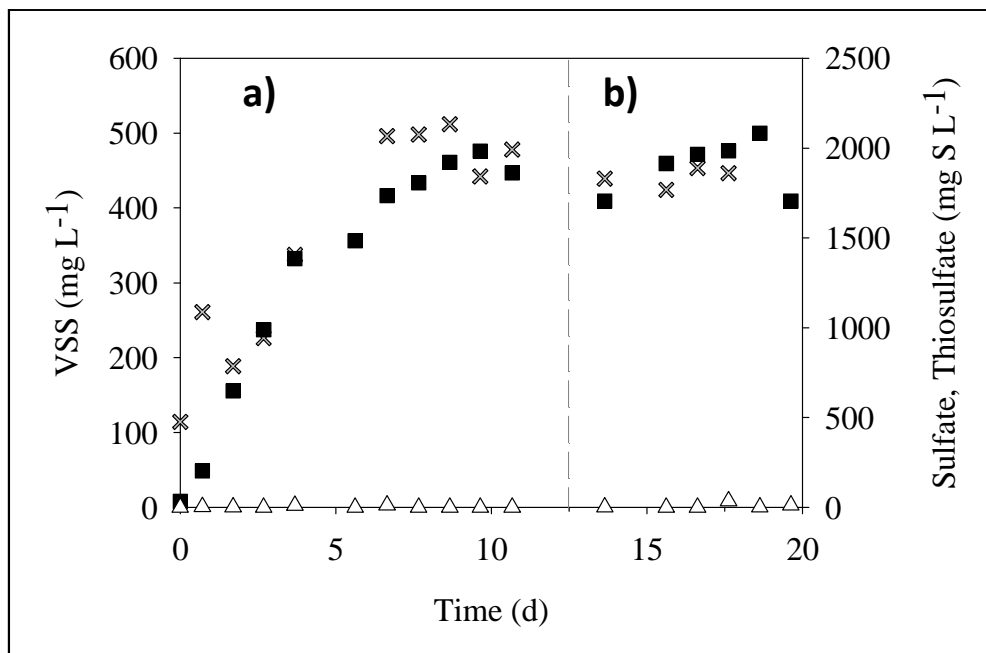
Figure. 8.1. SOB cultivation in a CSTR. (a) Unsteady state operation (b) Steady state operation. Sulfate (■), Thiosulfate (△) and Biomass (x).

Considering the biomass growth yield calculated, the stoichiometry of the overall oxidation reaction was obtained (Eq. 8.11) by solving the mass and charge balances according to Roels (1983), assuming $C_5H_7O_2N$ as typical biomass composition (Heijnen, 2002) and NH_4^+ as the nitrogen source.

$$0.5\ H_2S + 0.5\ HS^- + 1.64\ O_2 + 0.342\ CO_2 + 0.023\ HCO_3^- + 0.073\ NH_4^+ + 0.123\ H_2O \rightarrow$$

$$0.073\ C_5H_7NO_2 + SO_4^{2-} + 1.55\ H^+ \tag{8.11}$$
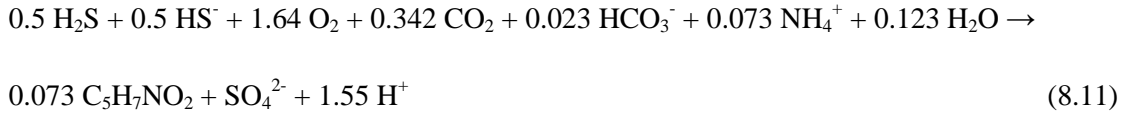
In Figure 8.2 the pyrosequencing analysis performed from the inoculum and the steady-state biomass samples collected from the CSTR are presented. As can be observed, the inoculum diversity (Figure 8.2a) was very low and the main specie found was *Thiothrix sp.* (95%) which was successfully preserved until the steady-state, where the composition was 99% (Figure 8.2b). This is a filamentous γ-proteobacterium that grows well under heterotrophic, mixotrophic or autotrophic conditions and forms intracellular deposits of elemental sulfur as intermediary product during sulfide oxidation. *Thiothrix sp.* is also capable of oxidizing thiosulfate and other reduced sulfur compounds (Nielsen et al., 2000).
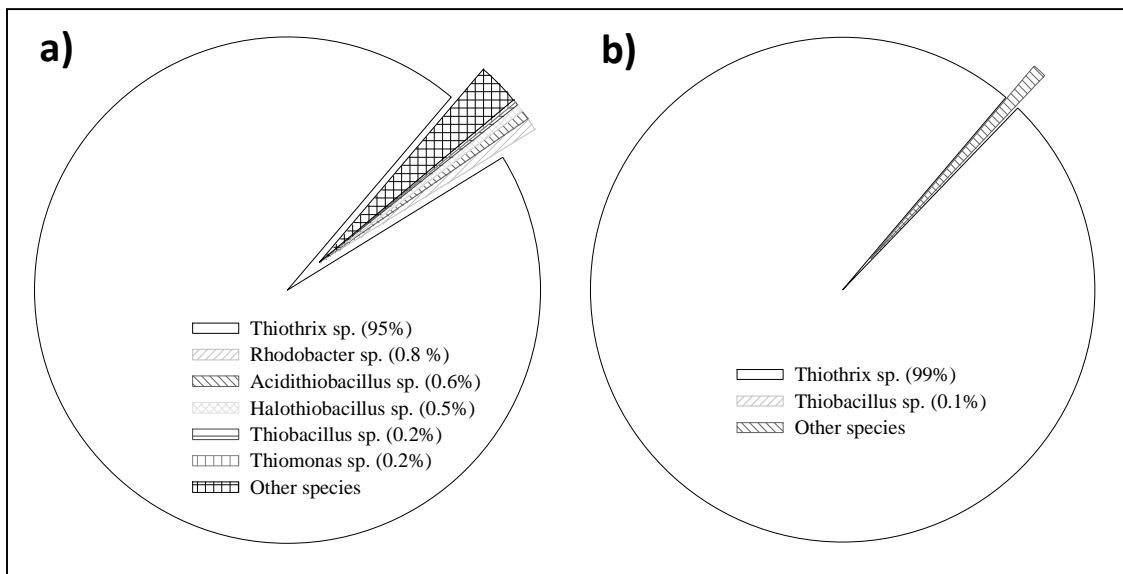
Figure 8.2. Pyrosequencing analysis of the biomass samples from the CSTR. (a)Inoculum microbial diversity (b) Steady state microbial diversity

From the previous results it was concluded that the CSTR operating conditions as well as the dilution rate set (0.015 h^{-1}) avoided the biomass washout and allowed the initial diversity preservation. This result indicates that the immobilized SO-NR mixed culture from the BTF acclimated well to suspended conditions.

From Eq. 8.10 a stoichiometric O_2/S ratio of 1.64 was obtained. This ratio is lower than that associated to the corresponding chemical reaction ($O_2/S=2$) (Eq. 8.3). This was expected since a higher amount of energy obtained from sulfide is required for biomass growth.

8.3.7. Mass transfer and sulfide stripping characterization

The stripping of sulfide was properly characterized by fitting the experimental data to the mathematical equations mentioned above (Eqs. 7.2 and 7.3). In Figure 8.3a the experimental and model data from the stripping test performed at 30 mg S L^{-1} and at 50 mL min^{-1} is presented. A K_La value of 0.075 ± 0.010 min^{-1} (4.5 ± 0.6 h^{-1}) was estimated. As expected, since the air is being diffused in the liquid phase, the K_La was higher than that obtained for a similar system just with a gassed headspace (0.739 h^{-1}, *see section 7.3.2*). Even so, the air flow used was 50 mL min^{-1} to minimize the H$_2$S stripping without limiting the dissolved oxygen concentration during respirometric tests. Therefore, K_La values obtained for different air flows are presented in Figure 8.3b.
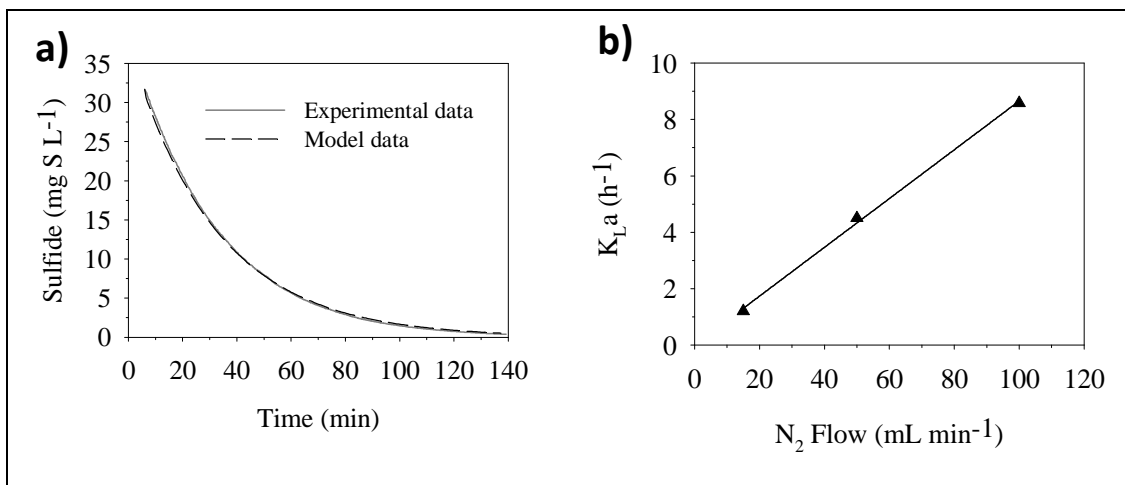
Figure 8.3. Experimental and modeled data obtained from H$_2$S stripping tests performed in the respirometer. (a) Stripping test performed at 30 mg S L^{-1} (b) Linear correlation between gas flow and K_La values. Experimental K_La (symbol), linear correlation between K_La and gas flow (black solid line).

As can be observed, a linear correlation was found to describe the relation between both variables. At 15 mL N$_2$ min^{-1} the K_La obtained allowed minimizing the

stripping of H_2S. However, in biotic experiments the recovery of the initial dissolved concentration after a substrate pulse was extremely long using this flow. This fact did not allow spiking several times the biomass suspension with substrate during the same experiment. On the other hand, a gas flow of 100 mL min^{-1} had a K_La associated of 0.143 ± 0.008 min^{-1} (8.6 ± 0.5 h^{-1}) which was too high to obtain a sensitive DO profile associated to a substrate pulse. For these reasons the gas flow was finally set at 50 mL min^{-1}.

8.3.8. Chemical oxidation of sulfide

Chemical oxidation of sulfide has been studied by many authors (Chen and Morris, 1972; Kuhn et al., 1983; Alper and Ozturk, 1985; Nielsen et al., 2003). Sulfide is a reactive specie that may be oxidized even without the presence of a catalyzer (Buisman et al., 1990). Since respirometric tests were performed under aerobic conditions (without trace elements solution to minimize specifically chemical reactions with sulfide), an abiotic test was performed with air and sulfide in order to verify this approach. In Figure 8.4 the experimental data obtained from the test is presented.

As expected, a minimum amount of thiosulfate is produced during the experiment. The chemical reaction that was taking place (Eq. 8.12) has been previously described with Eq. 8.13 by other authors (Buisman et al., 1990). In this case, this equation has also been used to properly fit the thiosulfate experimental data (Figure 8.4) and to estimate the corresponding kinetic parameters (k_{TS_ab}, a and b).

$$2\ HS^- + 2\ O_2 \rightarrow S_2O_3^{2-} + 2\ H_2O \tag{8.12}$$

$$r_{TS\_ab} = k_{TS\_ab} \cdot \left(S^{2-}\right)^a \cdot \left(O_2\right)^b \tag{8.13}$$

Where r_{TS_ab} is the oxidation rate (mg $S_2O_3^{2-}$-S L^{-1} min^{-1}), k_{TS_ab} is the rate constant for thiosulfate production ($k_{TS\_ab}=0.0030$ $_{\min \cdot (\text{mg S/L})^{-0.75} \cdot (\text{mg O}_2/\text{L})^{-0.77}}$) in abiotic conditions, a is the reaction order with respect to sulfide (a=0.25) and b is the reaction order with respect to oxygen (b=0.23).
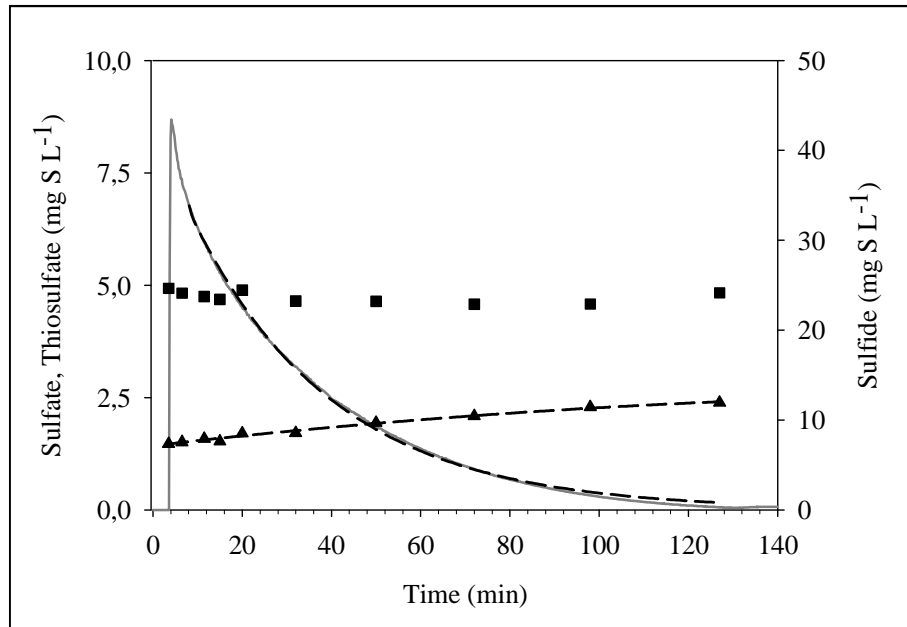
Figure 8.4. Experimental and model data obtained from sulfide chemical oxidation test performed in the respirometer without trace elements solution. Sulfate (■), Thiosulfate (▲), dissolved sulfide (grey solid line) and model data (black dashed line).

From the kinetic values estimated it was concluded that, under the conditions set to perform the respirometric tests, the chemical oxidation was not quantitatively important since the rate constant was extremely low. Even so, it was also observed that in terms of rate only 1 mg $S_2O_3^{2-}$-S L^{-1} was produced in 2h.

8.3.9. Biological sulfide oxidation mechanisms

The respirometric tests performed to calibrate the kinetic model were previously studied in order to elucidate which were the mechanisms of the process. By this way, from a single test (Test C-4, Figure 8.5) the mechanisms of the process were proposed and presented as shown in Figure 8.6. As can be observed, the first step was the partial sulfide oxidation to elemental sulfur but also to sulfite which were probably reacting in the presence of sulfide to form polysulfides (Kleinjan et al., 2005b) in the periplasmatic space of the cell and, subsequently, thiosulfate. This mechanism has been previously described by Chen and Morris (1972) through the reaction pathway of sulfide oxygenation and, as explained in the following lines, is in agreement with the results obtained in section 8.4.3 where the chemical oxidation of sulfide was studied. Finally, once the sulfide was completely depleted, the elemental sulfur that was intracellularly

stored and the chemically produced were further oxidized to sulfate, which was the end product of the reaction.
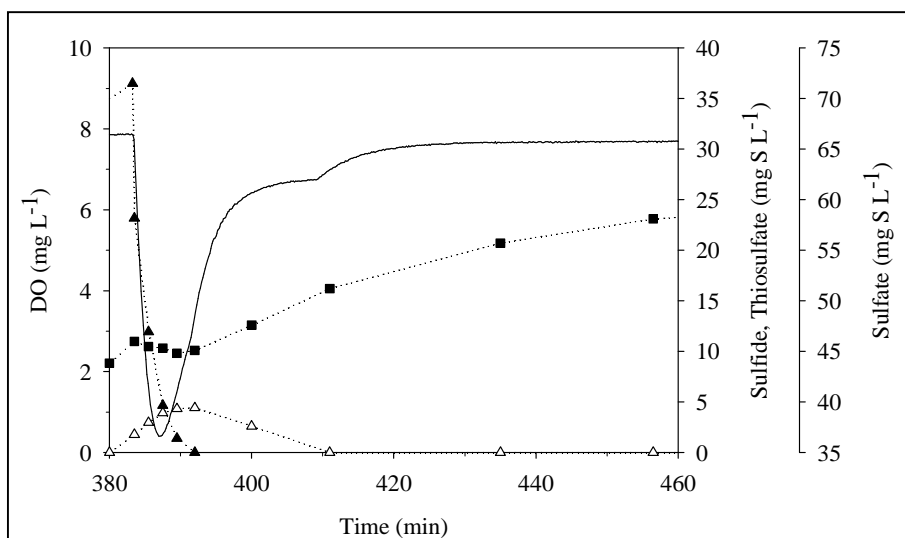
Figure 8.5. Respirometric profile obtained from Test C-4. Sulfide (▲), thiosulfate (△), sulfate (■), dissolved oxygen (solid line)
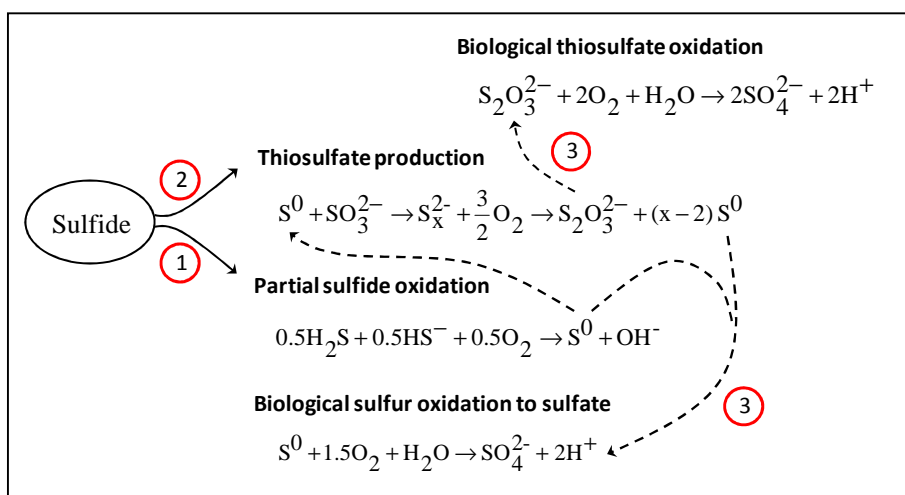
Figure 8.6. Mechanisms proposed for biological sulfide oxidation. (1) Partial sulfide oxidation to elemental sulfur (2) Thiosulfate production from polysulfide pathway (3) Biological oxidation of thiosulfate and intracellular elemental sulfur

Since the abiotic test showed that a much lower amount of thiosulfate was chemically produced compared to that produced in test C-4 (Figure 8.4), it is logical

that another specie not present in abiotic conditions was the responsible of thiosulfate formation. This could be the case of sulfite, which was only present during the biotic test and probably the key compound to obtain thiosulfate as an intermediate during biological sulfide oxidation. However, this hypothesis must be further investigated since, in this preliminary study, sulfite and polysulfides were not analyzed during respirometric tests. Moreover, biological thiosulfate formation has not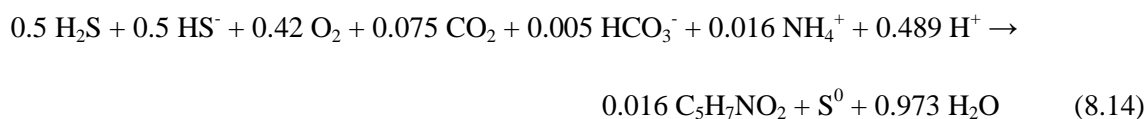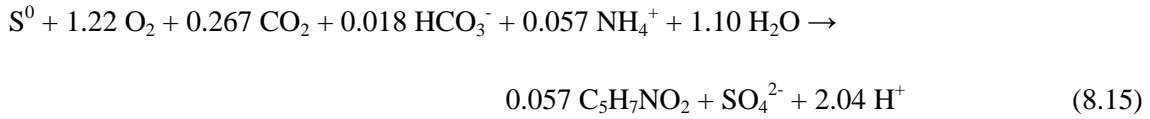 been previously reported by other authors at the conditions set in this study, probably because of the particular characteristics of the microbial culture studied herein. Therefore, there is no data available to be compared with that obtained in this chapter.

8.3.10. Stoichiometry of the process

The stoichiometry of the process was also solved using the profile presented in Figure 8.5 and the Eq. 8.11. From Figure 8.5 it was observed that during sulfide uptake the sulfate concentration was almost constant, which indicates that elemental sulfur was the main product obtained from this reaction. From this stage of the respirometric test (sulfide presence) the total oxygen used for sulfide oxidation to elemental sulfur was calculated by integrating Eq. 8.10. The ratio between the oxygen consumed and the sulfide consumed was 0.43 mg O_2 mg^{-1} S^{2-}. The remaining stoichiometric coefficients corresponding to the considered reaction (Eq. 8.14), including the biomass growth yield, were calculated as described above.

$$0.5\ H_2S + 0.5\ HS^- + 0.42\ O_2 + 0.075\ CO_2 + 0.005\ HCO_3^- + 0.016\ NH_4^+ + 0.489\ H^+ \rightarrow$$

$$0.016\ C_5H_7NO_2 + S^0 + 0.973\ H_2O \qquad (8.14)$$

A biomass growth yield of 0.016 mol biomass mol^{-1} substrate was calculated which represents a 22% of the experimental $Y_{x/s}$ obtained for the complete reaction (0.073 mol biomass mol^{-1} substrate). This result is coherent since in this reaction 25% of the electrons involved for the complete oxidation (2 of 8 mol e$^-$ mol^{-1} S^{2-}) were gained. From the combination of Eq. 8.11 and Eq. 8.14 the stoichiometry corresponding to the elemental sulfur oxidation reaction was solved (Eq. 8.15).

$$S^0 + 1.22\ O_2 + 0.267\ CO_2 + 0.018\ HCO_3^- + 0.057\ NH_4^+ + 1.10\ H_2O \rightarrow$$

$$0.057\ C_5H_7NO_2 + SO_4^{2-} + 2.04\ H^+ \qquad (8.15)$$

As can be observed a higher biomass growth yield was obtained from elemental sulfur oxidation to sulfate (0.057 mol biomass mol^{-1} substrate) since 6 mol e$^-$ mol^{-1} S are gained in this reaction.

Regarding to thiosulfate, a biomass growth yield of 0.071 mol VSS mol^{-1} S$_2$O$_3^{2-}$-S reported by Odintsova et al. (1993) for *Thiothrix ramosa* was used to solve the corresponding biological oxidation stoichiometry (Eq. 8.16).

$$S_2O_3^{2-} + 1.65\ O_2 + 0.333\ CO_2 + 0.022\ HCO_3^- + 0.071\ NH_4^+ + 1.12\ H_2O \rightarrow$$

$$0.071\ C_5H_7NO_2 + SO_4^{2-} + 2.05\ H^+ \qquad (8.16)$$
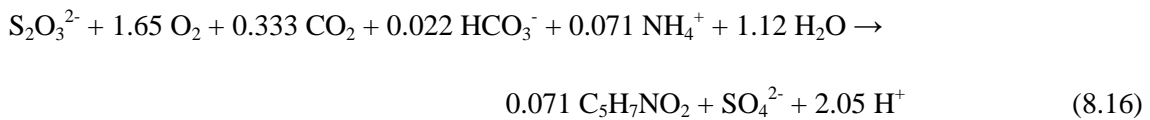
8.3.11. Kinetic model calibration

The kinetic model was calibrated with tests C-1 to C-4 which, as mentioned above, corresponded to 4 different substrate pulses performed in the same single respirometric test. In Figure 8.7 two of the modeled respirometric profiles are presented (C-2 and C-4). In Table 8.2 the corresponding kinetic parameters as well as the test in which have been calibrated are presented. Previously to model calibration the endogenous uptake rate (0.132 mg O$_2$ g^{-1} VSS min^{-1}) and the K$_L$a for oxygen (0.257 min^{-1} or 15.4 h^{-1}) were obtained.

As can be observed in Figure 8.7, the model described properly the experimental data although little differences were observed for dissolved oxygen concentration fitting when elemental sulfur was the remaining substrate (Test C-2). This difference was also found in tests C-1 and C-3 (*data not shown*) even though the kinetic constant corresponding to elemental sulfur oxidation (k$_{S0}$) was calibrated in each substrate pulse to describe properly the experimental data. It is possible that the shrinking particle model was not the most suitable to describe the respirometric profiles but was the best

134

fitting the experimental data since other kinetic equations as Monod, Haldane, zero-order and half-order equations were also used and, although sulfate profile was properly described, the dissolved oxygen profile was not well described from one elemental sulfur concentration to a higher one. Elemental sulfur oxidation was successfully described in previous chapters (*see section 7.3*) with a Monod equation because off-line sulfate monitoring is not as sensitive as the continuous dissolved oxygen monitoring is.
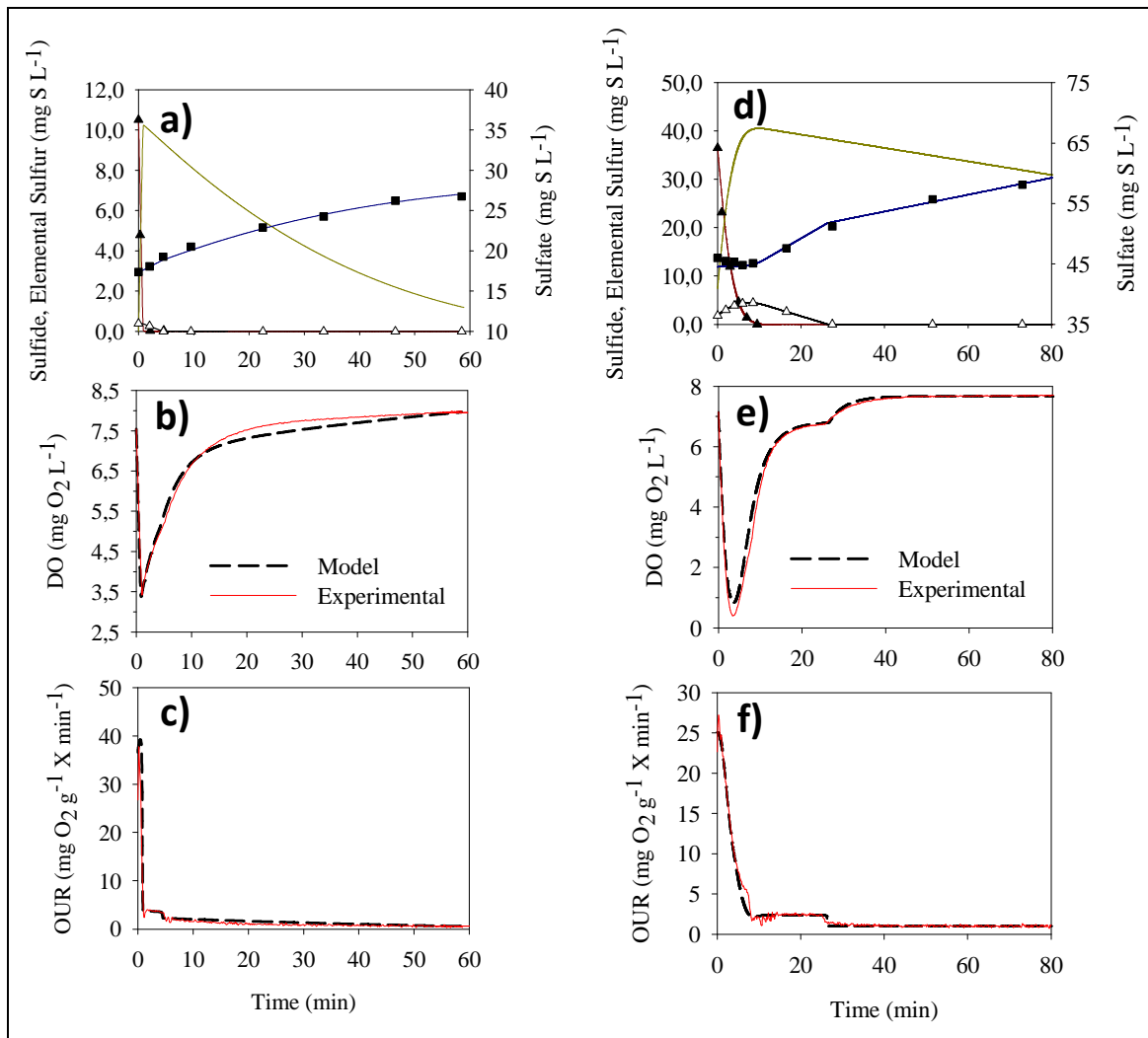
Figure 8.7. Calibration of the kinetic model proposed with the experimental respirometric profiles obtained from tests C-2 (a, b, c) and C-4 (d, e, f). Experimental and modeled sulfide concentration (▲ and dark red solid line, respectively), modeled elemental sulfur concentration (dark yellow solid line), experimental and modeled thiosulfate concentration (△ and black solid line, respectively), experimental and modeled sulfate concentration (■ and blue solid line, respectively).

Regarding to the kinetic variation, this has already been observed by Koenig and Liu (2001) when describing with a half-order kinetic equation elemental sulfur oxidation in a sulfur packed bed reactor. The authors eventually associated this variation to the sulfur particle size. Another explanation for kinetic variation could be the fact that part of the intracellular elemental sulfur was stored as orthorhombic α-sulfur which is most likely inaccessible to bacterial enzymes (Berg et al., 2014). Other authors have also observed kinetic variation when describing PHB degradation with the shrinking particle model (Tamis et al., 2014) which was associated to the number and size of the particles related to the biomass concentration. Therefore, the variation of k_{S0} obtained in this study was also associated to the particles size and the elemental sulfur speciation, which could have been changing during respirometric tests. However, further research is required in order to clarify which is the specific factor affecting k_{S0}.

Table 8.2. Kinetic parameters estimated from the fitting of the model proposed to the experimental respirometric profiles.

Parameter	Value	Value	Calibration test
μ_{max}	$6.6 \cdot 10^{-3}$	min^{-1}	C-1
	0.396	h^{-1}	
K_{s2-}	0.317	$mg\ S\ L^{-1}$	C-1
K_{is}	42.4	$mg\ S\ L^{-1}$	C-3
f_{max}	0.256	$mg\ S\ mg^{-1}\ VSS$	C-4
α	1.71	-	C-4
η_{TS}	0.030	-	C-3
K_{TS}	0.0023	$mg\ S\ L^{-1}$	C-3
k_{TS_p}	0.107	$mg\ S^{0.47}\ L^{-0.47}\ min^{-1}$	C-3, C-4
β	0.530	-	C-3, C-4
k_{S0}	[0.833-0.030]	$mg\ S^{1/3}\ mg^{-1/3}\ VSS$	C-1 to C-4
K_{switch}	0.455	$mg\ S\ L^{-1}$	C-4
$SOUR_{max}$	49.2	$mg\ DO\ g^{-1}\ VSS\ min^{-1}$	calculated
K_O	0.146	$mg\ O_2\ L^{-1}$	C-4

As presented in Table 8.2, the maximum growth rate obtained was 0.396 h^{-1} which was slightly higher to that found by Munz et al. (2009) (0.308 h^{-1}) for S-oxidizing biomass using elemental sulfur as substrate in a respirometer. The difference found is probably because the calibration of this parameter takes into account the maximum specific growth rate that describes only the sulfide oxidation to elemental sulfur, which had associated an extremely high specific consumption rate. This was somehow expected since S-oxidizing bacteria grow faster in sulfide than in elemental sulfur.

The S-oxidizing biomass obtained from the biotrickling filter presented high affinity for oxygen, sulfide and thiosulfate (*see K_O, K_{s2-} and K_{TS} values from Table 8.2*). The estimated inhibition constant for sulfide was also high (42.4 mg S L^{-1}), compared with those obtained in previous chapters, indicating that more than 80% of the maximum oxidation rate was reached for concentrations under 10 mg S L^{-1} of dissolved sulfide. It must be mentioned that during the operation of the biotrickling filter the dissolved sulfide concentration remained under 1 mg S L^{-1} (*data not shown*), which indicated that the biomass was not inhibited by sulfide.

As mentioned in previous sections, sulfide oxidation was also affected by the accumulation of intracellular sulfur. From the model calibration 25.6% of elemental sulfur was found to be the maximum capacity of sulfur storage inside the cells. No data is reported regarding sulfur storage capacity for S-oxidizing biomass under the same conditions but compared to PHB degraders (89% of PHB related to dry weight reported by Johnson et al. (2009)) the accumulation percentage was not especially high maybe because of the *Thiothrix sp.* morphology.

Regarding the substrate preference, no correlation between the O$_2$/S ratio and the product selectivity was found as concluded in previous chapters (*see Chapter 7*). This result is not in agreement with Gonzalez-Sanchez et al. (2009) who considered product selectivity depending on the O$_2$/S ratio available in the media. In this study the biomass was consuming preferentially sulfide, regardless of the O$_2$/S ratio, to convert it into elemental sulfur and thiosulfate in this particular case. All other substrates were consumed after sulfide depletion and presented the same inhibition-affinity constant (K$_{switch}$=0.455 mg S L^{-1}) which indicates a simultaneous biodegradation under the absence of sulfur. This result indicates that sulfide is energetically favorable so that it is

immediately oxidized to elemental sulfur, even with O_2/S ratio greater than the corresponding for the complete oxidation stoichiometry (Eq. 8.11). In fact, Visser et al. (1997) reported that sulfur formation was showed to occur when the maximum oxidative capacity of the culture was approached. This means that, in order to be able to oxidize increasing amounts of sulfide, the organism has to convert part of the sulfide to sulfur instead of sulfate to keep the electron flux constant regardless the oxygen concentration.

8.3.12. Validation of the kinetic model

The kinetic model was validated with the respirometric test V-1. In Figure 8.8 the experimental and respirometric profiles are presented. This test was performed with the same biomass used for the calibration tests (C-1 to C-4) but withdrawn from the CSTR in a different operation date.

An air flow of 15 mL min^{-1} and a biomass concentration of 260 mg VSS L^{-1} were used in order to validate the model at different conditions. A k_{S0} of 0.053 mg S$^{1/3}$ mg$^{-1/3}$ VSS was obtained since, as mentioned above, this constant must be calibrated in each profile. As expected, the K_La for oxygen was almost 3.5-fold less than that obtained for an air flow of 50 mL min^{-1} (0.069 min^{-1} or 4.14 h^{-1}).

As can be observed the dissolved oxygen profile was not perfectly described despite sulfate, thiosulfate and OUR profiles were properly fitted with the calibrated model. This result indicates that the model may be included in a general model describing aerobic desulfurization in the biotrickling filter. However, the kinetic constant related to elemental sulfur oxidation requires to be calibrated in each particular case since probably the elemental sulfur that is being formed inside the cells has different speciation, which affects directly to the oxidation rate. In any case, this process must be further investigated as mentioned above to find a mathematical equation describing better this biodegradation process.

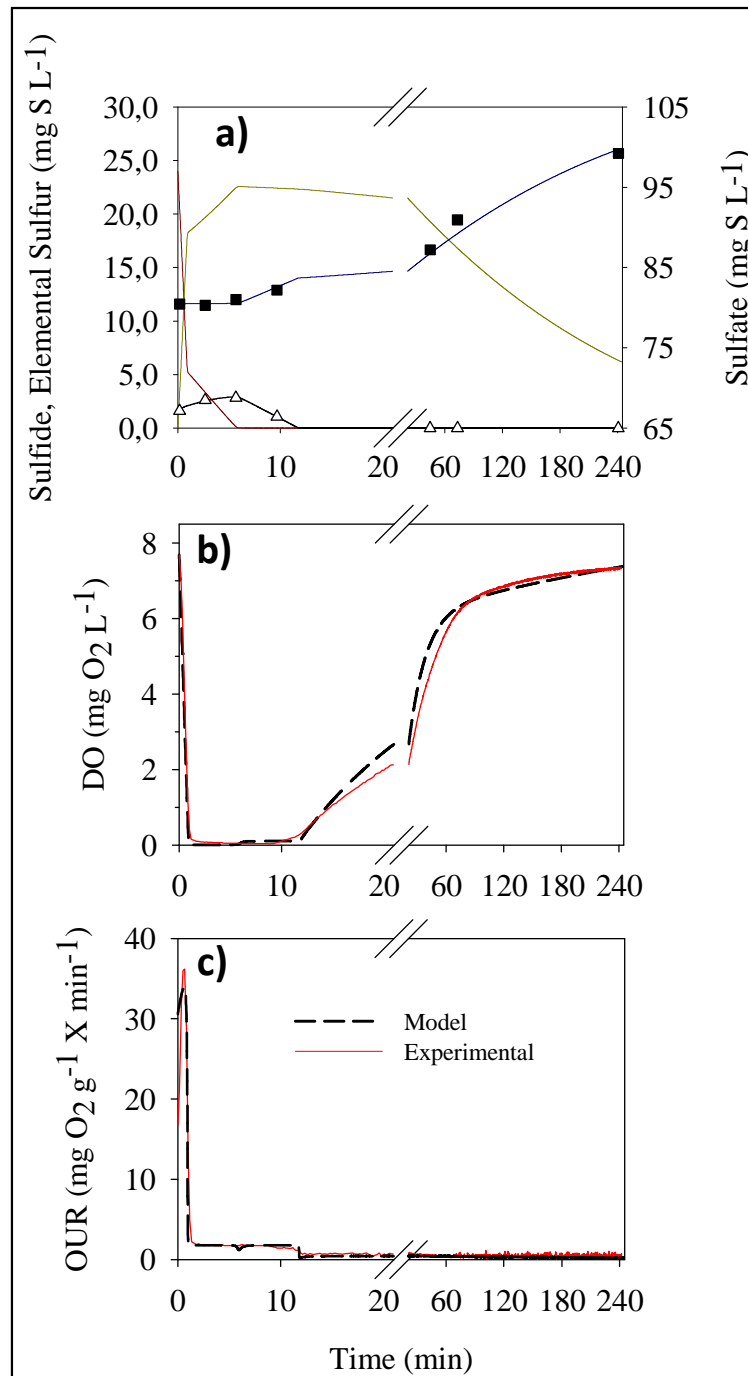**Figure 8.8.** Validation of the kinetic model with experimental data from respirometric test V-1. Modeled sulfide concentration (dark red solid line), modeled elemental sulfur concentration (dark yellow solid line), experimental and modeled thiosulfate concentration ($\triangle$ and black solid line, respectively), experimental and modeled sulfate concentration ($\blacksquare$ and blue solid line, respectively).

8.4. CONCLUSIONS

From the study presented in this chapter it was concluded that the LFS respirometry was again successfully implemented to characterize S-oxidizing biomass obtained from a desulfurizing biotrickling filter. The proposed mechanisms describing aerobic sulfide oxidation explained the intermediate production of thiosulfate. The kinetic model proposed was properly calibrated with the respirometric profiles and several kinetic parameters estimated from the calibration. Still further research related with elemental sulfur biodegradation is required since maybe the intracellular particles size and the elemental sulfur speciation variations were affecting the kinetics corresponding to its oxidation. For this reason further investigation is required in order to clearly find out which is the factor that influences negatively elemental sulfur biodegradation.

Chapter 9

PRELIMINARY STUDY ON THE APPLICATION OF HETEROGENEOUS RESPIROMETRY TO CHARACTERIZE H$_2$S OXIDIZING BIOFILM FROM DESULFURIZING BIOTRICKLING FILTERS

9. PRELIMINARY STUDY ON THE APPLICATION OF HETEROGENEOUS RESPIROMETRY TO CHARACTERIZE H_2S OXIDIZING BIOFILM FROM DESULFURIZING BIOTRICKLING FILTERS

This chapter is clearly the most ambitious of this thesis since the respirometric tests are performed directly with the biofilm attached to packing material obtained from a biotrickling filter. To this aim a new setup was constructed and a biofilter operated in order to study the mechanisms and kinetics of the desulfurization under aerobic conditions. The heterogeneous respirometer coupled to a novel mathematical model allowed estimating many parameters taking into account that morphological and physiological changes of the biofilm would be avoided with this new technique.

Abstract

The elimination capacity of gaseous H_2S by biofiltration can be limited either by mass transfer or bioreaction in the biofilm. The assessment of the biological activity of immobilized cells (biofilm) usually implies morphological and physiological changes during the adaptation of cells to respirometric devices operated with suspended cultures. In this chapter, heterogeneous respirometry is advised as a valuable technique for characterizing mass transport and the activity of S-oxidizing biofilms attached on two types of packed beds, originated from operative BTFs. Controlled flows of liquid and H_2S-containing air were circulated through a closed HR allowing a more realistic estimation of the biofilm activity by the experimental evaluation of the OUR. A mathematical model for the determination of kinetic-related parameters such as the maximum OUR and morphological properties of biofilm (i.e. thickness and fraction of wetted area of packing bed) was developed and calibrated. With the set of parameters obtained, the external oxygen mass transport to the wetted biofilm was found to limit the global H_2S biofiltration capacity, whereas the non-wetted biofilm was the predominant route for the gaseous O_2 and H_2S mass transfer to the biofilm. The oxygen diffusion rate was the limiting step in the case of very active biofilms.

A modified version of this chapter has been submitted for publication as :

9.1. INTRODUCTION

Several parameters can be monitored and controlled during waste gas biofiltration, such as inlet and outlet gaseous pollutant concentrations or flow rates, which allow calculating the overall removal performance. However, biodegradation kinetics are usually difficult to determine (Kim and Deshusses, 2003). Respirometry is a typical tool to assess the degradation activity of suspended cells cultures although performance of this assay with immobilized biomass leads to biofilm destruction, being modified the original physiology of cells as well as the mass transport phenomena occurring in the biofilm. Respirometry applied to characterize biofilms in suspended cultures generally leads to an overestimated biological activity as the biofilm structure and the mass transport are not considered (García-Peña et al., 2005). Therefore, the biodegradation activity measured from a sample of packed bed would allow improving the strategies to adequately operate and control biofilters.

Some methodologies to study biodegradation kinetics of immobilized biomass have been already proposed by using liquid and gas static phases (Ramirez-Vargas et al., 2013; Piculell et al., 2014) which are not the most suitable techniques to properly simulate the biofilm conditions in a BTF. The effect of external mass transfer resistance on the H_2S elimination seems to be significant for the performance of BTFs, and especially in aerobic process where the mass transport of gaseous oxygen to the biofilm could limit the global process (Montebello et al., 2012). Heterogeneous respirometry has been proposed as an alternative to the classical respirometric technique when characterizing immobilized biomass since heterogeneous respirometry allows a minimum handling of biofilms before and during the respirometric assay in order to mimic a biofiltration system (Govind et al., 1997; Kim and Deshusses, 2003). In HR, the liquid and gas phases are continuously circulated in closed-loop. The intrinsic OUR induced by the oxidation of H_2S in the biofilm is experimentally determined and compared to the theoretical value obtained from a mathematical model.

From the previous assumptions, the aim of this chapter was to propose and validate the heterogeneous respirometry as a valuable tool to characterize S-oxidizing activity and mass transport phenomena of specialized biofilms grown on packed beds of desulfurizing BTFs. Data and a mathematical model will allow identifying and

assessing the limiting steps in H$_2$S biofiltration and thereof propose actions to improve performance.

9.2. MATERIALS AND METHODS

9.2.1. Immobilized S-oxidizing biomass cultivation

The biomass was cultivated in three BTFs with different packing material that were connected through the liquid phase and operated at similar conditions (*see section 4.1.2*). The BTFs were inoculated with activated sludge from a municipal wastewater treatment plant to obtain an enriched neutrophilic S-oxidizing consortium. Initially, the inoculum was circulated through the packing material during 8h without liquid renewal and with a counter-current aeration flow of 0.03 m^3 h^{-1}. Afterwards, the BTFs were fed during 2 months reaching an H$_2$S inlet concentration of 300 ppm$_v$ while setting the EBRT to 30 s (48 g S m^{-3} h^{-1}). At the end of the operation the respirometric tests were performed with BTF-2a and BTF-2b which were packed with stainless steel PR and PUF, respectively (*see section 4.1.3*). The composition of the mineral medium used to grow up he immobilized culture contained (g L^{-1}): NaHCO$_3$ (3.5), NH$_4$Cl, (1); KH$_2$PO$_4$, (0.12); K$_2$HPO$_4$, (0.15); CaCl$_2$, (0.02); MgSO$_4$·7H$_2$O, (0.2); and trace elements solution, 1 mL L^{-1} (Fortuny et al., 2008).

9.2.2. Experimental approach of the heterogeneous respirometry

Abiotic and biotic experiments were conducted to characterize the mass transfer phenomena and the S-oxidizing activity of the biofilm. First, several abiotic assays were performed at different gas and liquid linear velocities with two types of packing material (PUF and PR) (Fortuny et al., 2008; Montebello et al., 2012) to estimate the overall volumetric mass transfer coefficient (K$_L$a$_{g-l}$) corresponding to oxygen.

The procedure to obtain the experimental data was applied as follows. A BTF with the same characteristics as BTF-2a and BTF-2b was filled with sterilized packing material and placed in the HR as the differential reactor unit. A volume of 126 mL of mineral medium was added to the liquid reservoir of the HR (*see section 4.1.3*). Afterwards, the gas and liquid phases were counter-currently circulated while all the

oxygen was stripped out from the HR by feeding nitrogen gas. Once the oxygen was absent, a controlled air flow (0.03 m^3 h^{-1}) was fed to the HR generating different time-depended oxygen concentration profiles in both phases. Different velocities for gas (43.4; 57.8; 77.1; 101.2 m h^{-1}) and liquid (6.9; 8.3; 10.8 m h^{-1}, respectively) were applied to assess the mass transfer phenomena in the BTF. Gaseous and dissolved oxygen profiles arising from the abiotic assays were used to estimate the corresponding K_La_{g-l}.

For the biotic assays, the colonized BTF (BTF-2a or BTF-2b) was placed as the differential reactor unit of the HR to obtain the respirometric profiles. The experiment started with the addition of 126 mL of mineral medium into the HR, which was continuously recycled and aerated for some hours in order to stabilize the biofilm and to allow exhausting the bioavailable substrates accumulated in the biofilm during the BTF operation (mainly H_2S and elemental sulfur). Afterwards, the HR was closed while recycling both phases (gas and liquid). Then, a pulse of gaseous pure H_2S (10 mL) was immediately injected in the gas phase to attain computed (He=0.41) equilibrium concentrations of 0.62 mmol L^{-1} (19.8 g m^{-3}) and 0.63 % (vol.) in the liquid and gas phases, respectively. Gas and liquid phases were circulated at linear velocities of 101.2 and 10.8 m h^{-1}, respectively, and the oxygen concentration evolution was continuously monitored for the corresponding analysis.

9.2.3. Experimental determinations in the packed bed

The amount of biomass attached to the packing support was quantified as follows. Once the corresponding assay was finished, the liquid pump was stopped and the packing material was immediately weighted (W_1). After draining the liquid for a period of 30 minutes, the support was weighted again (W_2). The weight difference between W_2 and W_1 was used to determine the static hold-up which, together with the dynamic hold-up, was used to estimate the volume fraction occupied by the liquid (ε_l). Once drained, the biofilm was mechanically and carefully withdrawn from the packing material to be suspended in a known amount of water. The clean packing was dried for 12 hours in an oven at 50 °C to determine the weight of the support (W_3). The suspended biomass was later centrifuged at 5000 rpm for 10 minutes and the supernatant was discarded to determine the weight of wet biomass (W_4) as well as it volume (V_1). The volume

fraction occupied by the biofilm (ε_b) was calculated by dividing V_1 by the volume of the packing material tested. The wet biofilm density was evaluated by dividing W_4 by V_1. Finally, the wet biomass was dried for 12 hours at 50 ° C to determine the dry weight of the biomass (W_5). The volume fraction occupied by the gas (ε_g) in the packed bed was also determined taking into account the space occupied by the abovementioned fractions of the packed bed, including the empty bed fraction of the packing material reported by the manufacturer (Table 9.1).

9.3. MATHEMATICAL MODEL DEVELOPMENT

Mass balances for oxygen and H_2S in the gas, liquid and biofilm phases for the HR were stated in Eqs. 9.1 to 9.6. Due to bench size and the operating mode as differential reactor, an ideally mixed regime was assumed in the HR for both bulk phases. The bioreaction was considered to occur entirely in the biofilm. Free volumes of gas in the upper and lower sections of the HR and the liquid recycling tank (i.e. reservoir) were also considered in mass balances. The mechanism proposed for H_2S removal in the BTF is shown in Figure 9.1. Both wetted and non-wetted portions of the biofilm were included in the model. As a common assumption often made in biofiltration modeling, mass transfer resistance in the gas boundary layer over the wetted and non-wetted biofilm was assumed negligible. More detailed model assumptions can be found elsewhere (Kim and Deshusses, 2003; González-Sánchez et al., 2009).
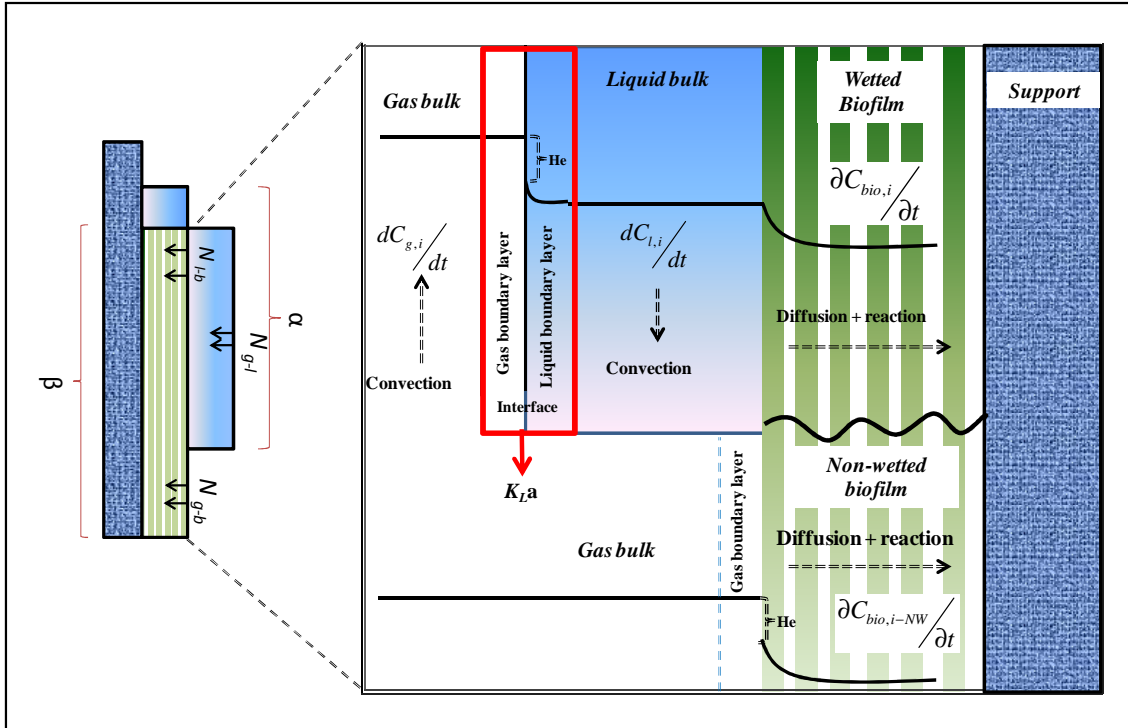
Figure 9.1. Schematic of the phenomena and mechanisms of the H$_2$S removal in a biotrickling filter assuming wetted and non-wetted biofilm. N$_{l\text{-}b}$, N$_{g\text{-}l}$, N$_{g\text{-}b}$ refer to mass fluxes between the different phases considered herein.

9.3.1. Mass Balance for the gas phase

Mass balances for the gas phase were considered in the packed bed and in the gaseous reservoir (*see section 4.1.3*).

- *In the packed bed*

$$\frac{dC_{g,i}^{Bed}}{dt} = \frac{Q_g}{V_{Bed}\cdot\varepsilon_g^{Bed}}\cdot\left(C_{g,i}^{Free}-C_{g,i}^{Bed}\right) - \frac{K_L\cdot a_{g-l}}{\varepsilon_g^{Bed}}\cdot\left(\frac{C_{g,i}^{Bed}}{He_i}-C_{l,i}^{Bed}\right) - \frac{K_B\cdot a_{g-b}}{\varepsilon_g^{Bed}}\cdot\left(\frac{C_{g,i}^{Bed}}{He_i}-C_{b-NW,i}\right) \qquad (9.1)$$

with the following initial condition: $\qquad t=0 \quad C_{g,i}^{Bed}=C_{g,i}^{0}$

- *In the gaseous reservoir*

$$\frac{dC_{g,i}^{Free}}{dt} = \frac{Q_g}{V_{g,i}^{Free}} \cdot \left(C_{g,i}^{Bed} - C_{g,i}^{Free} \right) \tag{9.2}$$

with the following initial condition: $\qquad t = 0 \quad C_{g,i}^{Free} = C_{g,i}^{0}$

The subscript *i* refers to oxygen or H_2S, the two different gaseous compounds considered in the model.

9.3.2. Mass Balance for the liquid phase

Mass balances for the liquid phase were considered in the packed bed and in the liquid reservoir (*see section 4.1.3*).

- *In the packed bed*

$$\frac{dC_{l,i}^{Bed}}{dt} = \frac{Q_l}{V_l^{Bed}} \cdot \left(C_{l,i}^{Res} - C_{l,i}^{Bed} \right) + \frac{K_L a_{g-l}}{\varepsilon_l^{Bed}} \left(\frac{C_{g,i}^{Bed}}{He_i} - C_{l,i}^{Bed} \right) - \frac{K_B \cdot a_{l-b}}{\varepsilon_l^{Bed}} \cdot \left(C_{l,i}^{Bed} - C_{b,i} \right) \tag{9.3}$$

with the following initial condition: $\qquad t = 0 \quad C_{l,i}^{Bed} = C_{l,i}^{0}$

- *In the liquid reservoir*

$$\frac{dC_{l,i}^{Res}}{dt} = \frac{Q_l}{V_l^{Res}} \cdot \left(C_{l,i}^{Bed} - C_{l,i}^{Res} \right) \tag{9.4}$$

with the following initial condition: $\qquad t = 0 \quad C_{l,i}^{Res} = C_{l,i}^{0}$

9.3.3. Mass Balance for the biofilm

Mass balances for the biofilm were considered in the wetted and non-wetted biofilm (Figure 9.1).

- *Wetted biofilm*

$$\frac{\partial C_{b,i}}{\partial t} = D_{eff,i} \frac{\partial^2 C_{b,i}}{\partial x^2} - r_{b,i} \tag{9.5}$$

with the following boundary conditions:

$$t = 0; C_{b,i} = C_{b,\ i}^0 \qquad\qquad x = 0; \quad C_{b,i} = C_{l,\ i} \qquad\qquad x = \delta; \quad \frac{\partial C_{b,i}}{\partial x} = 0$$

- *Non-wetted biofilm*

$$\frac{\partial C_{b-NW,i}}{\partial t} = D_{eff,i} \frac{\partial^2 C_{b-NW,i}}{\partial x^2} - r_{b-NW,i} \tag{9.6}$$

with the following boundary conditions:

$$t = 0; \quad C_{b-NW,i} = C_{b-NW,i}^0 \qquad\qquad x = 0; \quad C_{b-NW,i} = \frac{C_{g,i}}{He_i} \qquad\qquad x = \delta; \quad \frac{\partial C_{b-NW,i}}{\partial x} = 0$$

Where $C_{g,i}^{Bed}$, $C_{l,i}^{Bed}$, $C_{b,i}$ and $C_{b-NW,i}$ are the concentrations of component i in the bulk gas phase, bulk liquid, biofilm and non-wetted biofilm, respectively (g m^{-3}); $C_{g,i}^{Free}$ $C_{l,i}^{Res}$ are the concentrations of component i in the free gas volume and in the liquid reservoir tank respectively (g m^{-3}); He_i is the gas/liquid partition coefficient of component i (dimensionless); a, a_{g-l}, a_{l-b}, a_{g-b} (see Eqs. 9.8 to 9.10) represent the specific surface area per volume unit of packed bed, gas-liquid specific contact area, liquid-biofilm specific contact area and gas-biofilm specific contact area, respectively (m^2 m^{-3}); $D_{eff,i}$ is the diffusion coefficient of component i in the biofilm (m^2 h^{-1}); $r_{b,i}$, $r_{b-NW,i}$ are the consumption rates of component i in the wetted biofilm and in the non-wetted biofilm respectively (g m^{-3} h^{-1}); δ is the biofilm thickness (m) and N is the total number of layers of the discretized biofilm thickness for the numerical resolution of the mathematical model. According to Eq. 9.7, K_B is the external mass transfer coefficient

from external bulk phase to biofilm. The surface fraction of the packing material covered by biofilm (β) was estimated according to Eq. 9.11.

$$K_B = \frac{D_{eff,i} \cdot N}{\delta} \tag{9.7}$$

$$a_{g-l} = a \cdot \alpha \tag{9.8}$$

$$a_{l-b} = \beta \cdot a_{g-l} \tag{9.9}$$

$$a_{g-b} = \left(a - a_{g-l}\right) \cdot \beta \tag{9.10}$$

$$\beta = \frac{\varepsilon_b}{a \cdot \delta} \tag{9.11}$$

The set of partial differential equations was discretized in space along the biofilm thickness. Six points were used along the biofilm thickness. The resulting set of ordinary differential equations was solved using a Rosenbrock (stiff) integration method with Berkeley Madonna 8.3.18. Model predictions in the present work were checked by performing a statistical analysis based on a paired t-Student's test at 5% level of significance.

9.3.4. Microbial kinetic model

The OUR within the biofilm was described by a double Monod-Haldane type kinetic expression depending on dissolved oxygen and dissolved H₂S concentrations inside the biofilm (Eqs. 9.12 and 9.13). The H₂S uptake rate was computed from Eqs. 9.14 and 9.15 as a function of the stoichiometric yield of sulfide oxidation.

-   *Wetted biofilm*

$$r_{b,\cdot O_2} = OUR_{max} \cdot \left(\frac{C_{b,O_2}}{C_{b,O_2} + K_{S,O_2}} \right) \left(\frac{C_{b,H_2S}}{K_{S,H_2S} + C_{b,H_2S} + \frac{(C_{b,H_2S})^2}{k_I}} \right) \tag{9.12}$$

- *Non-wetted biofilm*

$$r_{b-NW,\cdot O_2} = OUR_{max} \cdot \left(\frac{C_{b-NW,O_2}}{C_{b-NW,O_2} + K_{S,O_2}} \right) \left(\frac{C_{b-NW,H_2S}}{K_{S,H_2S} + C_{b-NW,H_2S} + \frac{(C_{b-NW,H_2S})^2}{k_I}} \right) \tag{9.13}$$

- *Stoichiometric consideration*

$$r_{b,H_2S} = \frac{r_{b,O_2}}{Y_{O_2/H_2S}} \tag{9.14}$$

$$r_{b-NW,H_2S} = \frac{r_{b-NW,O_2}}{Y_{O_2/H_2S}} \tag{9.15}$$

9.3.5. Stoichiometry of H₂S oxidation

Recent reports (Klok et al., 2012) stated that elemental sulfur or sulfate production occur depending on the molar ratio of dissolved oxygen and sulfide species in the biofilm, namely $C_{b,O2}/C_{b,H2S}$ ratio. At molar ratio $C_{b,O2}/C_{b,H2S} \leq 1.0$ H₂S oxidation occurs through Eq. 9.16 at a stoichiometric yield $Y_{O_2/H_2S} = 0.5$ while Eq. 9.17 predominates at a stoichiometric yield $Y_{O_2/H_2S} = 2.0$ when the molar ratio $C_{b,O2}/C_{b,H2S} >$ 1.0. During modeling of respirometric assays, the molar ratio $C_{b,O2}/C_{b,H2S}$ in the biofilm was evaluated at every integration step of the set of differential equations in order to predict the fate of H₂S oxidation. A step switch function was programmed to use the corresponding molar yield.

$$H_2S + 0.5O_2 \rightarrow S^0 + H_2O \tag{9.16}$$

$$H_2S + 2O_2 \rightarrow SO_4^{2-} + 2H^+ \tag{9.17}$$

Furthermore, the calibrated model was used to predict the transient H₂S elimination capacity of the biotrickling filter bed (g H₂S m⁻³ bed h⁻¹) considering the fate of H₂S as well as the contribution of wetted and non-wetted biofilm to H₂S elimination according to Eq. 9.18.

$$EC_{H_2S} = \left[(r_{b,\cdot O_2} \cdot a_{l-b}) + (r_{b-NW,\cdot O_2} \cdot a_{g-b}) \right] \cdot \frac{\delta}{0.94 \cdot Y_{O_2/H_2S}} \tag{9.18}$$

9.3.6. Model parameters estimation

Physical and some biokinetic parameters included in the model were either experimentally determined or taken from literature while others were obtained from the packing materials manufacturers (Table 9.1). The experimental gaseous and dissolved oxygen concentration profiles generated from selected respirometric tests were used to calibrate the mathematical model described above. Only a biokinetic parameter (OUR$_{max}$) and two morphological parameters (biofilm thickness δ, and packing wetting ratio α) were determined by fitting the experimental data. Parameters estimation was performed following the least square method by minimizing the quadratic error between model predictions and measured gaseous and dissolved oxygen concentrations. Model simulations and parameters estimation were performed with Berkeley Madonna 8.3.18 software. A statistical analysis based on paired t-student tests at a 5% level of significance were performed for dissolved oxygen and oxygen gas in both packing materials in order to quantify the agreement between results predicted by the model with the optimized kinetic parameters and experimental data.

Table 9.1. Parameters included in the mathematical model

Parameter	Colonized PR		Colonized PUF		Units
	Value	*Ref.*	*Value*	*Ref.*	
ε_g	0.70	E.D.	0.85	E.D.	$m^3_{gas} \cdot m^{-3}_{bed}$
ε_b	0.02	E.D.	0.03	E.D.	$m^3_{biofilm} \, m^{-3}_{bed}$
ε_l	0.10	E.D.	0.09	E.D.	$m^3_{liquid} \, m^{-3}_{bed}$
ε_S	0.18	M.D.	0.03	M.D.	$m^3_{liquid} \, m^{-3}_{bed}$
a	354	M.D.	600	M.D.	$m^2 \, m^{-3}_{bed}$
$Ks_{,O2}$	0.03	[5]	0.03	[5]	$g \, m^{-3}$
$Ks_{,H2S}$	1.00	[13]	1.00	[13]	$g \, m^{-3}$
Ki	40.55	[15]	40.55	[15]	$g \, m^{-3}$
$\mathcal{D}_{iff_{O_2}}$	7.10×10^{-6}	ICAS[*]	7.10×10^{-6}	ICAS[*]	$m^2 \, h^{-1}$
$\mathcal{D}_{iff_{H_2S}}$	6.30×10^{-6}	[16]	6.30×10^{-6}	[16]	$m^2 \, h^{-1}$
He_{O2}	32.60	ICAS[*]	32.60	ICAS[*]	Dimensionless
He_{H2S}	0.41	[17]	0.41	[17]	Dimensionless
$K_L a_{g-l}$	29.31	E.D.	22.08	E.D.	h^{-1}
$V_{g \, res}$	6.30×10^{-4}	E.D.	6.30×10^{-4}	E.D.	m^3
$V_{l \, res}$	1.26×10^{-4}	E.D.	1.26×10^{-4}	E.D.	m^3
V_{bed}	6.10×10^{-4}	E.D.	6.10×10^{-4}	E.D.	m^3

* ICAS 13 data base, Denmark. E.D. Experimental determination. M.D. Manufacturer data

9.4. RESULTS AND DISCUSSION

9.4.1.   Biomass cultivation

In Figure 9.2 the operation of the BTFs system is presented. During the first three weeks the EBRT as well as the sulfur load were adequate to select and acclimate the biomass while obtaining removal efficiency (RE) over 98%. After 40 days the sulfur load was fixed in 48 g S m⁻³ bed h⁻¹ with an inlet H₂S concentration of 300 ppm$_v$ and an EBRT of 30 s. As observed from Figure 9.2, the RE was above 99% during almost the whole operation. Only two operational problems caused a RE drop under 80% on days 38 and 48. Even though, the system was rapidly recovered after 3 days. An additional

RE drop was observed on day 40 which was related to the sulfur load increase. The biomass was acclimated again to the new conditions in 2 days. The BTF system showed in general that at an EBRT of 30 s there were no limitations for a sulfur load of 48 g S m^{-3} h^{-1} and that the biomass also presented satisfactory recovery capacities after operational problems.
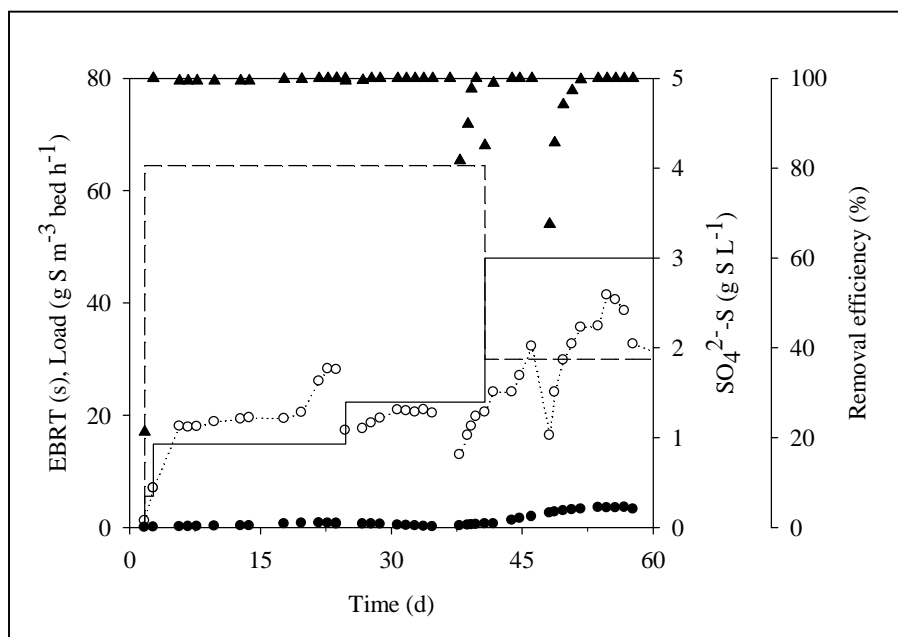

Figure 9.2. Operation of the BTFs system. Symbols: Removal efficiency (▲), elemental sulfur accumulated in the packed bed (●), sulfate (○). Lines: Empty bed residence time (dashed line), sulfur load (solid line).

9.4.2. Abiotic tests

In Figure 9.3 the K_La_{g-1} as a function of the hydrodynamic conditions for both packing materials is presented. Results from the abiotic tests indicated that the gas velocity had a larger impact on K_La_{g-1} compared to the impact of increasing the liquid velocity for both packing materials. Probably this increase of gas velocity on the K_La_{g-1} could be due to the excessive mixing of liquid, which caused a reasonable reduction of the resistance to the mass transport in the liquid side. Kim and Deshusses (2008) also suggested a proportional relationship of the liquid linear velocities to the oxygen K_La values, which was confirmed with the results obtained herein.

Regarding to the packing materials, both showed similar performance and values for the oxygen K_La_{g-l}. Despite of the lower specific surface area of PR compared to PUF, slightly higher K_La_{g-l} values for PR were found. Characterization of PUF in several works has shown that the reticulate structure of PUF provides a large accumulation of water in packed beds in the form of water droplets (Dorado et al., 2010). Both results suggest that such water accumulation in PUF does not necessarily improve G-L mass transfer if water is not well distributed as a thin layer over the surface of the packing material. In fact, Table 9.2 shows that α, the fraction of the packing surface covered with water, was estimated to be similar for PR and PUF. Then, the larger bulk porosity of PUF does not correspond to a better water trickling since a fraction of the water accumulated inside the foam may not be accessible for G-L mass transfer. Therefore, water and biofilm distribution over the surface of both packing materials might have a large impact in the performance of the system.

Finally, hydrodynamic conditions that lead to a K_La_{g-l} of around 20 h^{-1} (gas and liquid flow rates of 43.4 m h^{-1} and 10.8 m h^{-1}, respectively) were selected as convenient for biofiltration operation according to Kim and Deshusses (2003). Therefore, such conditions were set for subsequent biotic tests.
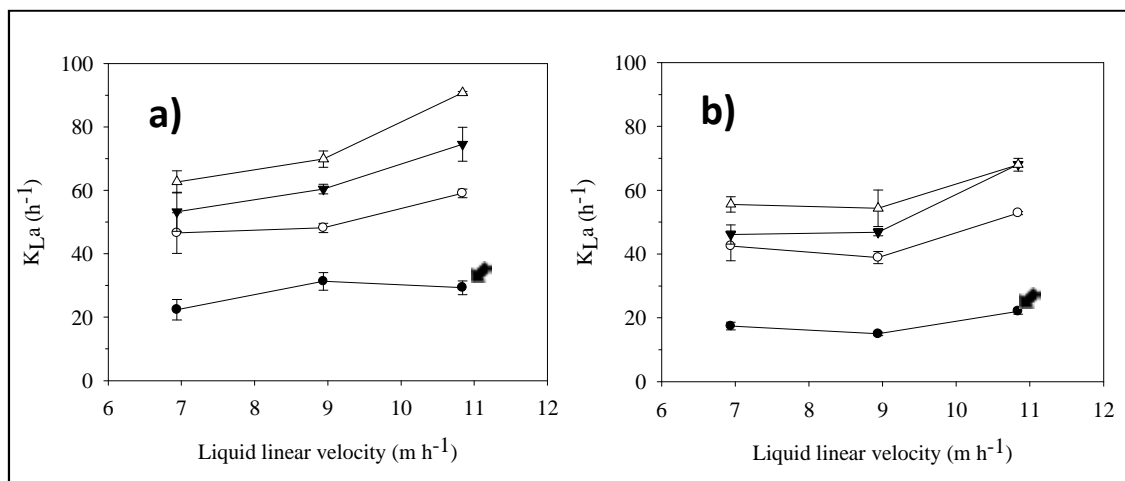

Figure 9.3. Mass transfer coefficient for the two different packing materials tested at different gas and liquid flow rates. (a) Stainless steel PR (b) PUF. Symbols: Gas velocity 43.37 m h^{-1} (●) Gas velocity 57.83 m h^{-1} (○) Gas velocity 77.11 m h^{-1} (▼), Gas velocity 101.21 m h^{-1} (△). Values marked with an arrow indicate the values used for biotic tests.

9.4.3. Biotic tests: estimation of kinetic parameters

Figure 9.4 shows the oxygen concentration changes in gas and liquid phases induced due to the biological H_2S oxidation in the corresponding packed bed tested. The total biofilm mass experimentally assessed on PR and PUF was 10.9 and 17.8 g VSS, respectively. Solid lines show the HR model predictions after optimization of OUR_{max}, δ and α for both packing materials. Overall, a good agreement was found for the oxygen profiles in the gas phase for both packing materials. Also, the dissolved oxygen concentration predicted for the PR packing was satisfactory (Figure 9.4a) while a slight overestimation of the oxygen consumption was found for PUF towards the end of the test. The t-tests executed for all variables in Figure 9.4 yielded absolute values in between the two t-test tails at a 5% level of significance indicating that the differences between dissolved oxygen and oxygen gas measured experimentally and those predicted by the model were not statistically significant in the studied period. The fitted parameters as well as other relevant parameters calculated from model estimates are shown in Table 9.2.
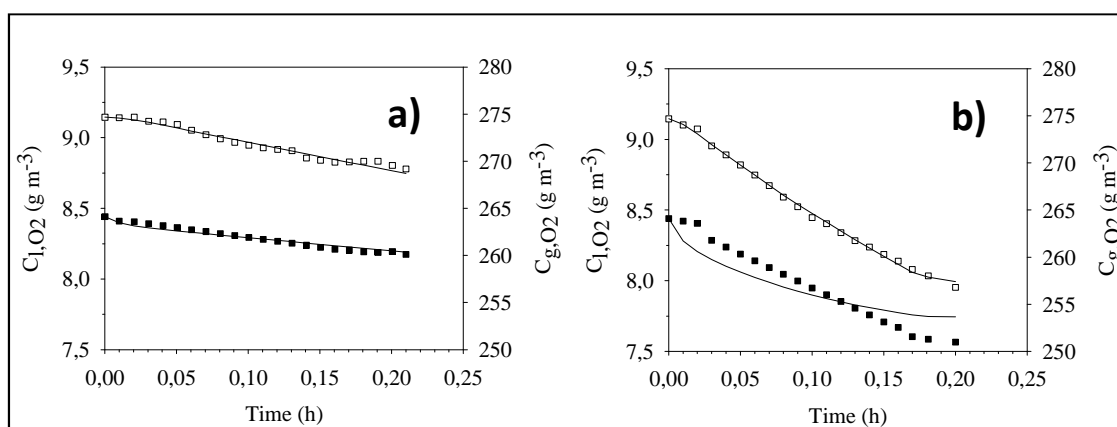
Figure 9.4. Experimental results and predicted profiles of the HR model obtained from the respirometric assays with a gas pulse of 10 mL of pure H_2S (a) Stainless steel PR (b) PUF. Symbols: Experimental oxygen concentration in the gas phase (□), Experimental oxygen concentration in the liquid phase (■). Model data (solid line).

Table 9.2 also shows the maximum elimination capacity (EC) estimated (EC_{max}) by the model corresponding to the maximum activity along the biotic test for each

packing material (Figure 9.5). Oppositely to that of PR, the EC estimated for the PUF indicated that H_2S was almost depleted at the end of the test. In the first 2 minutes an initial lag phase was found for both packing materials. As commonly found in respirometric tests performed with suspended cultures, such behavior was related to the wake up time needed by microorganisms for adapting to the test conditions after the endogenous phase.

Table 9.2. Fitted parameters for the calibration of the HR mathematical model to the respective PR and PUF assays and other relevant parameters computed. The average of triplicates and their corresponding standard deviation are presented.

Parameter	PR	PUF	Units
OUR_{max} (best fitted)	934±353	4762±1197	g O_2 m^{-3} biomass h^{-1}
δ (best fitted)	2.63x10^{-4} ±0.67x10^{-4}	1.20x10^{-4} ±0.15x10^{-4}	m
α (best fitted)	0.09 ±0.02	0.08± 0.01	m^2 liq. m^{-2} bed
EC_{max}	269.7±42.9	928.6±75.69	g H_2S m^{-3} h^{-1}
β	0.15	0.44	m^2 biofilm m^{-2} bed
q $O_{2\ max}$	2.64±1.00	13.52 ±3.41	mmol O_2 g^{-1} N min^{-1}
a_{l-b}	11.35	24.00	m^2 wetted-biofilm m^{-3}$_{bed}$
a_{g-b}	72.05	250.61	m^2 non-wetted biofilm m^{-3}$_{bed}$

From the abovementioned results, at the trickling rate tested (10.8 m h^{-1}), the fraction of biofilm covered by water (assuming to be proportional to α) was much smaller than that directly exposed to the gas for both packing materials. Even if the thickness of the biofilm on PUF was more than half that of the PR, the surface of packing covered by biofilm (β), the area of biofilm directly exposed to the gas phase (a_{g-b}) and the OUR_{max} were significantly larger for the PUF packing compared to those for the PR. Moreover, since wetted surfaces (a_{l-b}) were lower for PR and PUF compared to the non-wetted surface (a_{g-b}), the contribution of the G-L flux and that of the G-B flux was significantly different for both packing materials. According to the mass transport terms in Eq. 9.1, the oxygen G-B flux was 1.1 g O_2 m^{-2} h^{-1}, while the corresponding G-L flux was 0.24 g O_2 m^{-2} h^{-1} for PUF. Similarly, gas fluxes of 0.25 and

0.02 g O$_2$ m^{-2} h^{-1} for G-B and G-L fluxes, respectively, were found for PR. Nevertheless, the H$_2$S elimination capacity predicted by the model (Eq. 9.15), scrutinized in average that around 95% of the H$_2$S elimination capacity was due to the non-wetted biofilm part for the two packing materials tested.
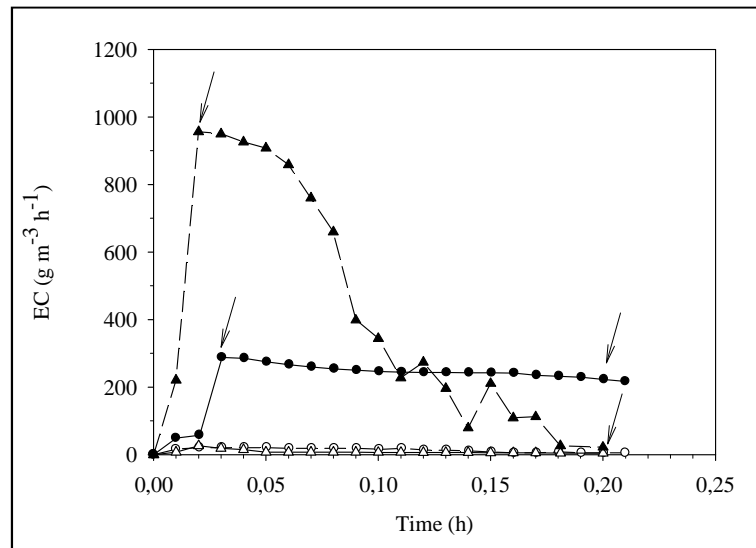

Figure 9.5. Predicted H$_2$S elimination capacity for the wetted and non-wetted fractions of colonized PUF and PR packing materials. Arrows indicate the time at which the rate controlling step was assessed (t$_{max}$, left arrows and t$_{end}$, right arrows). Symbols: wetted PR (○), non-wetted PR (●), wetted PUF (△), non-wetted PUF (▲).

However, an opposite behavior to the oxygen fluxes was computed for H$_2$S, resulting in a G-L flux slightly higher than the G-B flux, which can be explained in terms of the gradient concentrations conditioning the mass fluxes (Eq. 9.1). In the case of H$_2$S, these concentration gradients were similar either for G-L and G-B interfaces, which indicated that no external mass transfer limitation of H$_2$S occurred, mainly due to its much higher solubility than that of oxygen. Here the H$_2$S solubility can be sensibly enhanced by its absorption in aqueous solutions at pH> 7 (Gonzalez-Sanchez et al. 2007). In addition, experimental results about biomass density indicated that the biofilm amount on the PUF was almost twice larger that on PR, so different distribution in the bed leads to key consequences in terms of H$_2$S removal. In the case of PUF, a thinner biofilm as well as a surface colonized by biofilm were almost twice that in the PR

which lead to a PUF biofilm much more active (3 times compared with PR taking as reference the EC_{max}) with a larger capacity for H_2S degradation and concomitant oxygen consumption.

The model also predicted that maximum EC for H_2S occurred close to or under oxygen limiting conditions in both wetted and non-wetted biofilms. The reported H_2S elimination capacities are between 50 to 400 g H_2S m^{-3} h^{-1} (Kim and Deshusses, 2003; Aroca et al., 2007; Ramirez et al., 2009; Montebello et al., 2012) for different BTF packed with various materials and operated under similar conditions were in general much lower than the predicted by the calibrated mathematical model. This fact shows that conventional BTFs could not be optimally operated, meaning that the biofilm has to be exposed to optimal H_2S concentrations (non-limiting and non-inhibiting) as well as non-limiting oxygen concentration. These ideal conditions could be very difficult to reach, especially at full-scale BTF, where probably a large percentage of biofilm has low or no S-oxidizing activity. As pointed out by other authors, the use of intensive devices for O_2 transport to the liquid phase may help improving the performance of target compounds such as H_2S (Rodriguez et al., 2012) which is the main bottleneck when high loads of H_2S are removed.

9.4.4. Assessment of the rate controlling step

The calibrated HR model was used to assess the profiles of the electron donor and acceptor inside the biofilm at two particular times of the respirometry. First, at the time of reaching the EC_{max}, namely t_{max}, and secondly at the end of the test, namely t_{end} (Figure 9.5). Figure 9.6 shows the predicted concentrations of H_2S and dissolved oxygen inside of the wetted and non-wetted biofilm for both packing materials at both t_{max} and t_{end}. Figure 9.6a and 9.6b show, for the wetted biofilm, a similar behavior in both colonized packed beds independently of the time at which profiles were assessed. Almost the whole biofilm was active in both cases except in the inner layers of the PUF biofilm at t_{end} (Figure 9.6b) since H_2S had been almost completely consumed at the end of the test. Except in the latter case, no substrate limitation occurred in the wetted fractions of the biofilm. These results indicated that for the wetted biofilm, limited G-L oxygen transport compared to that of H_2S, i.e. solubility, could have conditioned the bioreaction rate at first layers of biofilm, due to slightly larger accumulation of H_2S at t_{max} in the wetted biofilm than the accounted for the non-wetted biofilm (Figure 9.6c

and 9.6d). A partial substrate inhibition of the H_2S degradation rate would explain that almost all wetted biofilm was active but not fast enough. The H_2S external transport was not relevant here because of its much higher solubility (He=0.41) compared to that of oxygen (He=32) under standard conditions.
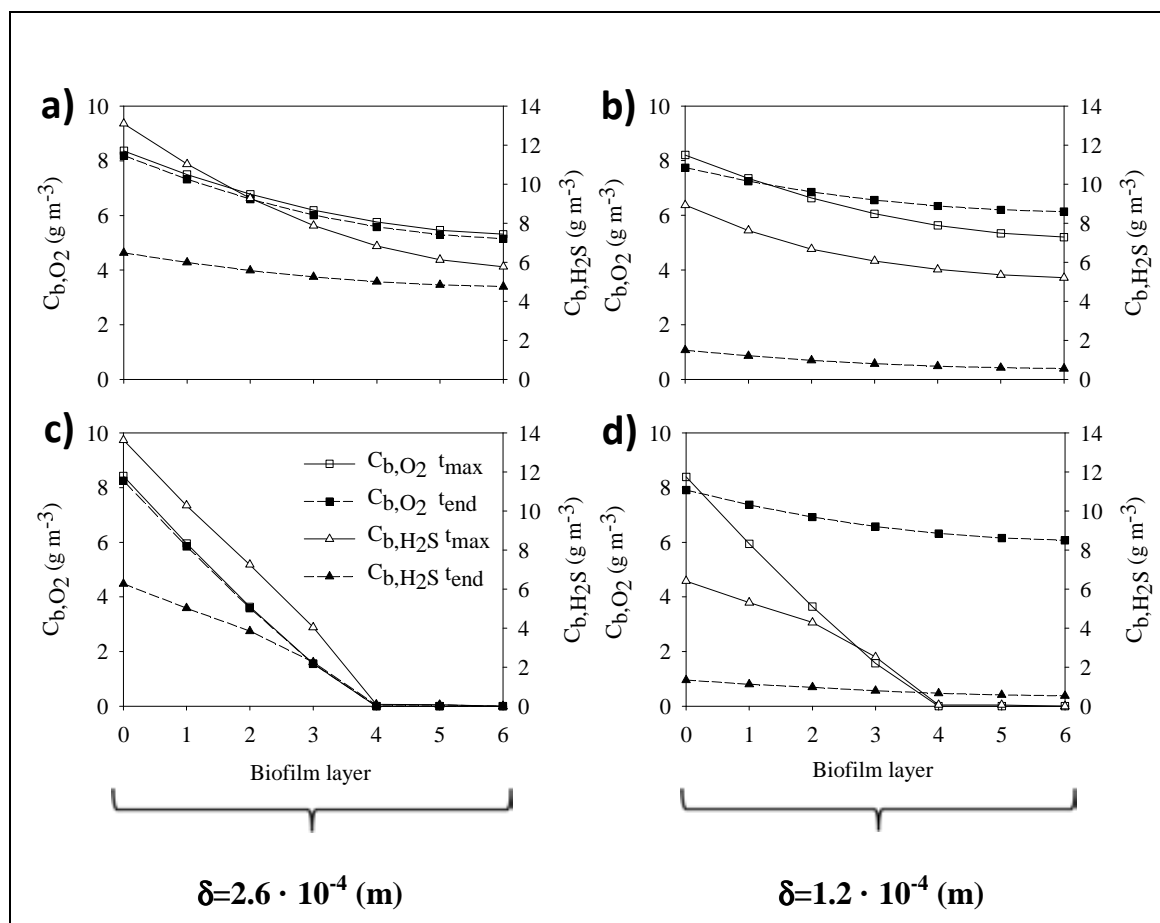

Figure 9.6. Simulated dissolved H_2S and oxygen concentration profiles inside the biofilm, at t_{max} and t_{end} for (a) wetted stainless steel PR (b) wetted PUF (c) non-wetted stainless steel PR (d) non-wetted PUF.

Oppositely, profiles for the non-wetted biofilm exhibited complete depletion before reaching the inner layers of the biofilm (Figure 9.6c and 9.6d). In the case of PUF at t_{max} (Figure 9.6d), the H_2S elimination capacity in the non-wetted biofilm was limited by the diffusion of oxygen through the biofilm. These results indicated that in the non-wetted biofilm, where no external mass transport resistance existed, bioreaction rates were maximized in the external layers but minimized in the deeper layers of the

biofilm. This means that both oxygen and H_2S diffusion rates through biofilm were limiting the activity of the biofilm which turned out to be inactive for both packing materials in the inner layers.

Also, model predictions helped understanding the different instant by-products production from H_2S biological oxidation in a range of situations. Since different H_2S and O_2 concentrations in the biofilm existed along time and biofilm depth, the H_2S elimination rates and its controlling factor depended on the molar $C_{b,O2}/C_{b,H2S}$ ratio which, in turn, defined the products of H_2S oxidation. Figure 9.7 shows the molar $C_{b,O2}/C_{b,H2S}$ ratio through the biofilm thickness computed at the same times than those in Figure 9.6. According to Eqs. 9.14 and 9.15, a combination of elemental sulfur and sulfate were being produced in both packing materials.
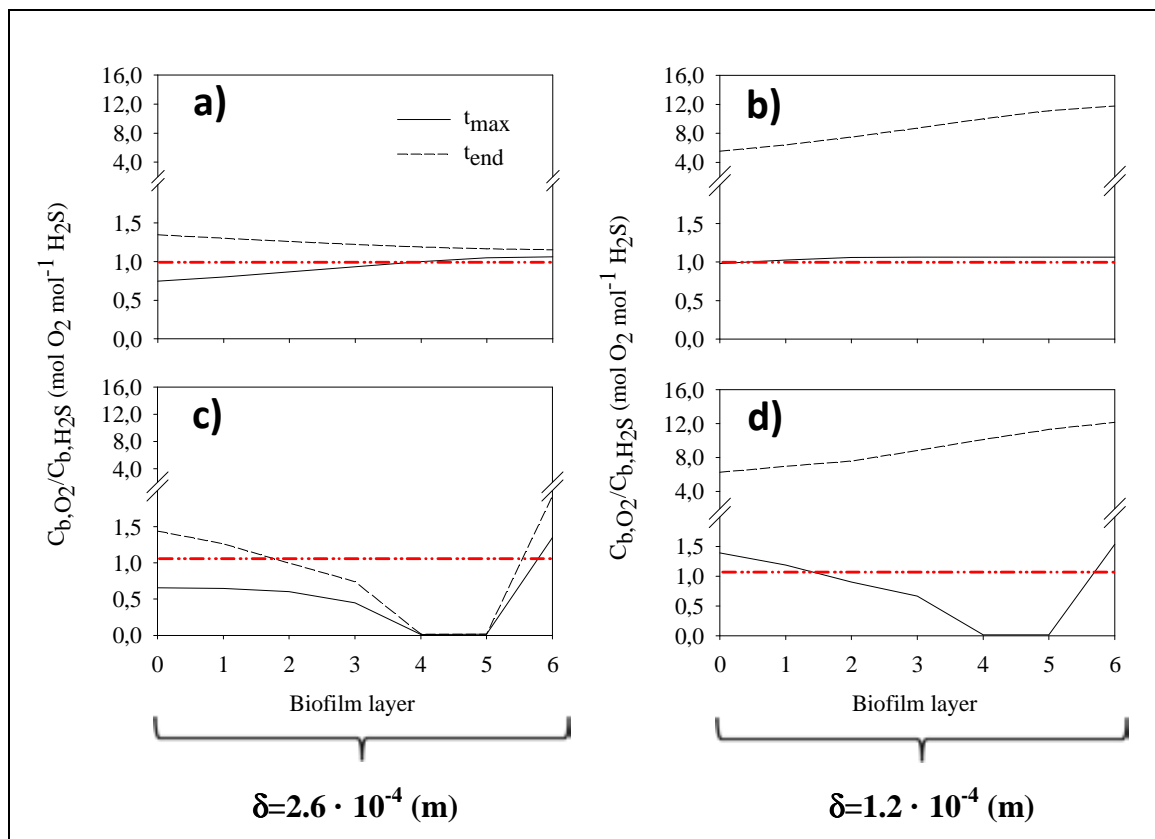

Figure 9.7. Dissolved oxygen and H_2S concentrations ratios inside the biofilm at t_{max} and t_{end} for (a) wetted stainless steel PR (b) wetted PUF (c) non-wetted stainless steel PR (d) non-wetted PUF. Dash-dotted lines correspond to the molar ratio at which stoichiometry switches occurs.

Although at the end of the tests an oxygen excess condition was reached and, concomitantly, sulfate was the main product of H_2S oxidation (Figure 9.7), in the case of PR, results indicate that elemental sulfur was produced at t_{max} in all biofilm fractions while sulfate was only produced in part of the biofilm only towards the end of the test (Figure 9.7a). Oppositely, sulfate was the end product of H_2S oxidation in the case of PUF at all times and all biofilm depths except in layers 3 and 4 at t_{max} (Figure 9.7d), corresponding to the existence of oxygen limitation. The molar ratios $C_{b,O2}/C_{b,H2S}$ predicted inside of the biofilm indicate that maximum elimination capacities should be reached under oxygen limiting conditions, but this means to overload the biofilm with H_2S. This could induce several performance risks, i.e. reaching toxic H_2S concentrations (>1 mM) or clogging the biofilter bed by excessive formation and accumulation of elemental sulfur. Instead, excess oxygen is desirable in terms of biofilter operation, but expensive because of the need to keep neutral pH (Eq. 9.14) as well as to promote adequate oxygen transfer if high loading rates of H_2S are treated (Fortuny et al., 2008). Other factors not considered herein such as the reticulate structure of PUF must be also included in order to analyze the performance of different packing materials based on the HR. As an example, the larger biomass retention capacity of PUF may be counterproductive when elemental sulfur is produced in the bed.

9.5. CONCLUSIONS

The use of bacterial biofilm as catalyst for the desulfurization of biogas in biotrickling filters is very convenient in terms of its easy design and operation, but difficult to keep good performance if not enough knowledge about the complex phenomena occurring in the biofiltration process is available.

Oppositely to respirometry performed with suspended cultures, the heterogeneous respirometry can mimic the hydrodynamic conditions found in a BTF allowing the estimation of the intrinsic biological activity of the biofilm by inducing comparative boundary layer properties of the mobile phases. Besides, the heterogeneous respirometric methodology described in this chapter considers and quantifies phenomena such as the partial wetting of both the packing material and biofilm that occur in real biotrickling filters. In this sense, heterogeneous respirometry was

successfully applied to characterize the basic biofiltration properties (i.e. transport and biological phenomena) using representative colonized packing material from an operating desulfurizing BTF in a short period of time, which allowed considering the biofilm properties as constant. Evaluation of mass transport by mimicking the BTF operation conditions during the respirometric assays allowed quantifying the contribution of wetted and non-wetted biofilm fractions to the overall removal of H_2S as well as to determine the limiting step.

From these results it was concluded that the non-wetted fraction of both packing materials tested in this study was the one that mostly contributed to the EC observed, which is consistent with the common experimental evidence that a higher water hold-up in BTFs leads to reduced EC and RE for poorly soluble compounds as O_2. This technique has shown to be highly adequate to study the kinetics of immobilized biomass, which is essential in those generic models describing biofiltration process, with the minimal handling of the biofilm.

Chapter 10

GENERAL CONCLUSIONS AND FUTURE WORK

10. GENERAL CONCLUSIONS AND FUTURE WORK

10.1.   CONCLUSIONS

The conclusions derived from this thesis could be grouped in three main topics: characterization of SOB under anoxic conditions, characterization of SOB under aerobic conditions and application of heterogeneous respirometry to characterize immobilized SOB.

10.1.1   Characterization of SOB under anoxic conditions

The conclusions related with the characterization of SOB under anoxic conditions arising from chapters 5, 6 and 7 are:

- A procedure to characterize mixed cultures obtained from desulfurizing BTFs was successfully developed and applied. The methodology allowed studying denitrification and sulfide oxidation mechanisms and kinetics. However, to apply this procedure the biofilm structure must be destroyed since suspended conditions of the biomass are required.

- Thiosulfate oxidation rate was influenced by the electron acceptor used and also inhibited by nitrite concentrations over 25 mg N L^{-1}.

- Nitrite inhibition over nitrite reduction, as well as sulfide inhibition over sulfide oxidation, was properly described through a Haldane kinetic equation

- Final products obtained from the biological reactions were affected by the initial S/N ratio employed but not the reaction rates. Then, nitrite accumulation did not depend on this ratio but on the initial nitrate concentration and on biomass characteristics.

- Two-step denitrification was successfully described with the stoichiometry calculated from the coupling of titrimetric and respirometric data.

- No competitive inhibition between nitrate and nitrite was detected during the respirometric tests when both were present in the medium.

- Acclimation of a SO-NR mixed culture to 150 mg NO_2^--N L^{-1} resulted in a denitritation rate a 37% higher than that of non-acclimated biomass. Thus, the acclimation of SO-NR biomass could be an effective solution for those anoxic BTF with operational problems caused by nitrite inhibition.

- An affinity-inhibition constant for elemental sulfur oxidation was included in the kinetic model describing two-step sulfide oxidation since it was confirmed that sulfide was preferentially consumed previous to other substrates present in the medium regardless of the S/N ratio.

- The kinetic models proposed, calibrated and validated in the abovementioned chapters described properly thiosulfate and sulfide oxidation under anoxic conditions.

10.1.2   Characterization of SOB under aerobic conditions

The conclusions related with the characterization of SOB under aerobic conditions arising from chapter 8 are:

- LFS respirometry was successfully implemented to characterize S-oxidizing biomass obtained from a desulfurizing biotrickling filter.

- An extremely high SOUR of 49.2 mg DO g^{-1} VSS min^{-1} was found to be consumed during sulfide oxidation indicating that *Thiothrix sp.* is a powerful bacteria for sulfide oxidation although causes serious clogging and operational problems due to its filamentous morphology.

- A maximum elemental sulfur fraction of 25% was estimated to be stored inside *Thriothrix sp.* cells, which was enough to inhibit the sulfide oxidation rate.

- An affinity-inhibition constant for elemental sulfur oxidation was included in the kinetic model describing two-step sulfide oxidation since it was confirmed that sulfide was preferentially consumed regardless the S/O_2 ratio present in the medium.

- Thiosulfate was produced from the chemical reactions between intermediary products of sulfide oxidation and characterized with a specific kinetic equation. This finding must be highlighted since this process has not been previously

reported at neutral conditions (to the author knowledge) and improves the elemental sulfur oxidation.

- Elemental sulfur biodegradation was not well described with a shrinking particle equation probably because intracellular particles size and the elemental sulfur speciation variations affected the kinetics corresponding to elemental sulfur oxidation.

- The kinetic model proposed was properly calibrated with the respirometric profiles and several kinetic parameters estimated.

10.1.3   Application of HR to characterize immobilized SOB

The conclusions related with the characterization of SOB under aerobic conditions arising from chapter 9 are:

- The heterogeneous respirometric technique has shown to be highly adequate to study the kinetics of immobilized biomass with the minimal handling of the biofilm.

- The HR mimics the hydrodynamic conditions found in a BTF allowing the estimation of the intrinsic biological activity of the biofilm by inducing comparative boundary layer properties of the mobile phases

- HR was successfully applied to characterize the basic biofiltration properties (i.e. transport and biological phenomena) using representative colonized packing material from an operating biotrickling filter

- Evaluation of mass transport during the respirometric assays allowed quantifying the contribution of wetted and non-wetted biofilms fractions to the overall removal of H_2S as well as to determine the limiting step.

- The non-wetted fraction of both packing materials tested was the one that mostly contributed to the EC observed. This is consistent with the common experimental evidence that a higher water hold-up in biotrickling filters leads to reduced EC and RE for poorly soluble compounds such as O_2.

10.2.   FUTURE WORK

In this thesis an extensive knowledge about sulfide, elemental sulfur and thiosulfate biological oxidation mechanisms has been acquired from the application of respirometric techniques to characterize SOB. However, further investigation is required in order to improve the procedure used to obtain kinetic and stoichiometric data.

Regarding to the homogeneous respirometer, the following modifications of the experimental setup could be performed in order to improve the data monitoring under anoxic conditions:

- Implementation of N_2O or NO in-line gas sensors. These compounds could be produced during denitrification and be removed from the respirometric vessel through the inert gas used to maintain the anoxic conditions. Their monitoring would provide more information about denitrification process.

- Implementation of nitrate or nitrite specific probes. This modification would provide more experimental data with less deviation associated. The analysis of these anions off-line through ionic chromatography entails less accurate data obtainment.

- Implementation of a redox probe. The monitoring of the redox potential helps to know which processes are taking place during the respirometric test and allows sampling better the system. Titrimetric data is very useful after the respirometric test, when the biological HPR is calculated. During the test is difficult to understand which process is taking place only with the monitoring of acid or base addition.

- Implementation of an off-line FIA monitoring system to monitor total dissolved sulfide in the liquid phase of the respirometer.

- Acquisition of a 3-L fermenter with sterilizable sensors and better sealing, culture agitation and temperature control to avoid the contamination of the original culture and to improve the homogeneity of the culture.

Moreover, further research related with the kinetic model used to describe the aerobic sulfide degradation (Chapter 8) is required in order to find out the exact mechanism behind thiosulfate production and, as well, the reason why elemental sulfur oxidation rate varies.

Regarding to the heterogeneous respirometer, future work focused on the improvement of the mathematical model must be performed in order to better describe the processes taking place during the respirometric test. The main objective of the following proposals is to get the standardization of the procedure in order to be used for desulfurizing biofilms characterization. The modifications related with monitoring tools to improve the experimental setup are:

- Implementation of a H_2S in-line sensor to monitor up to 10.000 ppm_v H_2S. In the experimental setup a H_2S sensor is currently installed although cannot be used during biotic tests since maximum concentrations of 200 ppm_v are allowed.

- Implementation of a redox probe. In this case is also helpful for real-time monitoring of the biological process.

- Modification of oxygen monitoring in the gas phase. Depending on the oxygen consumption during the respirometric test, the in-line oxygen sensor losses stability due to pressure changes. A pressure stabilizer or a different oxygen sensor with high sensitivity is required to improve the monitoring of this species.

- Improvement of liquid sampling. The monitoring of sulfate and thiosulfate off-line must be performed to characterize the whole biological process taking also into account intermediates production. However, this improvement is difficult since the system is completely sealed and the sampling implies pressure drop which affects the oxygen monitoring.

A part from these modifications, further research about the kinetics and stoichiometry of the reactions taking place inside the respirometer is required as well as the validation of the model with different experimental data.

Chapter 11

REFERENCES

Abatzoglou, N., Boivin, S., 2009. A review of biogas purification processes. Biofuels, Bioproducts and Biorefining 3, 42-71.

Almeida, J.S., Reis, M.A.M., Carrondo, M.J.T., 1995. Competition between nitrate and nitrite reduction in denitrification by *Pseudomonas fluorescens*. Biotechnol. Bioeng. 46, 476-484.

Almengló, F., Ramírez, M., Gómez, J.M., Cantero, D., Gamisans, X., Dorado, A.D. 2013. Modeling and control strategies development for anoxic biotrickling filtration. In: Proceedings of the 5th International Congress Biotechniques for Air Pollution Control and Bioenergy. Nîmes, France, 10-13 September, pp. 123-131.

Alper, E., Ozturk, S., 1985. Kinetics of oxidation of aqueous sodium sulfide solutions by gaseous oxygen in a stirred cell reactor. Chem. Eng. Commun. 36, 343-349.

An, S., Tang, K., Nemati, M., 2010. Simultaneous biodesulphurization and denitrification using an oil reservoir microbial culture: Effects of sulphide loading rate and sulphide to nitrate loading ratio. Water Res. 44, 1531-1541.

APHA, 2005. Standard Methods for the Examination of Water and Wastewater. American Publication Health Association, Washington, DC.

Aroca, G., Urrutia, H., Nunez, D., Oyarzun, P., Arancibia, A., Guerrero, K., 2007. Comparison on the removal of hydrogen sulfide in biotrickling filters inoculated with *Thiobacillus thioparus* and *Acidithiobacillus thiooxidans*. Electron. J. Biotechnol. 10, 514-520.

Artiga, P., Gonzalez, F., Mosquera-Corral, A., Campos, J.L., Garrido, J.M., Ficara, E., Mendez, R., 2005. Multiple analysis reprogrammable titration analyser for the kinetic characterization of nitrifying and autotrophic denitrifying biomass. Biochem. Eng. J. 26, 176-183.

Berg, J.S., Schwedt, A., Kreutzmann, A.C., Kuypers, M.M., Milucka, J., 2014. Polysulfides as intermediates in the oxidation of sulfide to sulfate by *Beggiatoa spp*. Appl. Environ. Microb. 80, 629-636.

Betlach, M.R., Tiedje, J.M., 1981. Kinetic explanation for accumulation of nitrite, nitric oxide, and nitrous oxide during bacterial denitrification. Appl. Environ. Microb. 42, 1074-1084.

Bogaert, H., Vanderhasselt, A., Gernaey, K., Yuan, Z.G., Thoeye, C., Verstraete, W., 1997. New sensor based on pH effect of denitrification process. J. Environ. Eng. 123, 884-891.

Brune, D.C., 1989. Sulfur oxidation by phototrophic bacteria. Biochim. Biophys. Acta. 975, 189-221.

Brüser, T., Lens, P.N.L., Trüper, H.G., 2000. The biological sulfur cycle. In: Environmental Technologies to Treat Sulfur Pollution. Principles and Engineering. IWA Publishing London, pp. 47-86.

Buisman, C., Uspeert, P., Janssen, A., Lettinga, G., 1990. Kinetics of chemical and biological sulphide oxidation in aqueous solutions. Water Res. 24, 667-671.

Buisman, C.J.N., Ijspeert, P., Hof, A., Janssen, A.J.H., Tenhagen, R., Lettinga, G., 1991. Kinetic parameters of a mixed culture oxidizing sulfide and sulfur with oxygen. Biotechnol. Bioeng. 38, 813-820.

Cabrol, L., Malhautier, L., Poly, F., Le Roux, X., Lepeuple, A.S., Fanlo, J.L., 2012. Resistance and resilience of removal efficiency and bacterial community structure of gas biofilters exposed to repeated shock loads. Biores. Technol. 123, 548-557.

Cai, J., Zheng, P., Qaisar, M., Xing, Y., 2013. Kinetic characteristics of biological simultaneous anaerobic sulfide and nitrite removal. Desalination and Water Treatment, 1-8.

Campos, J.L., Carvalho, S., Portela, R., Mosquera-Corral, A., Mendez, R., 2008. Kinetics of denitrification using sulphur compounds: Effects of S/N ratio, endogenous and exogenous compounds. Biores. Technol. 99, 1293-1299.

Can-Dogan, E., Turker, M., Dagasan, L., Arslan, A., 2010. Sulfide removal from industrial wastewaters by lithotrophic denitrification using nitrate as an electron acceptor. Water Sci. Technol. 62, 2286.

Cardoso, R.B., Sierra-Alvarez, R., Rowlette, P., Flores, E.R., Gomez, J., Field, J.A., 2006. Sulfide oxidation under chemolithoautotrophic denitrifying conditions. Biotechnol. Bioeng. 95, 1148-1157.

Claus, G., Kutzner, H.J., 1985. Physiology and kinetics of autotrophic denitrification by *Thiobacillus denitrificans.* Appl. Microbiol. Biotechnol. 22, 283-288.

Cline, J.D., Richards, F.A., 1969. Oxygenation of hydrogen sulfide in seawater at constant salinity, temperature and pH. Environ. Sci. Technol. 3, 838-&.

Cokgor, E.U., Insel, G., Aydin, E., Orhon, D., 2009. Respirometric evaluation of a mixture of organic chemicals with different biodegradation kinetics. J. Hazard. Mater. 161, 35-41.

Cox, H.H.J., Deshusses, M.A., 1998. Biological waste air treatment in biotrickling filters. Curr. Opin. Biotechnol. 9, 256-262.

Cox, H.H.J., Deshusses, M.A., 2002. Co-treatment of H_2S and toluene in a biotrickling filter. Chem. Eng. J. 87, 101-110.

Cuellar, A.D., Webber, M.E., 2008. Cow power: the energy and emissions benefits of converting manure to biogas. Environ. Res. Lett. 3.

Chen, K.Y., Morris, J.C., 1972. Kinetics of Oxidation of Aqueous Sulfide by O2. Environ. Sci. Technol. 6, 529-&.

Chung, Y.C., Huang, C.P., Pan, J.R., Tseng, C.P., 1998. Comparison of autotrophic and mixotrophic biofilters for H_2S removal. J. Environ. Eng. 124, 362-367.

Dahl, C., Prange, A., 2006. Bacterial sulfur globules: occurrence, structure and metabolism. Inclusions in prokaryotes. Springer, pp. 21-51.

Delhomenie, M.C., Nikiema, J., Bibeau, L., Heitz, M., 2008. A new method to determine the microbial kinetic parameters in biological air filters. Chem. Eng. Sci. 63, 4126-4134.

Dochain, D., Vanrolleghem, P.A., 2001. Dynamical modelling and estimation in wastewater treatment processes. IWA publishing.

Dogan, E.C., Turker, M., Dagasan, L., Arslan, A., 2012. Simultaneous sulfide and nitrite removal from industrial wastewaters under denitrifying conditions. Biotechnol. Bioproc. Eng. 17, 661-668.

Dorado, A.D., Baquerizo, G., Maestre, J.P., Gamisans, X., Gabriel, D., Lafuente, J., 2008. Modeling of a bacterial and fungal biofilter applied to toluene abatement: kinetic parameters estimation and model validation. Chem. Eng. J. 140, 52-61.

Dorado, A.D., Lafuente, F.J., Gabriel, D., Gamisans, X., 2010. A comparative study based on physical characteristics of suitable packing materials in biofiltration. Environ. Technol. 31, 193-204.

Estuardo, C., Marti, M.C., Huilinir, C., Lillo, E.A., von Bennewitz, M.R., 2008. Improvement of nitrate and nitrite reduction rates prediction. Electron. J. Biotechnol. 11.

Fajardo, C., Mora, M., Fernández, I., Mosquera-Corral, A., Campos, J.L., Méndez, R., 2014. Cross effect of temperature, pH and free ammonia on autotrophic denitrification process with sulphide as electron donor. Chemosphere 97, 10-15.

Fernandez, M., Ramirez, M., Perez, R.M., Gomez, J.M., Canter, D., 2013. Hydrogen sulphide removal from biogas by an anoxic biotrickling filter packed with pall rings. Chem. Eng. J. 225, 456-463.

Ficara, E., Canziani, R., 2007. Monitoring denitrification by pH-Stat titration. Biotechnol. Bioeng. 98, 368-377.

Ficara, E., Rozzi, A., Cortelezzi, P., 2003. Theory of pH-stat titration. Biotechnol. Bioeng. 82, 28-37.

Fortuny, M., Baeza, J.A., Gamisans, X., Casas, C., Lafuente, J., Deshusses, M.A., Gabriel, D., 2008. Biological sweetening of energy gases mimics in biotrickling filters. Chemosphere 71, 10-17.

Fortuny, M., Guisasola, A., Casas, C., Gamisans, X., Lafuente, J., Gabriel, D., 2010. Oxidation of biologically produced elemental sulfur under neutrophilic conditions. J. Chem. Technol. Biotechnol. 85, 378-386.

Friedrich, C.G., Bardischewsky, F., Rother, D., Quentmeier, A., Fischer, J., 2005. Prokaryotic sulfur oxidation. Curr. Opin. Microbiol. 8, 253-259.

Friedrich, C.G., Rother, D., Bardischewsky, F., Quentmeier, A., Fischer, J., 2001. Oxidation of reduced inorganic sulfur compounds by bacteria: emergence of a common mechanism? Appl. Environ. Microbiol. 67, 2873-2882.

Furumai, H., Tagui, H., Fujita, K., 1996. Effects of pH and alkalinity on sulfur denitrification in a biological granular filter. Water Sci. Technol. 34, 355-362.

Gabriel, D., Deshusses, M.A., 2004. Technical and economical analysis of the conversion of a full-scale scrubber to a biotrickling filter for odour control. Water Sci. Technol. 50, 309-318.

Gadekar, S., Nemati, M., Hill, G.A., 2006. Batch and continuous biooxidation of sulphide by *Thiomicrospira sp* CVO: reaction kinetics and stoichiometry. Water Res. 40, 2436-2446.

García-Peña, I., Hernández, S., Auria, R., Revah, S., 2005. Correlation of biological activity and reactor performance in biofiltration of toluene with the fungus *Paecilomyces variotii* CBS115145. Appl. Environ. Microbiol. 71, 4280-4285.

Gernaey, K., Bogaert, H., Massone, A., Vanrolleghem, P., Verstraete, W., 1997. On-line nitrification monitoring in activated sludge with a titrimetric sensor. Environ. Sci. Technol. 31, 2350-2355.

Gernaey, K., Petersen, B., Dochain, D., Vanrolleghem, P.A., 2002. Modeling aerobic carbon source degradation processes using titrimetric data and combined respirometric-titrimetric data: structural and practical identifiability. Biotechnol. Bioeng. 79, 754-767.

Glass, C., Silverstein, J., 1998. Denitrification kinetics of high nitrate concentration water: pH effect on inhibition and nitrite accumulation. Water Res. 32, 831-839.

Glass, C., Silverstein, J., Oh, J., 1997. Inhibition of denitrification in activated sludge by nitrite. Water Environ. Res. 69, 1086-1093.

Glass, J.B., Orphan, V.J., 2012. Trace metal requirements for microbial enzymes involved in the production and consumption of methane and nitrous oxide. Front. Microbiol. 3.

González-Sánchez A., Baquerizo G., GamisansX., Lafuente J. and Gabriel D. 2009. Short term characterization of a H_2S biotricking filter packing using a gaseous-liquid respirometer. In: Proceedings of the 3rd International Congress on Biotechniques for Air Pollution Control. Delft, The Netherlands, 28-30 September, pp. 255-260.

Gonzalez-Sanchez, A., Revah, S., 2007. The effect of chemical oxidation on the biological sulfide oxidation by an alkaliphilic sulfoxidizing bacterial consortium. Enz. Microbiol. Technol. 40, 292-298.

Gonzalez-Sanchez, A., Tomas, M., Dorado, A.D., Gamisans, X., Guisasola, A., Lafuente, J., Gabriel, D., 2009. Development of a kinetic model for elemental sulfur and sulfate formation from the autotrophic sulfide oxidation using respirometric techniques. Water Sci. Technol. 59, 1323-1329.

Govind, R., Wang, Z., 1997. Biofiltration kinetics for volatile organic compounds (VOCs) and development of a structure biodegradability relationship. In: Proceedings of the 90th Annual Meeting and Exhibition of the Air and Waste Management Association. Toronto, Canada, June 8-13.

Granger, J., Ward, B.B., 2003. Accumulation of nitrogen oxides in copper-limited cultures of denitrifying bacteria. Limnol. Oceanogr. 48, 313-318.

Gray, G.O., Knaff, D.B., 1982. The Role of a cytochrome C-552 cytochrome C-complex in the oxidation of Sulfide in *Chromatium Vinosum*. Biochim. Biophys. Acta. 680, 290-296.

Guerrero, R., Mas, J., Pedrosalio, C., 1984. Buoyant density changes due to intracellular content of sulfur in *Chromatium warmingii* and *Chromatium vinosum*. Arch. Microbiol. 137, 350-356.

Guisasola, A. 2005. Modelling biological organic matter and nutrient removal processes from wastewater using respirometric and titrimetric techniques. PhD Thesis, UAB, Barcelona.

Guisasola, A., Baeza, J.A., Carrera, J., Sin, G., Vanrolleghem, P.A., Lafuente, J., 2006. The influence of experimental data quality and quantity on parameter estimation accuracy: Andrews inhibition model as a case study. Educ. Chem. Engineers 1, 139-145.

Guisasola, A., Vargas, M., Marcelino, M., Lafuente, J., Casas, C., Baeza, J.A., 2007. On-line monitoring of the enhanced biological phosphorus removal process using respirometry and titrimetry. Biochem. Eng. J. 35, 371-379.

Hallberg, K.B., Dopson, M., Lindstrom, E.B., 1996. Reduced sulfur compound oxidation by *Thiobacillus caldus*. J. Bacteriol. 178, 6-11.

Hartler, N., Libert, J., Teder, A., 1967. Rate of sulfur dissolution in aqueous sodium sulfide. Ind. Eng. Chem. Proc. 6, 398-&.

Heijnen, J.J., 2002. Bioenergetics of Microbial Growth. Encyclopedia of Bioprocess Technology. John Wiley & Sons, Inc.

Hendriks, J., Oubrie, A., Castresana, J., Urbani, A., Gemeinhardt, S., Saraste, M., 2000. Nitric oxide reductases in bacteria. Biochim. Biophys. Acta. 1459, 266-273.

Janssen, A.J.H., De Keizer, A., Lettinga, G., 1994. Colloidal properties of a microbiologically produced sulphur suspension in comparison to a LaMer sulphur sol. Colloids and Surfaces 3, 111-117.

Janssen, A.J.H., Lens, P.N.L., Stams, A.J.M., Plugge, C.M., Sorokin, D.Y., Muyzer, G., Dijkman, H., Van Zessen, E., Luimes, P., Buisman, C.J.N., 2009. Application of bacteria involved in the biological sulfur cycle for paper mill effluent purification. Sci. Total Environ. 407, 1333-1343.

Janssen, A.J.H., Lettinga, G., de Keizer, A., 1999. Removal of hydrogen sulphide from wastewater and waste gases by biological conversion to elemental sulphur. Colloidal and interfacial aspects of biologically produced sulphur particles. Colloids and Surfaces 151, 389-397.

Jin, Y.M., Veiga, M.C., Kennes, C., 2005. Effects of pH, CO_2, and flow pattern on the autotrophic degradation of hydrogen sulfide in a biotrickling filter. Biotechnol. Bioeng. 92, 462-471.

Johnson, K., Jiang, Y., Kleerebezem, R., Muyzer, G., van Loosdrecht, M.C., 2009. Enrichment of a mixed bacterial culture with a high polyhydroxyalkanoate storage capacity. Biomacromolecules 10, 670-676.

Jubany, I., Baeza, J.A., Carrera, J., Lafuente, J., 2005. Respirometric calibration and validation of a biological nitrite oxidation model including biomass growth and substrate inhibition. Water Res. 39, 4574-4584.

Justin, P., Kelly, D.P., 1978. Growth kinetics of *Thiobacillus denitrificans* in anaerobic and aerobic chemostat culture. J. Gen. Microbiol. 107, 123-130.

Kelly, D.P., 1982. Biochemistry of the chemolithotrophic oxidation of inorganic sulfur. Phil. Trans. R. Soc. Lon. 298, 499-528.

Kelly, D.P., 2003. Microbial inorganic sulfur oxidation: the APS pathway. In: Biochemistry and Physiology of Anaerobic Bacteria. Springer, pp. 205-219.

Kelly, D.P., Shergill, J.K., Lu, W.P., Wood, A.P., 1997. Oxidative metabolism of inorganic sulfur compounds by bacteria. Anton. Leeuw. Int. J. 71, 95-107.

Khalid, A., Arshad, M., Anjum, M., Mahmood, T., Dawson, L., 2011. The anaerobic digestion of solid organic waste. Waste Manage. 31, 1737-1744.

Kim, S., Deshusses, M.A., 2003. Development and experimental validation of a conceptual model for biotrickling filtration of H_2S. Environ. Prog. 22, 119-128.

Kim, S., Deshusses, M.A., 2008. Determination of mass transfer coefficients for packing materials used in biofilters and biotrickling filters for air pollution control. Chem. Eng. Sci. 63, 841-855.

Kleerebezem, R., Mendez, R., 2002. Autotrophic denitrification for combined hydrogen sulfide removal from biogas and post-denitrification. Water Sci. Technol. 45, 349-356.

Kleinjan, W.E., de Keizer, A., Janssen, A.J.H., 2003. Biologically produced sulfur. In: Elemental Sulfur and Sulfur-Rich Compounds. Series: Top. Curr. Chem. 230, Springer, pp. 167-187.

Kleinjan, W.E., de Keizer, A., Janssen, A.J.H., 2005a. Equilibrium of the reaction between dissolved sodium sulfide and biologically produced sulfur. Colloids and Surfaces 43, 228-237.

Kleinjan, W.E., de Keizer, A., Janssen, A.J.H., 2005b. Kinetics of the reaction between dissolved sodium sulfide and biologically produced sulfur. Ind. Eng. Chem. Res. 44, 309-317.

Klok, J.B.M., de Graaff, M., van den Bosch, P.L.F., Boelee, N.C., Keesman, K.J., Janssen, A.J.H., 2013. A physiologically based kinetic model for bacterial sulfide oxidation. Water Res. 47, 483-492.

Klok, J.B.M., van den Bosch, P.L.F., Buisman, C.J.N., Stams, A.J.M., Keesman, K.J., Janssen, A.J.H., 2012. Pathways of sulfide oxidation by haloalkaliphilic bacteria in limited oxygen gas lift bioreactors. Environ. Sci. Technol. 46, 7581-7586.

Knowles, R., 1982. Denitrification. Microbiol. Rev. 46, 43-70.

Koenig, A., Liu, L.H., 2001. Kinetic model of autotrophic denitrification in sulphur packed-bed reactors. Water Res. 35, 1969-1978.

Kong, Z., Vanrolleghem, P., Willems, P., Verstraete, W., 1996. Simultaneous determination of inhibition kinetics of carbon oxidation and nitrification with a respirometer. Water Res. 30, 825-836.

Korner, H., Zumft, W.G., 1989. Expression of denitrification enzymes in response to the dissolved oxygen level and respiratory substrate in continuous culture of *Pseudomonas stutzeri.* Appl. Environ. Microbiol. 55, 1670-1676.

Krishnakumar, B., Manilal, V.B., 1999. Bacterial oxidation of sulphide under denitrifying conditions. Biotechnol. Lett. 21, 437-440.

Kuhn, A.T., Chana, M.S., Kelsall, G.H., 1983. A review of the air oxidation of aqueous sulphide solutions. J. Chem. Technol. Biotechnol. 33, 406-414.

Lee, E.Y., Lee, N.Y., Cho, K.S., Ryu, H.W., 2006. Removal of hydrogen sulfide by sulfate-resistant *Acidithiobacillus thiooxidans* AZ11. J. Biosci. Bioeng. 101, 309-314.

Lu, W.P., Kelly, D.P., 1988. Kinetic and energetic aspects of inorganic sulfur compound oxidation by *Thiobacillus tepidarius.* J. Gen. Microbiol. 134, 865-876.

Lynggaard-Jensen, A., 1999. Trends in monitoring of waste water systems. Talanta 50, 707-716.

Ma, Y.L., Yang, B.L., Zhao, J.L., 2006. Removal of H_2S by *Thiobacillus denitrificans* immobilized on different matrices. Biores. Technol. 97, 2041-2046.

Maestre, J.P., Rovira, R., Alvarez-Hornos, F.J., Fortuny, M., Lafuente, J., Gamisans, X., Gabriel, D., 2010. Bacterial community analysis of a gas-phase biotrickling filter for biogas mimics desulfurization through the rRNA approach. Chemosphere 80, 872-880.

Maki, J.S., 2013. Bacterial intracellular sulfur globules: structure and function. J. Mol. Microbiol. Biotechnol. 23, 270-280.

Manconi, I., Carucci, A., Lens, P., 2007. Combined removal of sulfur compounds and nitrate by autotrophic denitrification in bioaugmented activated sludge system. Biotechnol. Bioeng. 98, 551-560.

Manconi, I., Van der Maas, P., Lens, P., 2006. Effect of copper dosing on sulfide inhibited reduction of nitric and nitrous oxide. Nitric Oxide 15, 400-407.

Marcelino, M., Guisasola, A., Baeza, J.A., 2009. Experimental assessment and modelling of the proton production linked to phosphorus release and uptake in EBPR systems. Water Res. 43, 2431-2440.

Martin, R.W., Li, H.B., Mihelcic, J.R., Crittenden, J.C., Lueking, D.R., Hatch, C.R., Ball, P., 2002. Optimization of biofiltration for odor control: model calibration, validation, and applications. Water Environ. Res. 74, 17-27.

McMurray, S.H., Meyer, R.L., Zeng, R.J., Yuan, Z., Keller, J., 2004. Integration of titrimetric measurement, off-gas analysis and NOx biosensors to investigate the complexity of denitrification processes. Water Sci. Technol. 50, 135-141.

Mehra, R.K., 1974. Optimal input signals for parameter estimation in dynamic systems survey and new results. Automat. Contr., IEEE Trans. 19, 753-768.

Meulenberg, R., Scheer, E.J., Pronk, J.T., Hazeu, W., Bos, P., Kuenen, J.G., 1993. Metabolism of tetrathionate in *Thiobacillus acidophilus*. Fems. Microbiol. Lett. 112, 167-172.

Montebello, A.M., Bezerra, T., Rovira, R., Rago, L., Lafuente, J., Gamisans, X., Campoy, S., Baeza, M., Gabriel, D., 2013. Operational aspects, pH transition and microbial shifts of a H_2S desulfurizing biotrickling filter with random packing material. Chemosphere 93, 2675-2682.

Montebello, A.M., Fernandez, M., Almenglo, F., Ramirez, M., Cantero, D., Baeza, M., Gabriel, D., 2012. Simultaneous methylmercaptan and hydrogen sulfide removal in the desulfurization of biogas in aerobic and anoxic biotrickling filters. Chem Eng J 200, 237-246.

Mora, M., Fernández, M., Gómez, J., Cantero, D., Lafuente, J., Gamisans, X., Gabriel, D., 2014a. Kinetic and stoichiometric characterization of anoxic sulfide oxidation by SO-NR mixed cultures from anoxic biotrickling filters. Appl. Microbiol. Biotechnol. 1-11.

Mora, M., López, L.R., Gamisans, X., Gabriel, D., 2014b. Coupling respirometry and titrimetry for the characterization of the biological activity of a SO-NR consortium. Chem. Eng. J. 251, 111-115.

Mora, M., Guisasola, A., Gamisans, X., Gabriel, D., 2014c. Examining thiosulfate-driven autotrophic denitrification through respirometry. Chemosphere 113, 1-8.

Munz, G., Gori, R., Mori, G., Lubello, C., 2009. Monitoring biological sulphide oxidation processes using combined respirometric and titrimetric techniques. Chemosphere 76, 644-650.

Nelson, D.C., Jorgensen, B.B., Revsbech, N.P., 1986a. Growth pattern and yield of a chemoautotrophic *Beggiatoa sp.* in oxygen-sulfide microgradients. Appl. Environ. Microbiol. 52, 225-233.

Nelson, D.C., Revsbech, N.P., Jorgensen, B.B., 1986b. Microoxic-anoxic niche of *Beggiatoa sp*. Microelectrode survey of marine and fresh water strains. Appl. Environ. Microbiol. 52, 161-168.

Nielsen, A.H., Vollertsen, J., Hvitved-Jacobsen, T., 2003. Determination of kinetics and stoichiometry of chemical sulfide oxidation in wastewater of sewer networks. Environ. Sci. Technol. 37, 3853-3858.

Nielsen, P.H., de Muro, M.A., Nielsen, J.L., 2000. Studies on the in situ physiology of Thiothrix spp. present in activated sludge. Environ. Microbiol. 2, 389-398.

Obrien, D.J., Birkner, F.B., 1977. Kinetics of oxygenation of reduced sulfur species in aqueous solution. Environ. Sci. Technol. 11, 1114-1120.

Odintsova, E., Wood, A., Kelly, D., 1993. Chemolithoutotrophic growth of *Thiothrix ramosa.* Arch. Microbiol. 160, 152-157.

Oh, S.E., Kim, K.S., Choi, H.C., Cho, J., Kim, I.S., 2000. Kinetics and physiological characteristics of autotrophic dentrification by denitrifying sulfur bacteria. Water Sci. Technol. 42, 59-68.

Panwar, N.L., Kaushik, S.C., Kothari, S., 2011. Role of renewable energy sources in environmental protection: A review. Renew. Sust. En. Rev. 15, 1513-1524.

Pathak, H., Jain, N., Bhatia, A., Mohanty, S., Gupta, N., 2009. Global warming mitigation potential of biogas plants in India. Environ. Monit. Assess. 157, 407-418.

Peck, H.D., 1960. Adenosine 5'-Phosphosulfate as an intermediate in the oxidation of thiosulfate by *Thiobacillus thioparus*. Proc. Natl. Acad. Sci. USA 46, 1053-1057.

Perry, D.L., 2011. Handbook of Inorganic Compounds. CRC press.

Petersen, B., Gernaey, K., Vanrolleghem, P.A., 2002. Anoxic activated sludge monitoring with combined nitrate and titrimetric measurements. Water Sci. Technol. 45, 181-190.

Piculell, M., Welander, T., Jonsson, K., 2014. Organic removal activity in biofilm and suspended biomass fractions of MBBR systems. Water Sci. Technol. 69, 55-61.

Prange, A., Chauvistre, R., Modrow, H., Hormes, J., Truper, H.G., Dahl, C., 2002. Quantitative speciation of sulfur in bacterial sulfur globules: X-ray absorption spectroscopy reveals at least three different species of sulfur. Microbiol. 148, 267-276.

Ramadori, R., Rozzi, A., Tandoi, V., 1980. An automated system for monitoring the kinetics of biological oxidation of ammonia. Water Res. 14, 1555-1557.

Ramirez-Vargas, R., Ordaz, A., Carrion, M., Hernandez-Paniagua, I.Y., Thalasso, F., 2013. Comparison of static and dynamic respirometry for the determination of stoichiometric and kinetic parameters of a nitrifying process. Biodegradation 24, 675-684.

Ramirez, M., Gomez, J.M., Aroca, G., Cantero, D., 2009. Removal of hydrogen sulfide by immobilized *Thiobacillus thioparus* in a biotrickling filter packed with polyurethane foam. Biores. Technol. 100, 4989-4995.

Reyes-Avila, J.S., Razo-Flores, E., Gomez, J., 2004. Simultaneous biological removal of nitrogen, carbon and sulfur by denitrification. Water Res. 38, 3313-3321.

Richardson, D.J., Watmough, N.J., 1999. Inorganic nitrogen metabolism in bacteria. Curr. Opin. Chem. Biol. 3, 207-219.

Robertson, L.A., Kuenen, J.G., 2006. The colorless sulfur bacteria. The prokaryotes. Springer, pp. 985-1011.

Rodriguez, G., Dorado, A.D., Bonsfills, A., Sanahuja, R., Gabriel, D., Gamisans, X., 2012. Optimization of oxygen transfer through venturi-based systems applied to the biological sweetening of biogas. J. Chem. Technol. Biotechnol. 87, 854-860.

Rodriguez, G., Dorado, A.D., Fortuny, M., Gabriel, D., Gamisans, X., 2014. Biotrickling filters for biogas sweetening: oxygen transfer improvement for a reliable operation. Proc. Saf. Environ. 92, 261-268.

Roels, J.A., 1983. Energetics and kinetics in biotechnology. Elsevier Biomedical Press.

Roosta, A., Jahanmiri, A., Mowla, D., Niazi, A., 2011. Mathematical modeling of biological sulfide removal in a fed batch bioreactor. Biochem. Eng. J. 58-59, 50-56.

Rovira, R. 2012. Caracterització de l'operació i estudi metatranscriptòmic d'un bioreactor de dessulfuració d'alta càrrega d'H$_2$S. PhD Thesis, UAB, Barcelona.

Senga, Y., Mochida, K., Fukumori, R., Okamoto, N., Seike, Y., 2006. N$_2$O accumulation in estuarine and coastal sediments: the influence of H$_2$S on dissimilatory nitrate reduction. Estuar. Coast. Shelf Sci. 67, 231-238.

Sin, G., Malisse, K., Vanrolleghem, P.A., 2003. An integrated sensor for the monitoring of aerobic and anoxic activated sludge activities in biological nitrogen removal plants. Water Sci. Technol. 47, 141-148.

Sin, G., Vanrolleghem, P.A., 2004. A nitrate biosensor based methodology for monitoring anoxic activated sludge activity. Water Sci. Technol. 50, 125-133.

Soreanu, G., Beland, M., Falletta, P., Edmonson, K., Seto, P., 2008. Laboratory pilot scale study for H$_2$S removal from biogas in an anoxic biotrickling filter. Water Sci. Technol. 57, 201-207.

Soreanu, G., Beland, M., Falletta, P., Ventresca, B., Seto, P., 2009. Evaluation of different packing media for anoxic H$_2$S control in biogas. Environ. Technol. 30, 1249-1259.

Sorensen, J., Tiedje, J.M., Firestone, R.B., 1980. Inhibition by sulfide of nitric and nitrous oxide reduction by denitrifying *Pseudomonas fluorescens.* Appl. Environ. Microbiol. 39, 105-108.

Soto, O., Aspe, E., Roeckel, M., 2007. Kinetics of cross-inhibited denitrification of a high load wastewater. Enz. Microbiol. Technol. 40, 1627-1634.

Spanjers, H., Vanrolleghem, P., 1995. Respirometry as a tool for rapid characterization of waste water and activated sludge. Water Sci. Technol. 31, 105-114.

Spanjers, H., Vanrolleghem, P., Olsson, G., Dold, P., 1996. Respirometry in control of the activated sludge process. Water Sci. Technol. 34, 117-126.

Stefess, G.C., Torremans, R.A.M., deSchrijver, R., Robertson, L.A., Kuenen, J.G., 1996. Quantitative measurement of sulphur formation by steady state and transient state continuous cultures of autotrophic *Thiobacillus sp.* Appl. Microbiol. Biotechnol. 45, 169-175.

Steudel, R. 1989. On the nature of the elemental sulfur (S^0) produced by sulfur-oxidizing bacteria. A model for S^0 globules. In: Autotrophic Bacteria, Sci. Technol., Madison, pp 289-203

Steudel, R., Holdt, G., Göbel, T., Hazeu, W., 1987. Chromatographic Separation of higher polythionates and their detection in cultures of *Thiobacillus ferroxidans*; molecular composition of bacterial sulfur secretions. Angew. Chem. Int. Ed. Engl. 26, 151-153.

Steudel, R., Holdt, G., Nagorka, R., 1986. On the autoxidation of aqueous sodium polysulfide. Z. Naturforsch 41b, 1519-1522.

Suzuki, I., 1999. Oxidation of inorganic sulfur compounds: chemical and enzymatic reactions. Can. J. Microbiol. 45, 97-105.

Syed, M., Soreanu, G., Falletta, P., Béland, M., 2006. Removal of hydrogen sulfide from gas streams using biological processes - A review. Can. Biosyst. Eng. 48, 2.

Tamis, J., Marang, L., Jiang, Y., van Loosdrecht, M.C., Kleerebezem, R., 2014. Modeling PHA-producing microbial enrichment cultures; towards a generalized model with predictive power. N. Biotechnol. 31, 324-334.

Tang, K., Baskaran, V., Nemati, M., 2009. Bacteria of the sulphur cycle: an overview of microbiology, biokinetics and their role in petroleum and mining industries. Biochem. Eng. J. 44, 73-94.

Then, J., Truper, H.G., 1983. Sulfide oxidation in *Ectothiorhodospira abdelmalekii* - evidence for the catalytic role of cytochrome c551. Arch. Microbiol. 135, 254-258.

Timmertenhoor, A., 1981. Cell yield and bioenergetics of *Thiomicrospira denitrificans* compared with *Thiobacillus denitrificans*. Anton. Leeuw. J. Microbiol. 47, 231-243.

Tora, J.A., Lafuente, J., Baeza, J.A., Carrera, J., 2010. Combined effect of inorganic carbon limitation and inhibition by free ammonia and free nitrous acid on ammonia oxidizing bacteria. Biores. Technol. 101, 6051-6058.

Twining, B.S., Mylon, S.E., Benoit, G., 2007. Potential role of copper availability in nitrous oxide accumulation in a temperate lake. Limnol. Oceanogr. 52, 1354-1366.

US EPA (US Environmental Protection Agency), 2003. Toxicological Review of Hydrogen Sulfide. EPA/635/R-03/005, Washington, USA. (http://www.epa.gov)

Vaiopoulou, E., Melidis, P., Aivasidis, A., 2005. Sulfide removal in wastewater from petrochemical industries by autotrophic denitrification. Water Res. 39, 4101-4109.

Vanrolleghem, P.A., Spanjers, H., Petersen, B., Ginestet, P., Takacs, I., 1999. Estimating (combinations of) activated sludge model nº1; parameters and components by respirometry. Water Sci. Technol. 39, 195-214.

Vargas, M., Guisasola, A., Lafuente, J., Casas, C., Baeza, J.A., 2008. On-line titrimetric monitoring of anaerobic-anoxic EBPR processes. Water Sci. Technol. 57, 1149-1154.

Vishniac, W., 1952. The Metabolism of *Thiobacillus thioparus* I: the oxidation of thiosulfate. J. Bacteriol. 64, 363-373.

Visser, J.M., deJong, G.A.H., Robertson, L.A., Kuenen, J.G., 1996. Purification and characterization of a periplasmic thiosulfate dehydrogenase from the obligately autotrophic *Thiobacillus sp.* W5. Arch. Microbiol. 166, 372-378.

Visser, J.M., Robertson, L.A., VanVerseveld, H.W., Kuenen, J.G., 1997. Sulfur production by obligately chemolithoautotrophic *Thiobacillus sp.* Appl. Environ. Microbiol. 63, 2300-2305.

Wild, D., Vonschulthess, R., Gujer, W., 1995. Structured modeling of denitrification intermediates. Water Sci. Technol. 31, 45-54.

Williams, M., 2006. The Merck Index: an Encyclopedia of Chemicals, Drugs, and Biologicals. Merck Inc.

Yamamoto-Ikemoto, R., Komori, T., Nomura, M., Ide, Y., Matsukami, T., 2000. Nitrogen removal from hydroponic culture wastewater by autotrophic denitrification using thiosulfate. Water Sci. Technol. 42, 369-376.

Yavuz, B., Turker, M., Engin, G.O., 2007. Autotrophic removal of sulphide from industrial wastewaters using oxygen and nitrate as electron acceptors. Environ. Eng. Sci. 24, 457-470.

Young, J.C., Cowan, R.M., 2004. Respirometry for Environmental Science and Engineering. SJ Enterprises.